NOVA SCHOOL OF SCIENCE & TECHNOLOGY

DEPARTMENT OF PHYSICS

MARIA ANA NETO PARRA HENRIQUES

Bachelor of Science in Biomedical Engineering

ANALYSIS OF THE RELATIONSHIP BETWEEN EVOKED POTENTIALS AND ELECTRODERMAL ACTIVITY DURING THE APPLICATION OF VISUAL STIMULI IN INFANTS

MASTER IN BIOMEDICAL ENGINEERING

NOVA University Lisbon

October, 2023

NOVA SCHOOL OF
SCIENCE & TECHNOLOGY

DEPARTMENT OF PHYSICS

ANALYSIS OF THE RELATIONSHIP BETWEEN EVOKED POTENTIALS AND ELECTRODERMAL ACTIVITY DURING THE APPLICATION OF VISUAL STIMULI IN INFANTS

MARIA ANA NETO PARRA HENRIQUES

Bachelor of Science in Biomedical Engineering

Adviser: Carla Maria Quintão Pereira
Auxiliary Professor, NOVA University Lisbon

Co-adviser: Cláudia Regina Pereira Quaresma
Assistant Professor, NOVA University Lisbon

Examination Committee

Chair: Célia Maria Reis Henriques
Associate Professor, NOVA University Lisbon

Rapporteur: Hugo Filipe Silveira Gamboa
Associate Professor, NOVA University Lisbon

Adviser: Carla Maria Quintão Pereira
Auxiliary Professor, NOVA University Lisbon

MASTER IN BIOMEDICAL ENGINEERING

NOVA University Lisbon
October, 2023

Analysis of the relationship between evoked potentials and electrodermal activity during the application of visual stimuli in infants

This document was created with the (pdf/Xe/Lua)LaTeX processor and the NOVAthesis template (v7.1.7) [1].

Acknowledgements

I would like to express my gratitude to all those who played a pivotal role in completing this dissertation.

First and foremost, my profound thanks go to Professor Carla Quintão and Professor Cláudia Quaresma, my thesis advisers, for their invaluable mentorship and their constant commitment to assisting in the best way possible and dedicating their time to me and to this research. I would also like to express my profound gratitude to Dr. Ana Isabel Ferreira, whose expertise and unwavering support played a pivotal role in shaping this work. Her positive attitude and enthusiasm kept us motivated and cheerful even during the most challenging moments. It was the collective effort of this team that made all of this possible.

I must also express my gratitude to the NOVA School of Science and Technology (SST) and all the professors who, like my advisors, demonstrated a genuine interest in nurturing students' growth, both academically and as responsible citizens. They truly embodied the essence of the phrase "professors exist to help you, not to harm you". I extend special thanks to Professor Ricardo Vigário for his invaluable suggestions and willingness to provide assistance during moments of academic uncertainty.

From the very first day at SST, I was reminded that "you can't complete this course on your own." I sincerely thank all my friends and colleagues who made this statement a reality. Your messages of support and collaboration, spanning the past five years, have been invaluable. The mutual assistance within our course and among students has been remarkable, not only within our year but also with colleagues from higher years who empathized with our journey. A heartfelt thanks to Isabel Curioso, our course genius, whose willingness to help never wavered.

My little college family, André Rosa, Raquel Simão, and the rest of the family members, deserve special thanks for making my academic journey more special and complete. Back when I was a helpless freshman in the Biomedical course, they turned it into my second home (after Neves' place). My friends, who started this journey with me, as well as those who joined along the way from other years and courses, played a significant role. Your support and the moments we shared, whether to relieve the tension of projects and exams, late nights at the "7" of academic productivity, or just being there, made this journey possible. We've experienced significant growth, moments of despair, great happiness, and unforgettable, hilarious stories that we'll cherish for life, but that I will now keep between ourselves..

I extend my heartfelt thanks to my entire family, including my parents, sister, aunts,

uncles, and grandparents, as well as my partner Dinis. They patiently listened to my frustrations and provided unwavering emotional support, keeping me motivated. A special mention goes to my grandfather, who checked on my progress weekly since March, asking me every week: "Have you finished yet?" reminding me that I was running behind, but always with enjoyment, love and concern.

Lastly, I want to emphasize that this work would not have materialized without the invaluable support and encouragement of the entire academic community, my family, and friends. I wholeheartedly thank each of you for being an integral part of this remarkable journey.

”

“Towards the end, the elderly woman, in a state of ecstasy, exclaimed...”

— The Old Lady, Wise woman (en)

Abstract

Each year, more than 10% of infants are born prematurely, before reaching 37 weeks of gestational age. Premature birth, characterised by shorter gestation periods and exposure to different external environments compared to the womb, has significant implications for nervous system development. However, there remains a considerable gap in our comprehension of how to identify and mitigate the developmental hurdles that preterm infants may encounter. Evaluating preterm infants during their early months of life is particularly intricate due to ongoing neurodevelopment, and the available literature on this subject is limited.

This dissertation addresses the critical need for effective methods to assess and detect developmental immaturity in infants. Investigating infant responses to visual stimuli as a diagnostic tool can yield insights into their future prospects. Early diagnosis allows for timely intervention tailored to individual needs, increasing the likelihood of normative development into adulthood. Focusing on two key signals: Electrodermal Activity (EDA) and Visual Evoked Potentials (VEPs), the primary goal is to establish a connection between these signals to enhance our understanding of neurovisual system development in both full-term and preterm infants. To accomplish this goal, this study resorted to a systematic data collection, signal processing optimisations, parametrisation, and a comprehensive analysis.

Results from the analysis of full-term and preterm infants, focusing on data collected at 4 and 12 months, revealed a pattern with P100 latency typically decreasing, possibly showing signs of maturation. Some infants showed increased Skin Conductance Responses (SCRs) with age. Furthermore, the study revealed varying trends in Electrodermal Activity (EDA) Power values, with some infants exhibiting a decrease and others showing an increase, suggesting differing responses in development. Notably, the relationship between EDA and VEPs identified differences between these two infant groups, particularly in response to visual stimuli.

The methodologies demonstrated their effectiveness in analysing the signals and establishing a connection between neonate development and electrophysiology. This research sheds light on intricate signal interactions, which hold promise for enhancing diagnostic and analytical applications in the future, ultimately improving immaturity detection for infants.

Keywords: Preterm infants, Newborns, Nervous System Development, Electrodermal Activity, Visual Evoked Potentials, Visual Stimulus, Developmental Assessments

Resumo

Em cada ano, mais de 10% dos bebés nascem prematuramente, antes de atingirem as 37 semanas de gestação. O parto prematuro, caracterizado por períodos de gestação mais curtos e exposição a ambientes externos diferentes do útero, tem implicações significativas no desenvolvimento do sistema nervoso. Contudo, ainda existe uma lacuna considerável na nossa compreensão de como identificar e mitigar os obstáculos no desenvolvimento que os bebés prematuros podem enfrentar. Avaliar bebés prematuros nos primeiros meses de vida é particularmente complexo devido ao contínuo neurodesenvolvimento, e a literatura disponível sobre este tema ser limitada.

Esta dissertação aborda a necessidade de existirem métodos eficazes para avaliar e detetar imaturidades do desenvolvimento em bebés. Investigar as respostas dos bebés a estímulos visuais tem se demonstrado próspero e possivelmente relevante para este fim. O diagnóstico precoce permite intervenções atempadas adaptadas às necessidades individuais, aumentando a probabilidade de um desenvolvimento normativo na idade adulta. Deste modo, o estudo concentra-se em dois tipos de sinal: Atividade Eletrodérmica (EDA) e Potenciais Evocados Visuais (PEVs), com o objetivo principal de estabelecer uma ligação entre os mesmos para melhorar a nossa compreensão do desenvolvimento do sistema neurovisual em bebés nascidos a termo e pré-termo. Com isto em mente, foi implementada uma recolha de dados sistemática, aperfeiçoamento do processamento de sinais, parametrização e análise dos dados.

Os resultados da análise destes sinais registados em bebés de termo e pré-termo, aos 4 e 12 meses, revelaram um padrão em que a latência do P100 normalmente diminui, possivelmente revelando sinais de maturação. Alguns bebés apresentaram um aumento nas Respostas da Condutância da Pele (SCR) com a idade. O estudo revelou tendências variadas nos valores de Potência do EDA, com alguns bebés a apresentarem uma diminuição e outros a mostrarem um aumento, sugerindo variabilidade de respostas no desenvolvimento. Em adição, a relação entre EDA e PEVs identificou diferenças entre esses dois grupos de bebés, particularmente em resposta a estímulos visuais.

As metodologias demonstraram a sua eficácia na análise dos sinais e no estabelecimento de uma ligação entre o desenvolvimento neonatal e a eletrofisiologia. Esta investigação melhora o nosso conhecimento relativamente a interações complexas de sinais e espera-se que estas metodologias venham a contribuir para melhorar a capacidade de detetar imaturidades em bebés e de avaliação do desenvolvimento.

Palavras-chave: Prematuros, Recém-Nascidos, Desenvolvimento do Sistema Nervoso, Atividade Eletrodermica, Potenciais Evocados Visuais, Estímulos Visuais, Avaliação do Desenvolvimento

Contents

List of Figures

List of Tables

Glossary

binocular vision — Ability of an organism to perceive a single, three-dimensional image of the environment using both eyes simultaneously. This is made possible by the overlapping visual fields of the eyes, which provide the brain with two slightly different perspectives of the same scene [2].

conductance — Quantitative measurement of the ease with which electric current flows through a material, symbolized by "G" and measured in units of Ohm inverse (Ω^{-1}) or Siemens (S). It is the inverse of electrical resistance [3].

corrected age — Term used for premature babies to account for the duration of their prematurity, calculated from the estimated date of conception. As an example, consider a baby born with a gestational age of 28 weeks and 1 day. In this case, daily monitoring should continue until they reach 29 weeks, after which it transitions to a weekly monitoring routine until they reach 40 weeks. When the baby reaches 40 weeks, it aligns with their expected term age, which is the day they were originally due to be born [4].

Electrodermal Activity — Process that measures skin **conductance**, recorded in microsiemens (μS). It estimates Autonomic Nervous System responses, especially emotional or arousal states [3].

Electroencephalogram — Record of the electric signal, in voltage over time, generated by the cooperative activity of brain cells. It is a graphical representation of brain wave patterns, often used for diagnosing neurological conditions and studying brain function. Electroencephalography is the process of recording and interpreting those graphics [5].

fetus The developmental stage of an organism before birth, following the initial eight weeks after fertilization. It involves substantial growth, tissue and organ differentiation, and maturation of existing structures and is divided into trimesters for pregnancy monitoring and assessment [6].

Gastrulation Process in early embryonic development. It involves the transformation of a blastula, which is a hollow ball of cells, into a gastrula, a structure with distinct germ layers. Gastrulation is characterized by cell migration and rearrangement, creating of three primary germ layers: the endoderm (inner layer), mesoderm (middle layer), and ectoderm (outer layer). These germ layers give rise to various tissues and organs in the developing embryo [7].

myelination Biological process by which nerve fibres in the body are coated with a lipidic substance known as myelin. This fatty sheath acts as an insulator, increasing the velocity and efficiency of nerve signal transmission, and is crucial to the proper functioning of the nervous system, including the brain and spinal cord [8].

Neurulation Process in early embryonic development that leads to the formation of the neural tube, which serves as the foundation for the central nervous system (CNS) in vertebrate embryos. It involves the transformation of a flat neural plate into a neural tube that eventually differentiates into the brain and spinal cord. Any disruptions or malformations in neurulation can result in severe congenital neural tube defects, which can have profound implications for an individual's health and development [7].

visual acuity Term used in ophthalmology and optometry to describe the sharpness or clarity of vision. It refers to the ability of the eye to distinguish fine details and discriminate between objects at a given distance [9].

Visual Evoked Potential Electrical brain responses to visual stimuli recorded in electroencephalography. They help assess visual system functionality and diagnose visual or neurological issues [10].

zygote Cell resulting from the fusion of a sperm cell and an egg cell, during fertilization [11].

Abbreviations

ANS Autonomic Nervous System

CNS Central Nervous System

DDA Discrete Decomposition Analysis

EDA Electrodermal Activity
EEG Electroencephalogram

fVEP Flash Visual Evoked Potential

ISCEV International Society for Clinical Electrophysiology of Vision

MAC Maternidade Alfredo da Costa

nSCR number of Skin Conductance Responses

PNS Peripheral Nervous System
pVEP Pattern Visual Evoked Potential

SCL Skin Conductance Level
SCR Skin Conductance Response
SNS Sympathetic Nervous System
SSR Sympathetic Skin Response

USF Unidade de Saúde Familiar da Baixa

VEP Visual Evoked Potential

1

Introduction

The research work described in this dissertation was carried out in accordance with the norms established in the ethics code of Universidade Nova de Lisboa. The work described and the material presented in this dissertation, with the exceptions clearly indicated, constitute original work carried out by the author.

1.1 Context and Motivation

Each year, over 15 million babies are born prematurely, which accounts for more than 10% of all infants born worldwide. Despite this prevalence, there remains a lack of comprehensive understanding regarding the identification and prevention of developmental difficulties in these premature infants [12].

The distinction between preterm and term infants is based on the point of gestation at which birth occurs, with preterm birth defined as before 37 weeks and term birth defined as after 37 weeks. The primary difference between these two groups lies in their level of maturity at birth, as preterm infants have a shorter period of development in the womb, leading to an elevated risk of health issues [13].

Currently, evaluation methods primarily involve the clinical observation e.g., how the child sits and holds their head, along with developmental scales that assess their behaviour in response to specific stimuli e.g., objects and toys. Additionally, neurologic exams are sometimes conducted during the five behavioural stages, which include quiet sleep, active sleep, quiet wakefulness, active wakefulness, and crying, as outlined in [14]. Evaluating preterm infants during the early months of life presents numerous challenges, largely due to the continuous and dynamic nature of their nervous system development. This complexity hinders a comprehensive understanding of their responses to various stimuli and how these reactions may indicate potential issues. It is important to note that the existing literature remains significantly limited in addressing these assessments [15].

The motivation behind this dissertation is to establish an effective and practical methodology for assessing and identifying developmental immaturities in infants. This research endeavour aims to bridge the gap between electrophysiological signals and neonatal development, which holds considerable potential for pre-verbal infants incapable of describing their symptoms [16]. The investigation of infants' responses to visual sensory stimuli as a diagnostic tool for developmental immaturity has demonstrated considerable value, as it can provide valuable insights into the child's future developmental trajectory [17]. Early diagnosis facilitates prompt intervention and customisation aligned with the specific needs of each infant, consequently heightening the probability of the child adhering to a normative developmental trajectory throughout the journey of maturation into adulthood [18].

1.2 Objectives

This study is integrated within a broader research project duly approved by the ethics committee of the Centro Hospitalar Universitário Lisboa Central, with the purpose of studying the visuomotor competencies of preterm infants to optimize early-life intervention therapies. The present dissertation is part of a more comprehensive investigation under the purview of the Doctoral Program in Biomedical Engineering, entitled "Development of Visual and Motor Skills in Preterm Infants". The project, to be carried out by Dr. Ana Isabel Ferreira, seeks to analyse the physiological signals, Visual Evoked Potentials (VEPs) and Electrodermal Activity (EDA), of both term and preterm infants across various months of age, thereby facilitating a comparative assessment of the developmental trajectories of these two populations throughout their growth stages.

This research builds upon the findings of two prior dissertations, [19] and [20]. The former focused on investigating the EDA in infants exposed to visual stimuli, while the latter revolved around the study of babies' VEPs. Both studies shared the goal of identifying an objective method for evaluating infant development. The present research focuses on simultaneously measuring VEPs and EDA in healthy infants. The aim of this dissertation is to:

1. Examine the behaviour of signals over time and how they evolve with age.
2. Explore the relationship between VEPs and EDA, and their correlation with demographic data.
3. Establish a normative reference for comparing preterm and full-term infant populations to enable early detection of any differences between the two groups.

These objectives will be achieved by creating a computer platform designed for the processing and organization of electrophysiological parameters. This method will also include the analysis of signals and their parametrisation. This analysis is critical in further understanding sensory processing development in babies and providing a basis for creating an effective clinical intervention plan, ensuring a development trajectory for preterm babies similar to that of full-term babies [18].

The purpose of this dissertation is to provide an overview of the key concepts, literature, and methods necessary to address the problem at hand. It is organized as follows:

Chapter 1 - Introduction: Contextualization, motivation, and objectives.

Chapter 2 - Theoretical Concepts: Anatomical, physiological, and electrophysiological foundations.

Chapter 3 - State of the Art: Reviews relevant studies about the use of EDA and VEPs to access visual competencies in different populations.

Chapter 4 - Materials and Methods: Sample characterisation, tools, procedures and parametrisation.

Chapter 5 - Results: The results are presented.

Chapter 6 - Discussion and Conclusions: Synthesizes and discusses findings, limitations and outlines prospects.

2

Theoretical Concepts

This chapter is organized into four distinct sections. It begins with “Sensory Processing”, delving into how our senses interpret the surrounding environment. Within this, the subsection “Sensory Processing Development” examines the evolution of these senses as we mature. Transitioning to section two, “Visual Processing”, we explore how we perceive visual stimuli, followed by subsection “Development of Visual Processing”, which details the maturation of our visual abilities. Section three, “Visual Evoked Potentials (VEPs)”, introduces a method to measure brain responses to visual stimuli, encompassing “Signal Acquisition” and “Signal Processing” subsections. Concluding the chapter, the section “Electrodermal Activity (EDA)” investigates the measurement of skin conductance changes, providing a comprehensive understanding of our physiological responses to visual stimuli. This investigation encompasses three subsections: “Anatomy of the Skin”, “Signal Acquisition”, and “Signal Processing”.

2.1 Sensory Processing

Sensory processing is a function of the nervous system that pertains to how the Central Nervous System (CNS) perceives and responds to sensory information received from the Peripheral Nervous System (PNS). The CNS is composed of the brain and spinal cord, while the PNS is made up of nerves branching from the CNS, transmitting information between it and the rest of the body. The PNS is comprised of the Somatic System, responsible for voluntary functions, and the Autonomic System, which can be further subdivided into the Sympathetic and Parasympathetic branches, that collectively regulate involuntary bodily functions, for example, temperature regulation [9, 21]. The Sympathetic Nervous System (SNS) and Parasympathetic Nervous System are crucial for managing physiological arousal and recovery. The Sympathetic system, often associated with the "fight or flight" response, contrasts with Parasympathetic processes that facilitate the body’s return to homeostasis following stress [22].

Sensory information is received by specific receptors located in the eyes, ears, skin, and other sensory organs. These receptors are designed to be differentially sensitive to particular stimuli. For instance, light receptors are not susceptible to temperature changes. When a stimulus occurs, the receptors are excited and transform the energy of the stimulus (e.g., light, sound, mechanical energy, etc.) into action potentials generated by their membranes. Thus, the stimulus is translated into electrical information our nervous

system can understand. The peripheral nerves then transmit the electrical information to the CNS, where it is processed, and an adaptive response to the situation is generated [9].

2.1.1 Sensory Processing Development

The development of the nervous system begins during gestation, a period lasting approximately 38 to 42 weeks. This gestational phase is subdivided into three trimesters, with the initial trimester further categorised into three stages: germinal, embryonic, and fetal [8].

The germinal stage occurs during the first 2 weeks after conception, where the zygote undergoes numerous cell divisions and differentiation [8]. The embryonic stage spans between the 3^{rd} and 8^{th} weeks of gestation and comprises various processes. The process of Gastrulation leads to the formation of three distinct layers: ectoderm, endoderm, and mesoderm. During this period, Neurulation occurs and gives rise to the neural tube, which is the foundation for the CNS. As illustrated in Figure 2.1, ectoderm thickens to create the neural plate, folding over to form the neural groove, which eventually merges into a hollow tube, the neural tube. This structure differentiates into the primary brain and spinal cord. Simultaneously, the formation of organs commences, as well as the maturation of the head and facial structures and early formation of limb protrusions [7, 23].

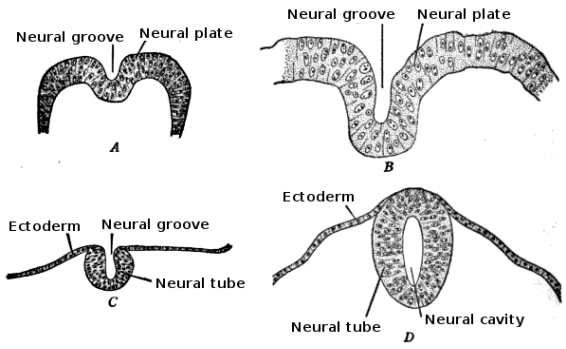

Figure 2.1: Process of Neurulation from [7]. *A*: Neural plate folds; *B*: Neural groove is created; *C*: Groove keeps folding; *D*: Merging of the edges and Neural tube formation.

The fetal stage begins in the 9^{th} week, extending until the completion of pregnancy, during which organs and systems continue to develop, and neurons migrate to specific areas, forming synapses. During this stage, the first reflexes emerge, primarily in the limbs. Subsequently, the fetus enters the second trimester, which spans from the 14^{th} week and is characterised by significant growth. During this period, the nervous system becomes more responsive, and the brain and sensory nerves develop, allowing for the emergence of the sense of touch in the fetus. At the commencement of the third trimester, which starts around the 27^{th} week, the fetus prepares for birth [6, 8].

During the fetal period, most reflexes that involve the spinal cord and brain stem reach maturity within the 3^{rd} to 4^{th} months of gestation. Nevertheless, the functions of the

nervous system that implicate the cerebral cortex are not yet fully formed at birth. It is important to highlight that the process of myelination in several crucial brain tracts may continue for up to one year after birth [24].

Premature birth has significant implications for the development of the nervous system, leading to less mature brains and notable differences in structural, functional, and connectivity levels compared to term babies. These differences can manifest as challenges in sensory processing, cognitive abilities, and behavioural development [21, 25].

2.2 Visual Processing

Visual processing is a fundamental aspect of sensory processing as the eyes, along with the brain, are the primary means of capturing and translating visual information into perceptible content for the nervous system. The process involves capturing information related to colour, light, and space, which are then transmitted to the brain for further processing [26].

The eye is a complex organ that comprises a variable aperture system, the pupil, whose iris controls the light entering the eye, and a system of lenses with four refractive interfaces. These regions include the cornea, aqueous humour, the eye lens, and vitreous humour, as shown in Figure 2.2 a). At the posterior of the eye lies the retina, containing two types of photoreceptors: the cones, responsible for colour vision, and the rods, responsible for black-and-white vision and night vision, as seen in Figure 2.2 b). The fovea is a part of the retina responsible for visual acuity, the ability to distinguish detail in an object [27].

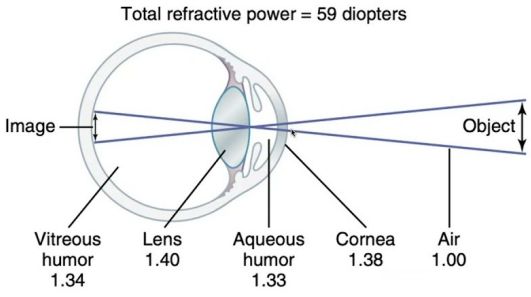

a) Layers of the eye and their refractive indices from [27].

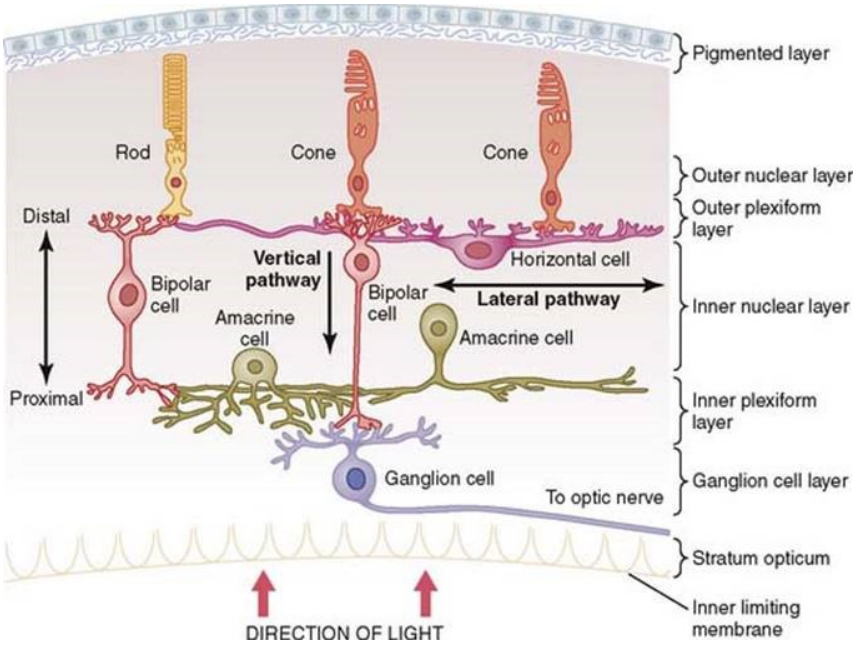

b) Different Layers of the Retina from [28].

Figure 2.2: The Layers of the eye and different Layers of the Retina.

The visual process begins with the entry of light into the eye, passing through the lens system until it reaches the distal area of the retina, where it stimulates the photoreceptors, as depicted in Figure 2.2 b). Subsequently, the signal traverses the neural layers of the retina, reaching the ganglion cells and, finally, the optic nerve fibres and cerebral cortex [28].

2.2.1 Development of Visual Processing

The visual system begins to develop during early gestation and continues to mature throughout childhood and early adulthood. The retina is formed from the same embryonic structures that give rise to the nervous system, namely the neural tube, and starts to develop around 40 days after conception [29].

Infants and young children undergo several stages of visual development. In the first few months of life, their ability to perceive contrasts is limited, and their recognition of larger objects is confined to fixed outlines e.g., just basic shapes without much detail. However, between 1 to 3 months of age, their visual acuity improves, allowing them to discriminate details better and perceive colours. They also start to exhibit eye to eye contact, eye movement development, fixation and tracking of human faces, and the ability to follow and recognize objects and animals [2].

Between 6 to 10 months of age, the development of binocular vision and sensitivity to contrast enables infants to perceive depth and have three-dimensional vision. They can then get around and avoid obstacles, explore small objects, and recognize people. They also develop the ability to voluntarily control their eye movements, focusing and fixing on objects and people at different distances, and can discriminate and name colours, shapes, and sizes [2].

The overall visual development of infants involves the myelination of the optic nerve, the maturation of the fovea, and the development of binocular vision, which all contribute to improvements in visual acuity, depth perception, and contrast discrimination [2, 29]. Newborns consistently exhibit a preference for specific visual stimuli. They tend to respond more to patterns with bull's-eyes or checkerboard shapes instead of stripes and solid forms, moving versus static patterns, and high contrasts, such as black and white images [29].

2.3 Visual Evoked Potentials (VEPs)

VEPs are a neurophysiological technique used to assess the brain's electrical activity in response to specific visual stimuli, typically an intermittent flash of light or a pattern reversal. The derived signal, measured as voltage over time, is extracted from an Electroencephalogram (EEG) (i.e., Records of the electrical activity in the brain), captured during the application of these visual stimuli [5, 10, 30].

2.3.1 Signal Acquisition

To obtain VEPs, a conventional electrode placement scheme is typically followed, according to the recommendations outlined by the International Society for Clinical Electrophysiology of Vision (ISCEV). These guidelines prescribe specific electrode locations, namely O_Z, $P0_8$, and $P0_7$, with F_Z serving as the reference electrode. Ground electrode placements commonly chosen include the forehead, vertex (C_Z), mastoid, earlobe, or linked earlobes [30]. These electrode positions are illustrated in Figure 2.3.

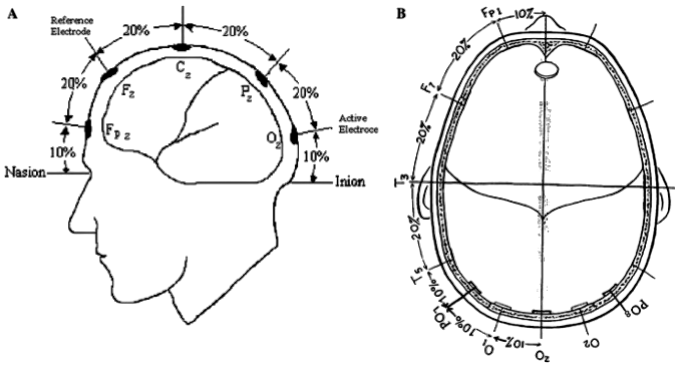

Figure 2.3: ISCEV standard electrode placement from [30]. A: Location of active and reference electrodes for standard responses; B: Locations of the lateral active electrodes.

When the visual sensory pathway is stimulated, an electrical discharge is generated and travels to the cerebral occipital cortex, resulting in waves that are predominantly observed in Brodmann areas 17, 18, and 19. These areas correspond to the primary visual cortex (V1), peristriate cortex and parastriate cortex, respectively, and play a crucial role in eye fixation movements. The electrical discharges can be captured by the electrodes and analysed to assess the speed and quality of the nerve signals reaching the brain [31, 32].

2.3.2 Signal Processing

Sudden head and body movements, including yawning, crying, or pacifier usage, can generate significant broad-band electrical artefacts. Adressing these artefacs is essential, using algorithms to filter out unwanted interference and extract clean and accurate neural responses. In addition to artefact removal, sensory evoked potentials often necessitate an amplifier, because they produce small responses compared to the background noise. The evoked response is consistent in time and magnitude when using the same stimulus pattern. Through the calculation of the average of multiple responses to the same stimulus, we can effectively enhance the signal of interest in comparison to the background noise, as the random noise tends to cancel out, while the consistent signal from the stimulus accumulates [10, 33, 34].

The recorded data produces a voltage graph over time, where the stimulus elicits an initial artefact followed by a series of peaks and valleys corresponding to the neuronal response. Information such as peak amplitude, latency (i.e., the time interval between

the stimulus and peak), and inter-peak latency (i.e., the time interval between successive peaks) can be extracted from the data [10].

Figure 2.4 represents a normal pattern-reversal VEPs response. The waveform consists of N75, P100 and N135 peaks, where the P100 positive peak is of primary interest. The latency of the P100 peak shifts to around 100 ms before six months of age, as seen in Figure 2.5. Prolonged latency can indicate visual impairment [30, 35, 36].

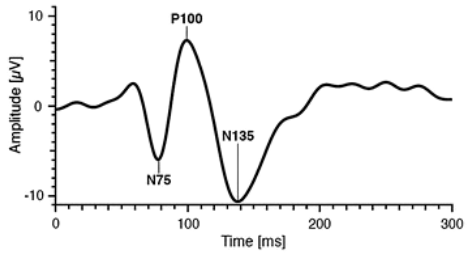

Figure 2.4: ISCEV standard pattern-reversal VEPs from [30].

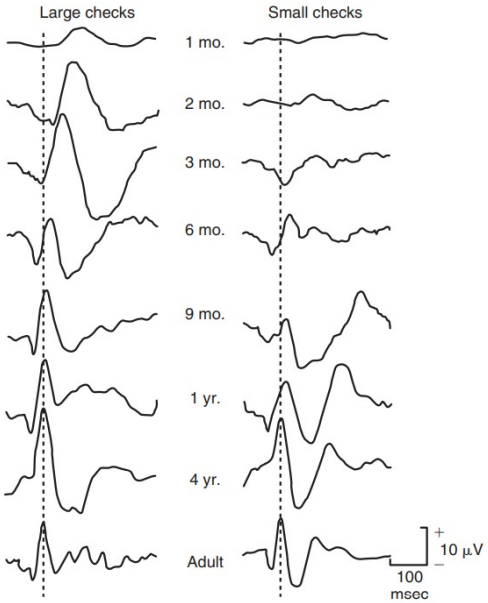

Figure 2.5: Pattern-reversal transient VEPs recorded from infants, children, and adults with normal vision. Response to both large (60-min) and small checks (15-min) at arc, from [36].

The timing of the P100 peak is influenced by various non-pathophysiological parameters, including pattern size, pattern contrast, mean luminance, signal filtering, patient age, refractive error, fixation quality, and pupil size, both extremely large and small. When analysing VEPs, it is often necessary to compare the acquired signal to a baseline reference (for example Figure 2.4) to identify the different peaks and draw conclusions from the data [30, 35, 36].

2.4 Electrodermal Activity (EDA)

The EDA measures changes in the electrical properties of the skin induced by the Autonomic Nervous System (ANS), specifically the SNS. It is represented as the variation in skin conductance over time, i.e., ease with which electric current flows through a material [3].

2.4.1 Anatomy of the skin

The skin's conductance is the property with the most significant impact on EDA. The skin is composed of two layers, the dermis and the hypodermis, with one of its components being sweat glands responsible for sweat production. The cell membranes of the skin cells have the ability to store energy and can be polarised. By applying an external electrical current, the skin behaves like an electric circuit, and its ducts can be considered a set of resistances connected in parallel [3, 37]. The skin in preterm infants is characterised by the development of distinct keratin patterns and the formation of essential anatomical structures within the epidermis. Importantly, the skin in preterm infants is notably more immature and thinner when compared to full-term infants, rendering it particularly vulnerable to external factors and influences. This underdeveloped epidermal barrier, distinguished by fewer cornified layers (i.e., composed of dead skin cells), increases preterm infants' vulnerability to harmful agents, excessive water loss, delayed skin maturation, potential skin damage, and the risk of infection [38, 39].

There are two types of sweat glands, eccrine and apocrine. Eccrine glands are found throughout the body and produce odourless sweat that helps regulate body temperature, while apocrine glands are primarily found in the axillary and groin regions, producing sweat that causes body odour. The eccrine sweat glands are composed of a secretory region located in the hypodermis that is innervated by nerves of the SNS and a duct located in the dermis that conducts sweat to the pores, releasing it directly onto the skin's surface [3, 40].

During the presentation of a visual stimulus, information is transmitted from the eye to the visual cortex, as discussed in section 2.2. Subsequently, it passes to the hypothalamus, which sends the information to the spinal cord, activating the SNS, traveling through the efferent nerves to the effector organs, in this case, the sweat glands. This process establishes communication between the visual stimulus, the CNS, and the ANS [28].

Sympathetic activation induces the rise of a sweat column in the duct, whose concentration and quantity depend on the degree of activation. The rising column causes a decrease in the duct's resistance, increasing its conductance. The larger the sweat column, the lower the resistance and the higher the conductance. The variation of conductance properties of the ducts of the numerous sweat glands produces visible changes in the EDA signal [3, 37].

2.4.2 Signal Acquisition

There are two methodologies for collecting EDA signals: endosomatic and exosomatic, with the latter being easier to analyse. The difference between them is that endosomatic methods use only the differences of potential originating in the skin itself, without the use of any external current source, while exosomatic methods use an external current applied to the skin [3, 37].

Exosomatic methodology uses Ohm's Law to determine skin conductance. Firstly, two electrodes are placed in distinct points in contact with the skin's surface. An electric current is then passed through the electrodes, creating a difference of potential between them (U), causing skin conductance changes. By applying a continuous current (I) and knowing that conductance (G) is the inverse of resistance (R) (Equation 2.1), its value can be calculated using Equation 2.2 [3, 41].

$$U = R \times I \qquad \text{(Ohm's Law)}$$

$$G = \frac{1}{R} \tag{2.1}$$

$$G = \frac{I}{U} \tag{2.2}$$

2.4.3 Signal Processing

Some equipment used for acquiring EDA signals, such as *Biosignalsplux*® and *Bitalino*®, may not measure the signal in standard SI units. In such cases, it is necessary to convert the raw data into microsiemens (symbol: µS), using Equation 2.3 [19].

$$\text{EDA} = \frac{\frac{\text{ADC}}{2^n} \times \text{VCC}}{0.12} \tag{2.3}$$

The variables in the equation represent the following: EDA (µS) denotes the EDA value in microsiemens, ADC (Analog to Digital Converter) is the value acquired from the EDA sensor channel, VCC represents the voltage value used, and n stands for the number of bits of the channel.

The EDA signal has two components, as shown in Figure 2.6 a). The tonic component, slowly varying Skin Conductance Level (SCL), is a relatively stable and continuous signal over time, used as a baseline measure. The phasic component, Skin Conductance Response (SCR), refers to the rapid changes in skin electrical conductance that occur in response to an emotional or physiological stimulus. These changes are typically short-lived, quickly returning to the baseline after removing the stimulus. The tonic/phasic decomposition of the signal allows for the identification of the specific SNS activity that triggered a specific phasic shift. From an isolated SCR signal, it is possible to take quantitative amplitude and time measurements, as shown in Figure 2.6 b) [42].

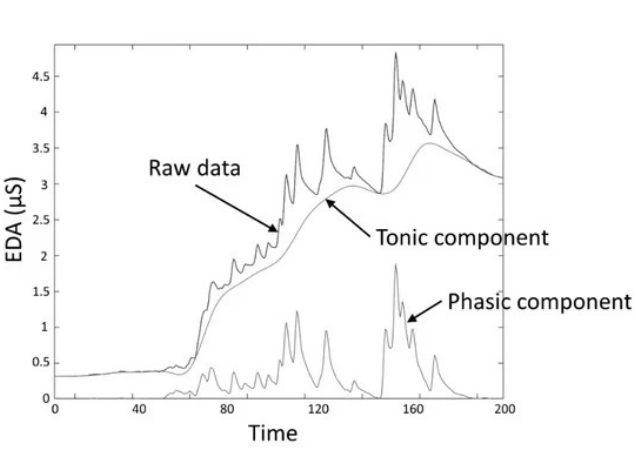

a) EDA signal decomposition into tonic and phasic components from [42].

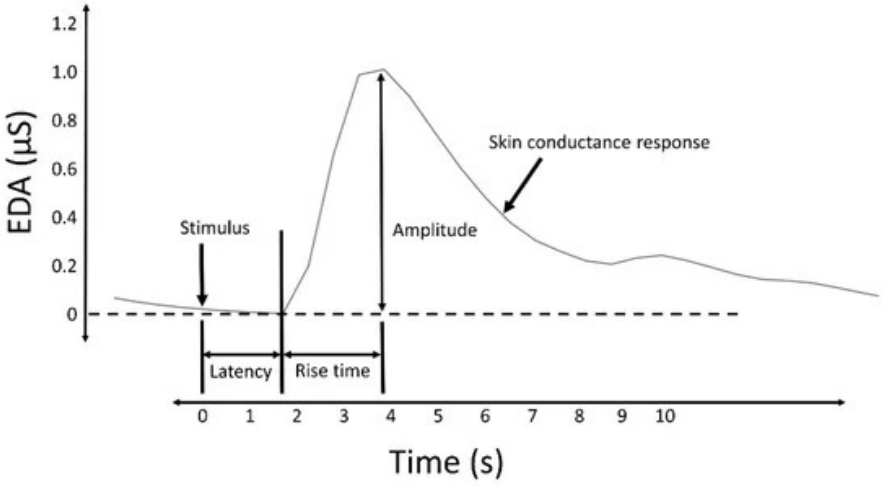

b) SCR signal and derived measures from [42].

Figure 2.6: EDA signal decomposition and SCR derived measures.

A substantial number of parameters can be derived from the signal. However, the literature suggests that the most informative parameters for studying the signal are the ones listed below [3]:

1. Amplitude - Sum of the amplitudes of all responses in the defined time window.
2. Area - Sum of the areas of all responses found in the defined time window.
3. nSCR - Number of responses to the stimuli.
4. Latency time - The time delay between the onset of a stimulus and the observable response to it.
5. SCL - Mean level of conductance.

The EDA signal varies from person to person, with different responses to stimuli. The electrodermal response may differ for the same individual depending on distinct stimuli or emotional conditions. The signal can also be affected by temperature fluctuations, patient movement and noise, which can easily be mistaken for response signals [43].

3

State of the Art

Presently, assessment methodologies predominantly encompass the observation of a child's posture, head control, developmental scales for evaluating their responses to objects and toys, and neurological examinations. Multiple studies underscore the importance of enhancing early diagnostic and intervention approaches for addressing developmental immaturity in children [14, 44]. Low birth weight and premature birth increase the risk of infant mortality and morbidity. Early and intensive intervention, including rehabilitation programs, significantly improves the neurodevelopment and motor skills of premature infants [14]. While various studies have employed VEPs or EDA to investigate responses to visual stimuli, none have explored the correlation between both signals, particularly in the context of term and preterm infants, and at such small age, to the best of our knowledge. This study distinguishes itself from existing research.

3.1 Studies on Visual Evoked Potentials

Studies utilising evoked potentials have been employed to evaluate visual development in children non-invasively. For example, Roy et al. [45] used Pattern Visual Evoked Potentials (pVEPs) to test both term and preterm infants in the first six months of life and found that this test helps monitor the visual development of both groups. Balachandran et al. [46] used Multifocal VEPs perimetry tests to diagnose diseases of the optic pathways in children aged 5 to 16 years, which objectively documented the visual fields of children and demonstrated that optical pathway maturity is associated with age.

Ruberto et al. [47] compared the visual pathway development of healthy preterm and full-term infants using Flash Visual Evoked Potentials (fVEPs) and pVEPs. Results varied with different visual stimuli, but the study concluded that similar neural groups develop at different time intervals for each population. In contrast, Birtles et al. [48] found that preterm infants exhibited reduced neural responses to orientation-specific visual stimuli compared to full-term infants, suggesting that these differences may be attributed to maturation delays in the visual cortex of preterm infants. However, their responses to motion-specific stimuli were similar to those of full-term infants.

Feng et al. [49] examined the development of fVEPs in preterm infants between 1 and 18 months of age and determined that the signals maturation is comparable to that of full-term infants. However, deficiencies in electrophysiological visual maturation were detected in very low birth weight infants. Through high-density electrode arrays, Tremblay et al. [50] reported that some premature infants experience delayed development of the primary visual pathway, as evidenced by electrophysiological findings, suggesting that preterm infants require specialized attention for visual development. Michalczuk et al. [51]

investigated the impact of birth weight, gestational age, and Apgar score on pVEPs in children with a history of prematurity. They found that birth weight and gestational age significantly affected the pVEPs, with lower birth weight and shorter gestational age resulting in delayed visual system development. Still, the Apgar score did not significantly impact the signal.

Kharal et al. [52] used fVEPs to evaluate stable preterm and term infants at 6 months of age. They found that preterm infants showed abnormal fVEPs, potentially indicating dysfunction of the visual pathways.

In summary, VEPs are adequate for evaluating visual development in children. Using distinct types of evoked potentials, several authors found differences in the visual function between preterm and full-term infants. Preterm infants may need special attention due to delayed primary visual pathway development and neural response differences to certain visual stimuli compared to full-term infants.

3.2 Studies on Electrodermal Activity

This section discusses several studies that explore the use of EDA in assessing emotional states and developmental processes in different populations. Article [53], by Martínez et al., describes a method for classifying the arousal level of ageing adults using EDA, which proves to be effective in assessing the emotional state of this population. Similarly, heart rate and skin conductance are explored for the assessment of behaviour inhibition in Mauritian children in article [54] by Scarpa et al., which found that inhibited children had a greater heart rate and skin conductance level in response to stress. Fowles, Kochanska and Murray [55] investigated the relationship between EDA and temperament in preschool children, finding that preschoolers with certain characters had greater EDA in response to stress. The results suggest that EDA may be a valuable measure for assessing individual differences in temperament.

Skin conductance is used to examine stress response in preterm infants during heel stick procedures, in article [56] by Storm. It was found that preterm infants significantly increased skin conductance during the procedure, indicating a stress response. Additionally, changes in skin conductance in full-term infants over the first year of life are investigated by Hernes et al. [57], suggesting that skin conductance changes during the first year of life and may be related to neurological maturation.

Further research has explored the feasibility of measuring infant skin conductance, with Ham and Tronick [58] presenting a procedure to that end, validating the use of a clap-induced startle. The study highlights the potential for assessing emotional states and reactivity in infants using skin conductance measurements.

An additional study by Ellaway et al. [59] investigates the relationship between sweat production and the Sympathetic Skin Response (SSR), suggesting that measuring both can provide a more accurate assessment of the ANS. Finally, Visnovcova et al. [60] highlights the utility of entropy-based measures of EDA as a method for detecting physiological

changes in sympathetic activity in the early postnatal days of healthy full-term newborns. The findings suggest that EDA analysis could offer a non-invasive means for early diagnosis, aiding in the timely identification of pathological conditions linked to autonomic dysregulation or dysmaturation during the neonatal phase. Overall, these studies provide insight into the potential applications of EDA in assessing emotional states and developmental maturation across different populations.

3.3 Previous work

This work builds on two previous dissertations, "Study of Electrodermal Activity in Babies subjected to Visual Stimuli" [19] and "Study of Visual Evoked Potentials in Babies" [20]. Both studies employed a checkerboard pattern-reversal visual stimulus, alternating every second for a total duration of 2 minutes, resulting in 120 stimuli.

In the first study [19], the primary objective was to explore the EDA signal's response in infants exposed to a visual stimulus. The study aimed to derive reference values for EDA signal parameters from distinct groups of participants, including full-term infants, preterm infants, and adults. Furthermore, the investigation aimed to examine potential connections between EDA values and participants' ages.

The analysis of various parameters, such as the number of responses, amplitude, area, latency time, and skin conductance level, was conducted among the three participant groups. Notably, preterm infants exhibited higher values in all parameters except the number of responses, compared to both full-term infants and adults.

While adults and children older than 12 months displayed an inverse relationship between age and stimulus reactivity, the findings were distinct for full-term and preterm infants. These groups exhibited a different trend, indicating higher stimulus reactivity as the age increases. This phenomenon could potentially be attributed to developmental factors. The study yielded unexpected results, revealing robust evidence of a direct response to the presented stimulus. Surprisingly, this response manifested approximately once per stimulus inversion, coinciding with a frequency of 1 Hz.

To achieve these results, the study required the synchronisation of the equipment *Biosignalsplux*®, *opensignals*® (EDA acquisition software), and *E-prime*® (software containing the visual stimuli), along with the connection between *E-prime*® and *g.Nautilus*® (records VEPs and trigger events) to obtain trigger-related information. The MATLAB code employed for processing and analysing the EDA signal in this study includes the following tools:

1. **Load and Read Data:** MATLAB is used to extract information from the raw signal, which is then downsampled to 100 Hz.

2. **Conversion and Noise Reduction:** The conversion formula from raw data to microsiemens (μS) is applied using Equation 2.3, with specified values for power

voltage (3 V) and resolution (16 bits), used for *Biosignalsplux*®. Subsequently, a moving average filter with a 50-point window is applied to reduce signal noise without compromising relevant information for analysis.

3. **Segmentation:** From *Opensignals*®, the two markers denoting the start and end of the stimulation period are extracted, while *g.Nautilus*® provides all 120 triggers that occur during the data collection. The MATLAB code generates an events file containing trigger information and a data file containing EDA information. The *Ledalab*® tool from MATLAB is employed to segment the signal with 120 markers.

4. **Parametrisation:** The Discrete Decomposition Analysis (DDA) function decomposes electrodermal responses into phasic and tonic components. Parameters $\tau 1$ and $\tau 2$, which minimise the discrepancy between the measured and reconstructed signal, are determined using the optimisation function in *Ledalab*®. Subsequently, the signal's parameters are extracted into an Excel file. The extraction encompasses responses commencing within 0.5 to 1 second after stimuli, featuring amplitudes surpassing 0.01 μS. This approach aids in capturing the response to a particular stimulus prior to the subsequent one.

The study conducted in [20] delved into the dynamics of VEPs within the premature infant population, specifically examining those at 4 and 6 months of corrected age, i.e., age adjusted to account for the duration of their prematurity [4]. Central to this investigation was an exploration of the responsiveness of these infants to visual stimuli, with a particular emphasis on understanding the impact of gestational age on the latency of the P100 component, an essential metric for assessing neural processing speed.

For preterms at four months of corrected age, the study revealed a more subtle correlation between gestational age and P100 latency, indicating a weaker relationship. However, in a bid to expand the scope of inquiry, the study encompassed full-term infants at 4 months, unravelling a consistent trend of diminished P100 latency with an augmentation in gestational weeks. Evidently, gestational age wielded influence over the developmental trajectory of premature infants, evoking divergent P100 latencies even at similar corrected ages.

An extension of the study encompassed premature twin siblings. A discernible disparity in developmental progression was noted among these twins at both 4 and 9 months of corrected age. This developmental incongruence could be attributed to the inherent variability often found within twin pairs, an element that resonated through the produced VEPs.

While adults exhibited consistent VEPs waveforms, indicative of mature neural pathways, premature infants presented markedly erratic waveforms, indicative of their ongoing neurological development. Remarkably, full-term infants at 4 months displayed P100 latencies more closely aligned with the anticipated norm of 100 ms, in contrast to the majority of premature. This reinforced the consistent pattern of delayed latencies in premature infants at various developmental milestones.

The findings revealed a significant correlation between gestational age and P100 latency, indicating that as the gestational age increases, the P100 latency tends to decrease. This highlights the importance of considering gestational age in visuomotor development therapies.

To conduct this study, it was necessary to synchronise *E-prime*® with *g.Nautilus*®. The MATLAB code utilised for processing the VEPs signal encompasses the following tools:

1. **Load and Read Data:** The files generated by *g.Nautilus*® are in `.hdf5` format. The hierarchical data structure and directories are determined using the `hdf5info` command, while the `hdf5read` command is employed to visualise the data, creating a matrix with each row containing information from one channel.

2. **Noise Reduction:** The DC (Direct Current) component is removed by subtracting the mean value from each signal to itself, centering the signals around zero, removing the offset. A Butterworth bandpass filter of $4^t h$ order with 2 Hz and 30 Hz cutoff frequencies is applied using the MATLAB Filter Designer tool. The filtfilt function is used to prevent phase shifts that could influence the P100 latency and affect the results.

3. **Segmentation and Average:** The signal is segmented into 120 segments, with each segment corresponding to a stimulus. Cuts are made 100 milliseconds before and 700 milliseconds after the precise stimulus moment to ensure the visibility of the entire evoked response. The segments are then averaged, and a Butterworth low-pass filter of $4^t h$ order with a cutoff frequency of 10 Hz is applied after this stage to reduce noise.

4. **Artefact Removal and parametrisation:** Signal artefacts are removed by discarding segments with a standard deviation 0.6 times greater than the entire signal's standard deviation. To analyse the signal, an interface is created using MATLAB's GUIDE tool, allowing for the identification of the P100 peak by comparison with a reference signal similar to the one shown in Figure 2.4.

In the same context, a pilot study [61] was developed to investigate the electrophysiological answer to a checkerboard stimulus. The experimental protocol involved two female preterm infants aged 4 and 6 months corrected age. Initial findings demonstrate that the P100 latencies and amplitude deviate from those observed in adults and older children. Notably, the older infant's outcomes more closely resemble those of adults, indicating a more developed visual system. The study also observed EDA, revealing that the older infant exhibited increased stimulus responses, higher skin conductance, and shorter latency compared to the younger infant. These trends align with nervous system maturation. Significant differences were discernible between premature infants with a 2-month age gap. Furthermore, the experiment highlighted that visual stimuli influence age-correlated visual and electrodermal responses, potentially enhancing developmental correlation analyses.

4

Materials and Methods

This chapter starts by providing an overview of the sample characteristics, detailing the test groups and outlining the inclusion and exclusion criteria. Subsequently, the materials employed in conducting this investigation are presented. The process for collecting data in the experiment is further explained. The signal processing tools are introduced, some of which have been adapted from prior studies due to their proven suitability, along with the modifications made to enhance outcomes. Furthermore, the Parametrisation section clarifies the specific parameters extracted from each signal and outlines the methodology employed for their extraction.

The procedures for the execution of this study were as follows:

1. Collection of VEPs and EDA from infants at 4, 6, 9 and 12 months.
2. Development of adequate signal processing code and visualisation platforms.
3. Processing, parametrisation and analysis of collected data.
4. Finding the relationship between the two signals and how they evolve with age.

4.1 Sample Characterisation

The present study analysed data from ten infants categorised into two groups: five full-term infants and five preterm infants. This same cohort underwent comprehensive evaluations at multiple time points, precisely at 4, 6, 9, and 12 months of age for full-term infants and corrected age for preterm ones, as shown in Figure 4.1. At 12 months the acquisition was recorded two times (Take 1 and Take 2) with a ten minute interval in between, approximately. Nevertheless, the current research exclusively focused on analysing data obtained from the initial and concluding assessments, which occurred at 4 and 12 months, respectively. The data collection was conducted by Dr. Ana Ferreira, and prior to the commencement of data collection necessary parental consent was diligently obtained.

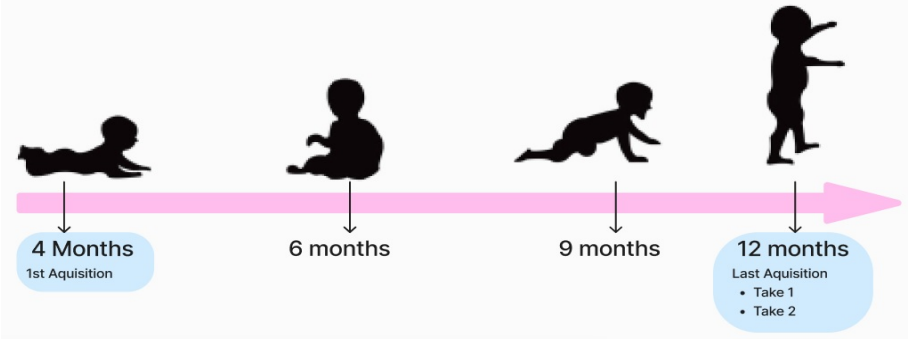

Figure 4.1: Schematic of the data acquisitions.

EDA and VEPs data were collected for full-term infants at Unidade de Saúde Familiar da Baixa (USF) and preterm infants at Maternidade Alfredo da Costa (MAC). The study sample comprised Group FT (5 full-term infants) and Group PT (5 preterm infants).

Inclusion criteria were specific: Group PT and Group FT included participants who were 4 months at the commencement of the study and remained enrolled until 12 months (corrected age for preterm), at which point the final data collection occurred. For Group FT, full-term status without dysfunction/pathology was required; Group PT included preterm infants without dysfunction/pathology.

Exclusion criteria were stringent. Data with technical glitches, connectivity issues between software, or behavioural incongruence were removed. These exclusions encompassed situations involving restlessness, electrode detachment, or the presence of noisy signals. Regarding the data acquired at 12 months of age, the exclusion criteria for selecting between Take 1 and Take 2 were as follows: the primary choice was Take 1, with Take 2 serving as a replacement option in cases where the behavioural analysis of the first take was suboptimal or when stimulus-associated patterns in VEPs were unidentifiable. The behavioural analysis of the subjects can be found in Appendix A.

4.2 Materials

This study integrates various equipment components. A computer system was utilised for the synchronisation of all equipment. The research required effective synchronisation of *Biosignalsplux*® and *opensignals*®, along with *E-prime*® and *g.Nautilus*® systems. To achieve this, a parallel port facilitated the connection between *g.Nautilus*® and *E-prime*®, while *Biosignalsplux*® and *E-prime*® were linked using a socket mechanism to capture stimulus-triggered events. Data processing and analysis were conducted using MATLAB®, and *Tableau*® software was used to obtain a descriptive analysis of the data. Some of the equipment can be found in Appendix B. A more detailed description of the aforementioned materials is given below.

Computer - Dell Computer (Intel ® Core (TN) 2DUO, 4,00 GB) where all equipment runs, that projects the image for a LG flatron W1934s;

***E-prime*® -** Software used to create visual stimuli. The stimulus is presented as a checkerboard pattern. The centre of the pattern features a red cross, which serves as a fixation point for the observer, as depicted in Figure 4.2.

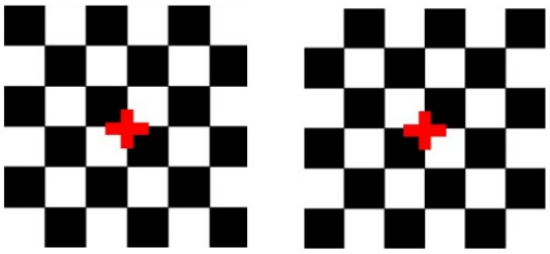

Figure 4.2: Pattern created using the Software E-Prime from [20].

***g.Nautilus*® -** It contains a cap with 32 electrodes (Serial number NB-2017.08.77), with software *g.Recorder*® (version 5.16.00) that records the VEPs signal. Specific wearable EEG headset for kids, which features its own integrated ground electrode (GND), near the F_Z location, within the electrode cap. We employed the O_Z, $P0_8$, $P0_7$, and C_Z electrodes, all functioning as active electrodes. However, we also incorporated an earlobe reference electrode as an inertial point [62].

***Biosignalsplux*® and EDA sensor -** Used to collect EDA data. The sensor is equipped with two channels that are connected to electrodes.

***Opensignals*® -** Software used to record EDA data.

MATLAB® - Programming software used for signal processing analysis.

***Tableau*® -** Software for Data Analysis.

It is worth noting that the ISCEV Guidelines, mentioned in Section 2.3.1, were designed for the standard adult population. Consequently, they may prove inadequate when applied to infants, particularly due to the evolving and small nature of their skull and brain geometries. These structures are not yet stabilised and are subject to rapid growth and change over few months, making electrode placement more challenging, specially considering that this study involves acquisitions from the same subject at 4, 6, 9 and 12 months of age. In pediatric VEPs recordings, to enhance cooperation, an infant may observe the stimulus while being held on a lap or placed over the shoulder [30, 34].

4.3 Experimental Protocol

During the initial phase of acquisition, which occurred at the age of 4 months, the parents were provided with a comprehensive document elucidating the study's objectives and a parental consent form. These documents are available in Appendix C.

1. **Parent Approval -** The experimental procedure is presented to the parents. They must approve and sign a permission document.

2. **Setup -** The infant is positioned on an adult's lap, with a monitor displayed at a distance of approximately 70 centimetres from the infant's face.

3. **Equipment Placement -** The EDA sensors are securely attached to the plantar surface of the right foot. The electrode cap is placed on the head, and the electrodes of interest are prepared to collect the signal. The gel is distributed over the electrodes.

4. **Acquisition Software initialisation -** *Opensignals*® is started and connected to *Biosignalsplux*®. *g.Nautilus*® Software is initialised and prepared to collect the data. Acquisition rates are selected (250 Hz for *g.Nautilus*® and 500 Hz for *opensignals*®).

5. **Signal Acquisition -** The recordings are started, and *E-prime*® displays the pattern. The colour of the squares (black and white) will alternate every second for a duration of 120 seconds (120 stimuli, each lasting 1 second).

6. **Acquisition Conclusion -** The programs are shut down, and the equipment is removed.

4.4 Signal Processing and Parametrisation

The signal processing code was developed by building upon the foundational work of preceding dissertations. These techniques are comprehensively elucidated in Section 3.3, encompassing the stages of Load and Read Data, Noise Reduction, Segmentation and Parameterisation of both signals. However, modifications were introduced to optimise signal reconstruction and visualisation while refining the outcomes. These modifications primarily encompassed alterations in the artefact removal technique and the enhancement of the GUIDE platform's capabilities in facilitating the analysis and parametrisation of VEPs signals. The modifications are further elucidated with images in Appendix D.

4.4.1 Artefact Removal in VEPs

Regarding artefact removal, a previous methodology (outlined in [20]) involved calculating the standard deviation of the complete EEG signal and subsequently excluding segments that surpassed a threshold of 0.6 times the calculated standard deviation. While this approach yielded satisfactory results for the sample used in the earlier study, it introduced certain limitations.

Calculating the standard deviation of the entire signal inherently included the artefacts embedded within it. Consequently, these artefacts significantly influenced and negatively impacted the resulting standard deviation value. This outcome was attributed to the fact that artefacts often possess magnitudes substantially more significant than those of the signal containing VEPs data. Moreover, the choice of 0.6 as the threshold for exclusion, constituting a relatively small fraction of the standard deviation, had unintended consequences. In scenarios with fewer artefacts and higher-quality signals, this threshold excluded a substantial portion of the signal with VEPs data, resulting in a notable loss of essential information. An example of this is demonstrated in Appendix D.

A new approach was adopted for artefact removal in response to these limitations. This new strategy involves directly selecting an interval from the preprocessed signal, characterised by its lack of offset and filtration treatment (explained in 3.3 Noise reduction for VEPs). This interval is chosen based on its observable minimal artefact presence. Subsequently, the standard deviation of this chosen interval is computed. Notably, this computation is executed in a manner that is more devoid of the pronounced negative impact of artefacts. In this updated methodology, signal segments where the signal exceeds 1.5 times the computed standard deviation are systematically identified and subsequently removed.

Adopting this new methodology for calculating the standard deviation effectively disentangles artefact influences and mitigates their negative repercussions. By eliminating the undue influence of artefacts, this approach offers a more accurate representation of the signal's underlying characteristics. Furthermore, introducing a new threshold mechanism ensures that only signal segments displaying substantial deviations from the computed standard deviation are excluded. This prevents the accidental removal of segments containing important VEPs information.

4.4.2 GUIDE platform for VEPs

The interface has been refined to incorporate four graphs. These graphs illustrate the signals emanating from the four active electrodes (O_Z, $P0_8$, $P0_7$, C_Z), each having undergone preprocessing (i.e., signals with no offset and filtered). A pivotal step in this process involves the selection of an interval for standard deviation calculation within the platform. Executing this interval selection before engaging upon other functionalities available through the interface is imperative.

A sequence of graphs is presented upon providing the desired filename and subsequently activating the "Save" function, as demonstrated in Figure 4.3. From these graphs, it is necessary to identify intervals exhibiting minimal artefact interference.

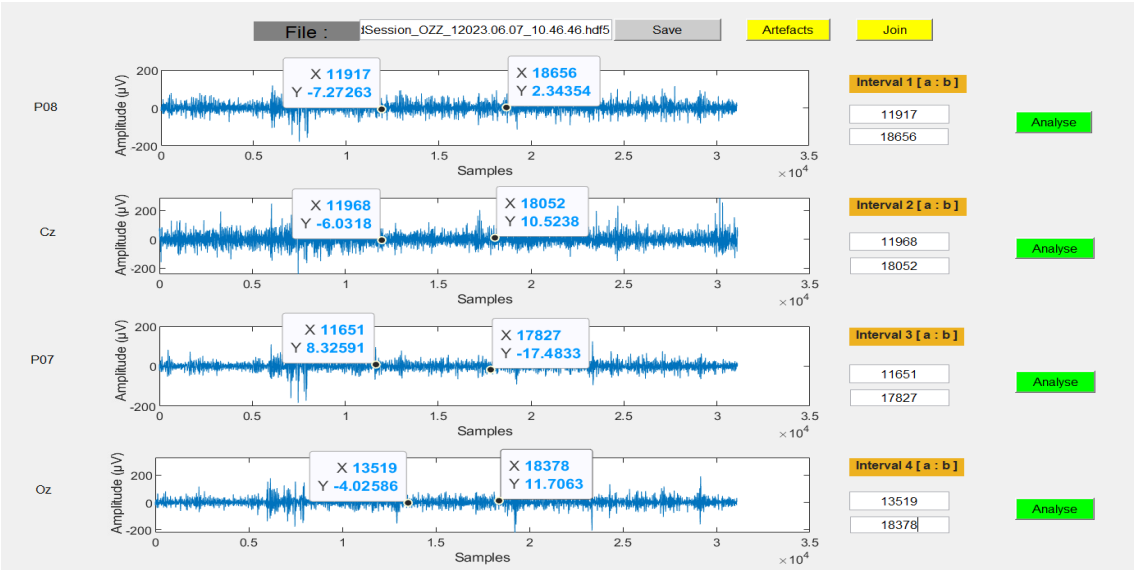

Figure 4.3: GUIDE platform cover.

Following the identification of artefact-lean intervals, it is necessary to duly record the interval values within designated variables labelled "a" and "b". This step makes engaging with the "Analyse" function aligned with the specific electrode possible. Activation of this function facilitates an in-depth exploration of the signal's attributes intrinsic to the selected electrode. Upon its activation, a new page unfolds, showcasing a set of 12 plots. The initial six plots visually represent the cumulative signal aggregated at intervals of every 20 stimuli. The final six plots offer insight into specific signal portions and each of these portions encapsulates information about a consecutive sequence of 20 stimuli, as depicted in Figure 4.4 a).

The analysis page has been enhanced by incorporating the "Mean" feature. Upon activation, this feature generates a page (Figure 4.4 b)) that visually presents the averaged signal, incorporating the chosen portions only (placed beside the "Mean" button). This functionality allows researchers to meticulously choose coherent segments that vividly showcase visual stimuli responses while efficiently disregarding components that lack significant information.

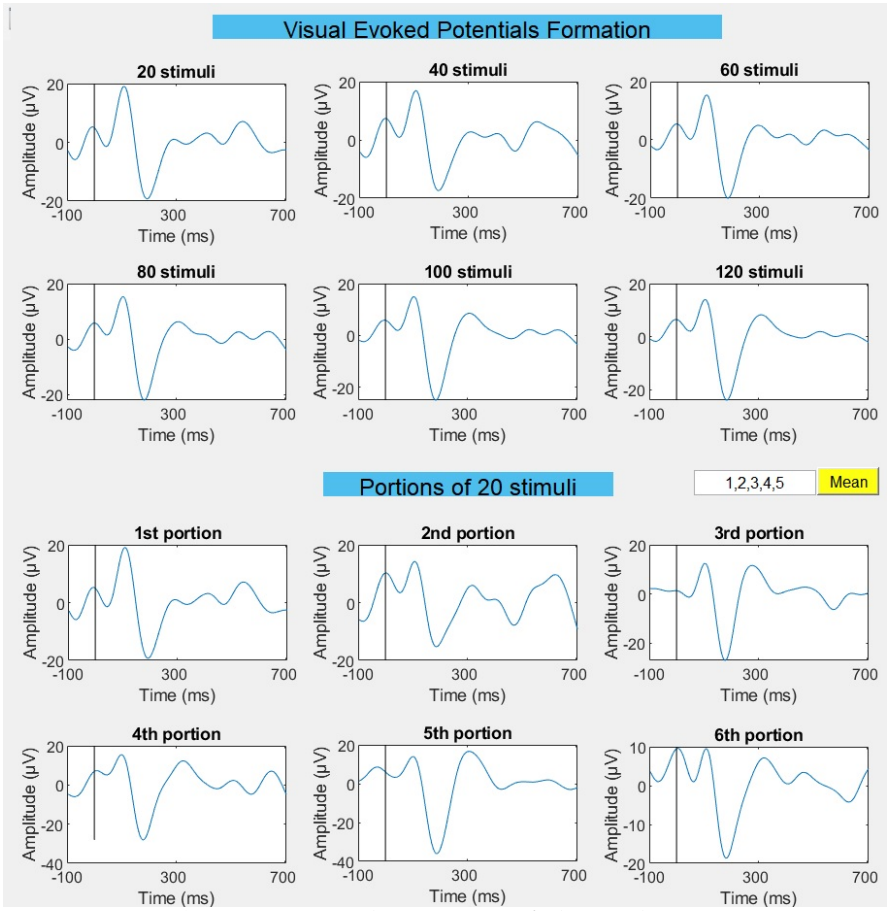

a) GUIDE "Analyse" page of electrode $P0_8$.

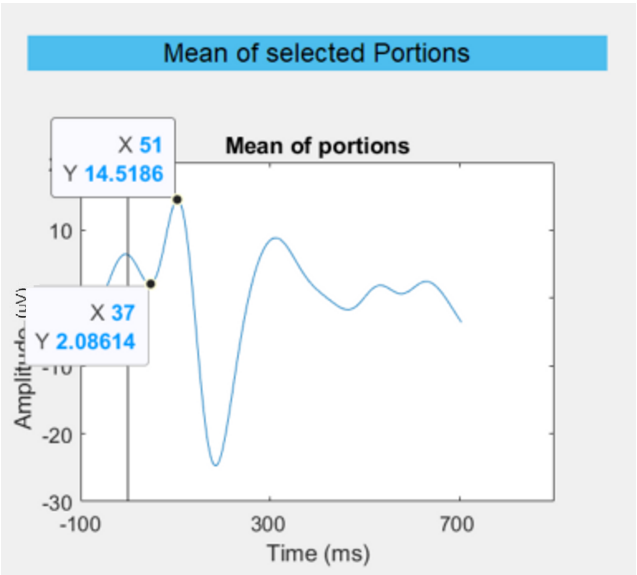

b) GUIDE "Mean of selected portions" page.

Figure 4.4: GUIDE platform "Analyse" and "Mean of selected portions" pages.

The validity of this method is highlighted by the lack of more productive alternatives available to date. Our approach retains segments of genuine relevance by excluding non-attentive portions from the two-minute data collection interval, thereby upholding the integrity of stimuli related signal representation. However, selecting a minimum of three segments out of the six available is essential to prevent undue reliance on a restricted data set that could disproportionately influence the outcomes.

When identifying specific parameters in VEPs in infants, limitations arise that are not present when collecting data from adults who are given explicit instructions to maintain focus. This is because factors such as sleep, hunger, and infants' natural tendency to explore can affect the study. Assuring consistent attentiveness during the two-minute data acquisition proves notably challenging. The selection of "optimal" portions endeavours to

alleviate the limitations arising from the intrinsic inability of infants to sustain attention.

4.4.3 Parametrisation

Within Appendix E, a comprehensive description of the parametrization process is provided. In the context of evoked potentials, an in-depth analysis was conducted on each of the four distinct electrodes (O_Z, $P0_8$, $P0_7$, and C_Z). This analysis was carried out using the platform detailed in Section 4.4.2 for both the initial and final acquisition files.

Following a rigorous examination in the "Analyse" page and obtaining the final signal in the "Mean of selected portions" page, the significant N75 and P100 peaks were identified meticulously. This identification process involved comparing the acquired signals with reference VEPs signals, such as the one depicted in Figure 2.4. The latencies extracted from the graphical representations are initially presented in terms of the number of samples denoted as X, as illustrated in Figure 4.4 b). Given an acquisition rate of 250 samples per second, the conversion from sample count X to milliseconds is calculated using Equation 4.1:

$$\text{Time [ms]} = \frac{X \times 1000}{250} \tag{4.1}$$

Given that the graphical representation encompasses a span of 100 milliseconds before and 700 milliseconds after the precise stimulus onset, ensuring comprehensive visualisation of the entire evoked response and the activity before stimuli (as depicted in Figure 4.4 b)), an adjustment is necessary to align the conversion Equation 4.1 to the exact stimulus application moment (Time [ms] = 0) for accurate latency calculation. Thus, to convert the sample information to milliseconds, Equation 4.2 is employed:

$$\text{Latency [ms]} = \frac{(X - 25) \times 1000}{250} \tag{4.2}$$

Any electrodes without VEPs patterns were carefully excluded from further analysis. To simplify the assessment, only two parameters - N75 latency and P100 latency (for each evaluation, at 4 and 12 months) - were calculated by averaging the peak latencies across the remaining electrodes that were not excluded, obtaining a table similar to E.2.

There are several reasons for excluding specific electrodes from the analysis. One such reason is when electrodes experience short circuits due to inconsistencies in the gel. Given the small size of the infant's head and the proximity of certain electrode placements, the gel applied for one electrode can inadvertently connect with the gel of another electrode placement. This situation can result in electrodes displaying results that combine data from multiple electrode locations, potentially offering valuable insights for identifying peak phenomena or, conversely, introducing distortions that render the data unusable [16]. Moreover, the C_Z electrode is inherently marked by distinct limitations, primarily stemming from its heightened vulnerability to the geometrical intricacies of the infant's skull and cerebral architecture. Furthermore, the susceptibility of the C_Z electrode to perturbations induced by ocular movements and the mechanical ramifications ensuing from the infant's interactions with a pacifier accentuate its limitations [63].

For the EDA data, the initial step involved uploading the *opensignals*® and triggers data to the *Ledalab*® software, resulting in the creation of a *.mat* file for both the initial and final acquisitions. Subsequent to performing the Discrete Decomposition Analysis (DDA), a *.mat* file similar to the one depicted in Figure 4.5 was obtained.

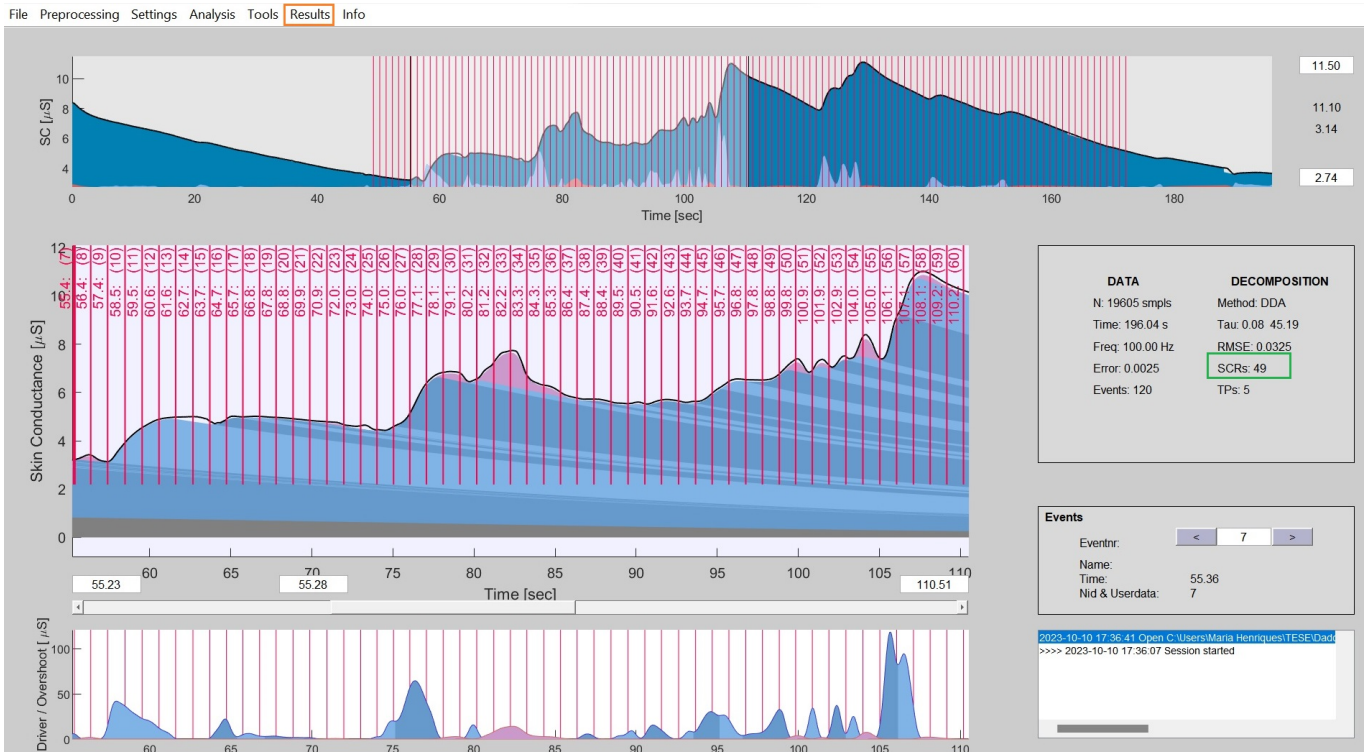

Figure 4.5: Ledalab® software after DDA process. The top graphic shows the complete EDA signal, the middle one displays the tonic component, and the bottom one exhibits the phasic component. The red lines represent the triggers. "Results" menu and SCRs are highlighted in orange and green, respectively.

To extract parameters into an Excel spreadsheet, we followed these steps: In the "Results" menu of the *Ledalab*® software, we selected a response window ranging from 0.5 to 1.4 seconds with a 0.01 microsiemens amplitude, i.e., threshold value for SCR detection. This allowed us to collect data from each stimulus without overlap with information from the next or previous one. Next, we computed the SCRs and Power metrics.

The first parameter, SCRs, corresponds to the sum of skin conductance responses recorded during the entire data collection period and is directly obtained from the *Ledalab*® platform, highlighted in green in Figure 4.5. The second parameter involves calculating the average of values in the "Global.Mean [µS]" column, which includes the mean skin conductance values within the selected response window, as seen in Table E.3.

4.5 Data Analysis

In the present work, examinations were undertaken to validate the appropriateness of the processing tools developed throughout the dissertation for the examination of EDA and VEPs signals in infants aged 4 to 12 months, both full-term and preterm. This descriptive data analysis was executed with the *Tableau*® software.

5

Results

In this chapter, we present the findings derived from the analysis of VEPs and EDA signals acquired from the sample characterised in Section 4.1. Due to the small sample sizes and significant diversity between cases, especially within the preterm group, a comprehensive statistical analysis is not feasible. Therefore, we have chosen to conduct a case-by-case study to explore how the methods presented enable the visualisation of various scenarios and behaviours. The dataset used to obtain these results can be found in Appendix F.

The first section of this chapter is dedicated to the individual analysis of VEPs parameters, including both the N75 and P100 latencies. Subsequently, we provide a comprehensive overview of these parameters, their temporal evolution, and comparisons across the FT and PT study Groups. The second section delves into an analysis of EDA parameters, with a specific focus on SCRs and Power. This analysis involves an assessment of the temporal dynamics of each parameter for each subject. In the final part of this chapter, we explore the potential correlations between EDA and VEPs, observing the transformations that occur during the developmental journey of the individuals under investigation, from 4 months to 12 months.

Our primary objective in presenting these results is to demonstrate the effectiveness of the developed processing code and tools in achieving the goals outlined in this thesis.

5.1 Visual Evoked Potentials Analysis

The values obtained for the N75 and P100 latency parameters can be found below, in Figure 5.1 and Figure 5.2, respectively.

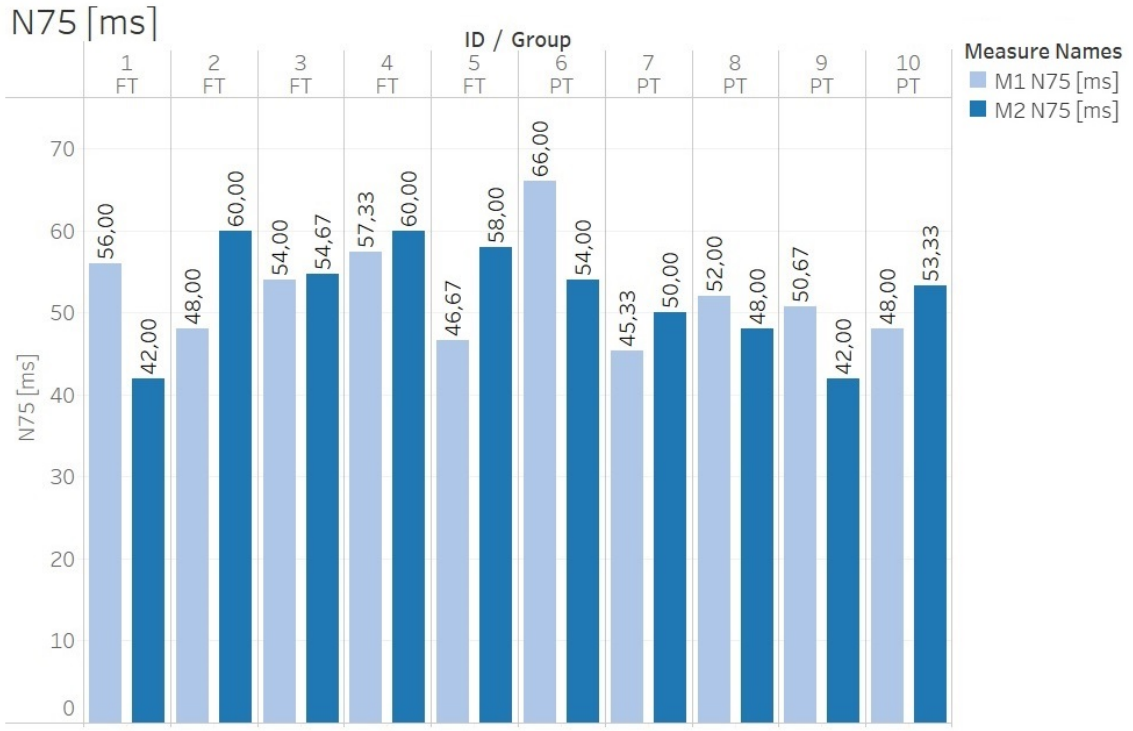

Figure 5.1: N75 Latency Parameter values for Individual Subjects in FT and PT Groups at 4 Months (M1) and 12 Months (M2).

In Figure 5.1, we observe the progression of the N75 parameter for individual subjects within each study group (FT and PT). It is evident that, in some cases, the N75 value shows an upward trend, and that in others, exhibits a contrary pattern where the N75 parameter decreases over time. It is essential to mention that during the evaluation of VEPs, the presence of the N75 component appeared inconsistent at times. This inconsistency may be attributed to the developmental stage of the subjects, as some infants might not have developed this particular marker yet, which means the parameter may be less reliable in some instances.

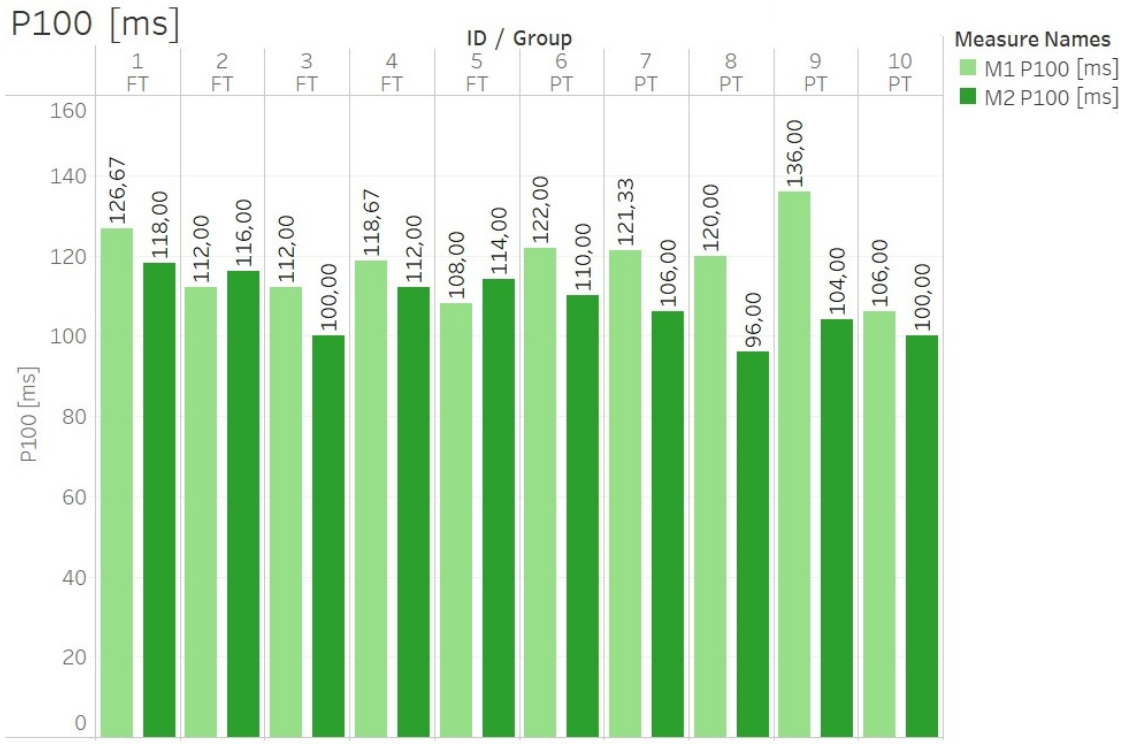

Figure 5.2: P100 Parameter values for Individual Subjects in FT and PT Groups at 4 Months (M1) and 12 Months (M2).

In Figure 5.2, we can observe the developmental trajectory of the P100 parameter among individual subjects in both the FT and PT study Groups. For subjects 1, 3, 4, 6, 7, 8, 9, and 10, the P100 latency value decreases from 4 months to 12 months of age, converging to approximately 100 milliseconds. However, infants 2 and 5 display an increase in the P100 parameter at the 12-month mark. Nevertheless, it's crucial to highlight that the disparity between the 4-month and 12-month measurements in these cases is not significant, only a few milliseconds apart, and remains close to the 100 milliseconds threshold.

In Figure 5.3, we can see the mean values of N75 and P100 latencies at 4 months (M1) and 12 months (M2) of age for both Group FT and Group PT.

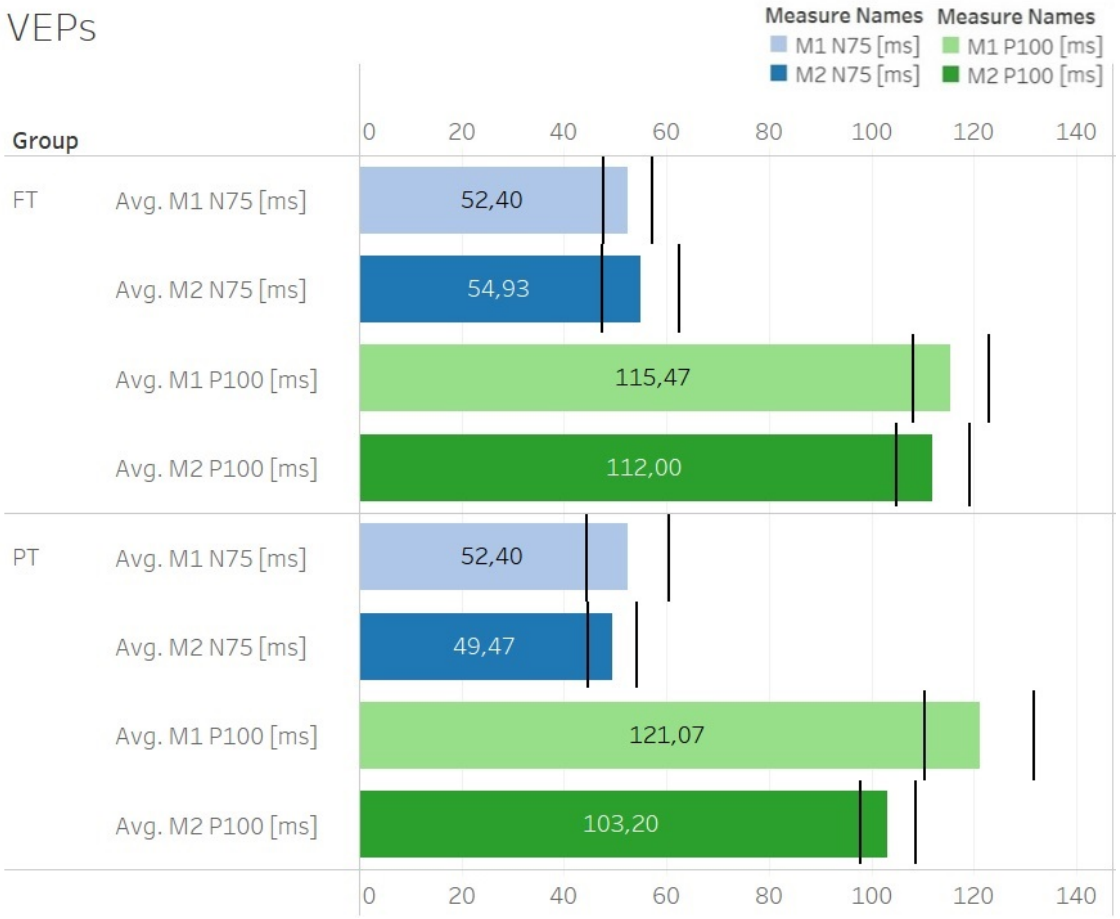

Figure 5.3: N75 and P100 Parameter mean values for FT and PT Groups at 4 Months (M1) and 12 Months (M2).

Regarding the N75 latency, within the FT Group, there is an observed increase in the mean value from 4 to 12 months, while within the PT Group a decrease is evident, albeit with substantial standard deviation error bars. It is important to note that these groups represent a small sample size, which may contribute to the variability observed in the data. Conversely, for the mean P100 latency, the FT and PT Groups tend to decrease from 4 to 12 months, converging closer to the 100 milliseconds mark. It is particularly noteworthy that the PT Group, in the majority of cases, seems to show a more pronounced evolution in the P100 parameter.

5.2 Electrodermal Activity Analysis

Similarly to the previous section, the data on the quantification of SCRs and EDA Power parameters are presented in Figure 5.4 and Figure 5.6, respectively.

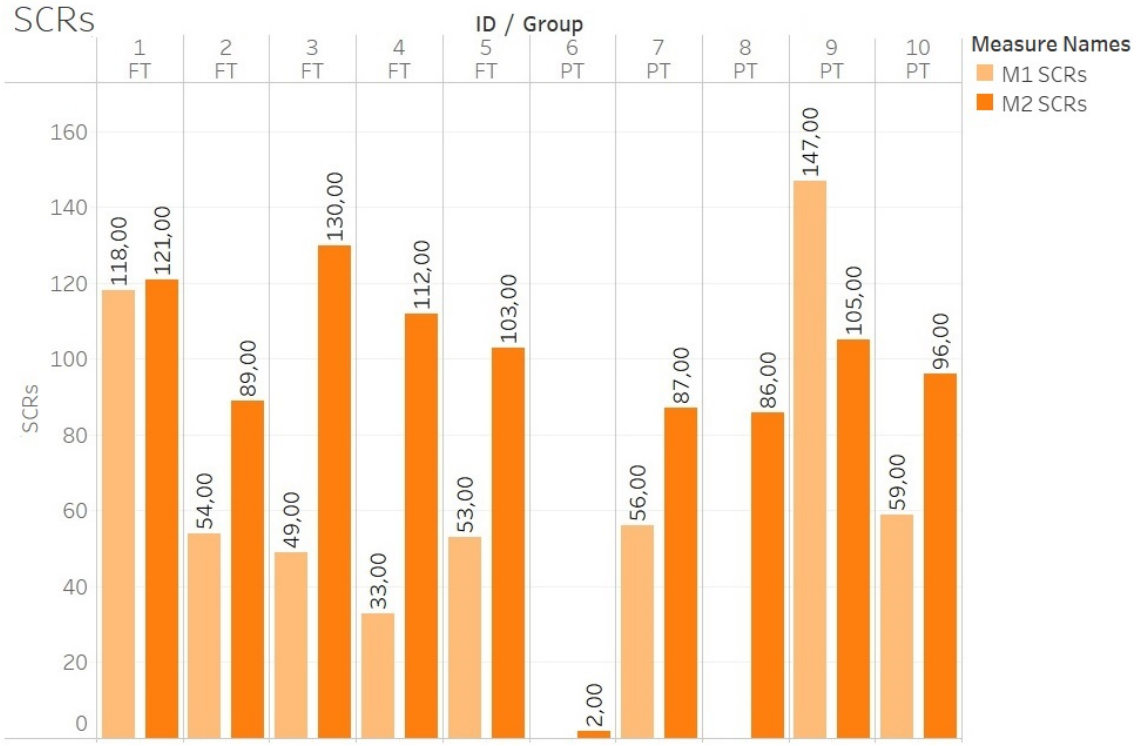

Figure 5.4: SCRs Parameter values for Individual Subjects in FT and PT Groups at 4 Months (M1) and 12 Months (M2).

Figure 5.4 illustrates that for subjects 1, 2, 3, 4, 5, 7 and 10 the SCRs exhibits a higher count at the 12-month mark (M2) compared to the 4-month measurement (M1). In subject 1 the increase is not very significant.

An exception is observed in the case of subject 9, where the SCRs exhibit a decrease with age. However, it is noteworthy that at the 12-month mark, subject 9's SCRs value aligns more closely with the values observed in the rest of the study group. A more comprehensive analysis of the EDA signal of subject 9 at 4 months is presented in Figure 5.5. In this analysis, it is evident that in certain segments, the infant's SCR demonstrates rhythmicity, synchronizing with the moments of stimulus presentation, particularly in the 30 to 58 seconds interval. Nonetheless, in other segments, such as from 97 to 148 seconds, increased agitation is apparent. The signal exhibits higher amplitude, and some of the peaks appear non-coincident with the trigger, indicating that factors beyond the visual pattern may be contributing to the infant's stimulation.

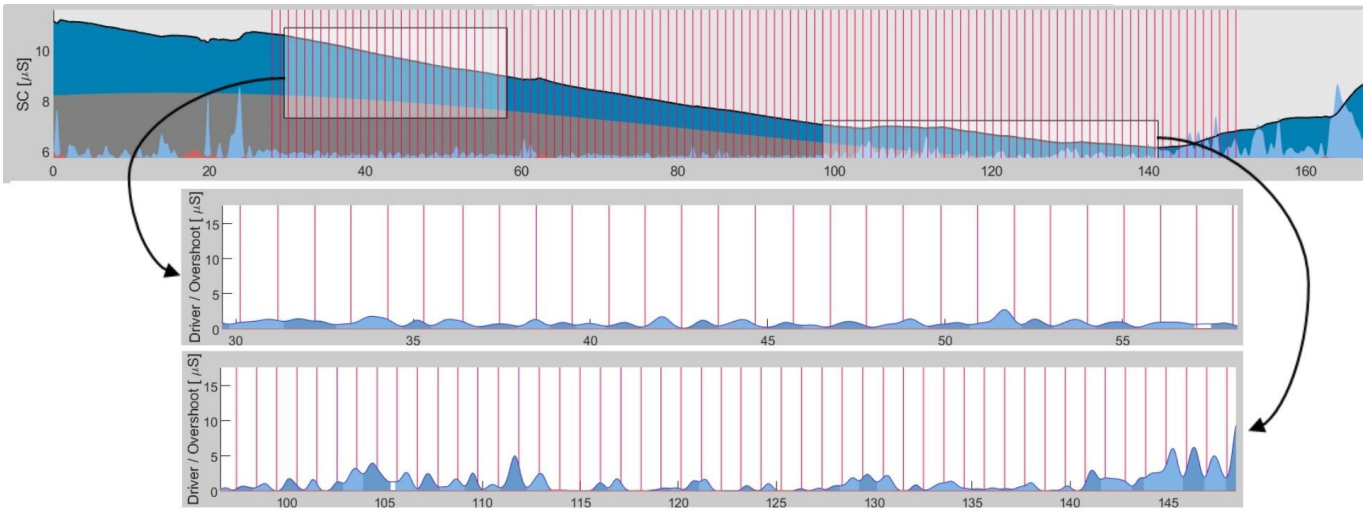

Figure 5.5: EDA signal for subject ID 9 at 4 months. The first graphic is the entire EDA signal, the middle one is the phasic component from 30 to 58 seconds, and the bottom graphic is the phasic component from 97 to 148 seconds.

Regarding subjects 6 and 8 from the PT Group, it is noteworthy that neither of them displayed any SCRs during the 4-month assessment. This absence of response can be attributed to the saturation of the EDA signal. This phenomenon of saturation in premature infants is linked to their underdeveloped and delicate skin, as elucidated in Subsection 2.4.1. The unique characteristics of their skin negatively impact electrical conductivity. Additionally, their inherently thin skin, as discussed earlier, leads to an increased release of moisture, resulting in the saturation of EDA signals [39]. Upon reaching 12 months of age, these infants' skin is typically more mature, which is associated with distinct SCRs outcomes compared to the saturation observed at 4 months. Subject 8 shows clear improvement in this regard at 12 months, showing results similar to the other subject at that age, whereas subject 6 does not demonstrate a significant change in their SCRs.

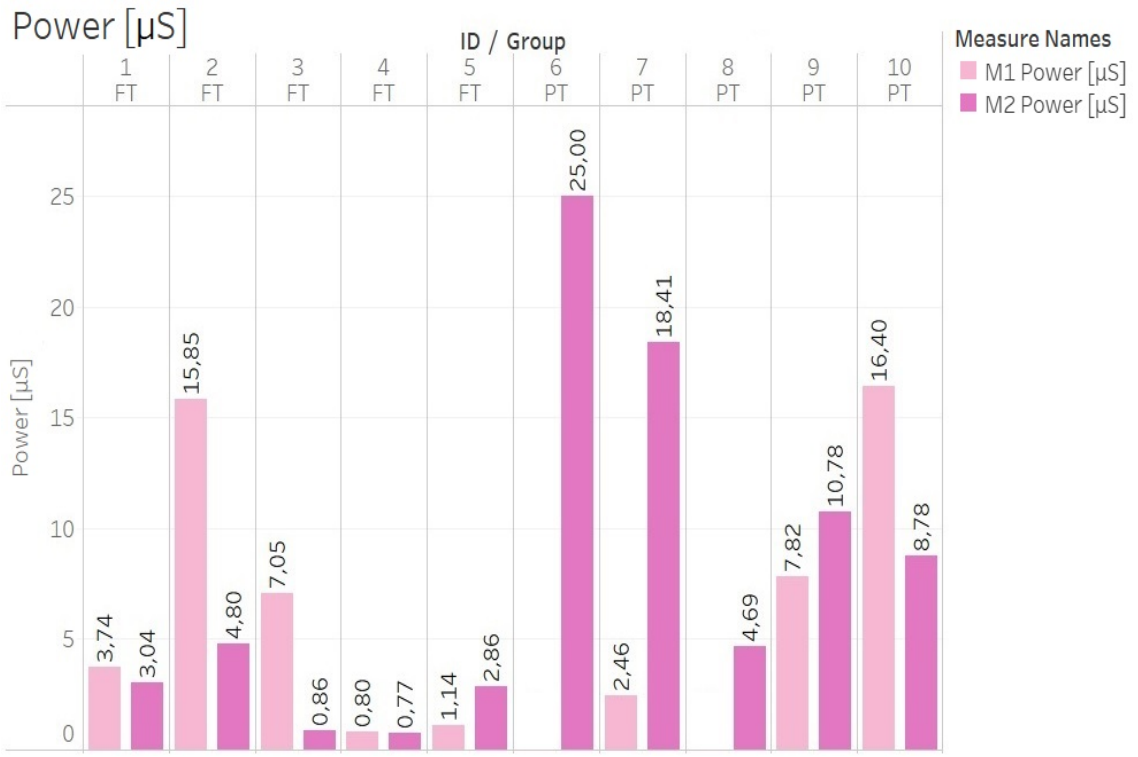

Figure 5.6: EDA Power Parameter values for Individual Subjects in FT and PT Groups at 4 Months (M1) and 12 Months (M2).

The EDA Power values for each infant are visualised in Figure 5.6. Subjects 1, 2, 3, and 10 display a reduction in EDA Power values from 4 to 12 months, with the decrease being relatively minor for subject 1. Notably, subjects 2 and 10 exhibit significantly higher values at 4 months compared to the other individuals. Subject 4 also experiences a decrease, although it is minimal, resulting in a nearly consistent value.

Conversely, subjects 5, 7, and 9 demonstrate an increase in EDA Power values, with subjects 7 and 9 displaying considerably higher values than subject 5.

Subjects 6 and 8 only have results available for 12 months (due to signal saturation at 4 months). Subject 6 exhibits an exceptionally high EDA Power value, while subject 8 appears to have a value more in line with the rest of the subjects.

5.3 Relation Between VEPs and EDA

The subsequent Figures 5.7 a), b) and c) present scatterplots illustrating the correlation between the SCRs and the P100 latency value. Each dot represents an individual in these plots, with blue dots referring FT Group and yellow dots to PT Group. Initially, in a), this correlation is depicted for the M1 moment, denoting 4 months of age. Subsequently, in b), the same correlation is displayed for the M2 moment, corresponding to 12 months of age. Lastly, in c), a consolidated graph integrates both temporal instances, M1 and M2, allowing observing the developmental trajectory of each individual concerning these parameters over time.

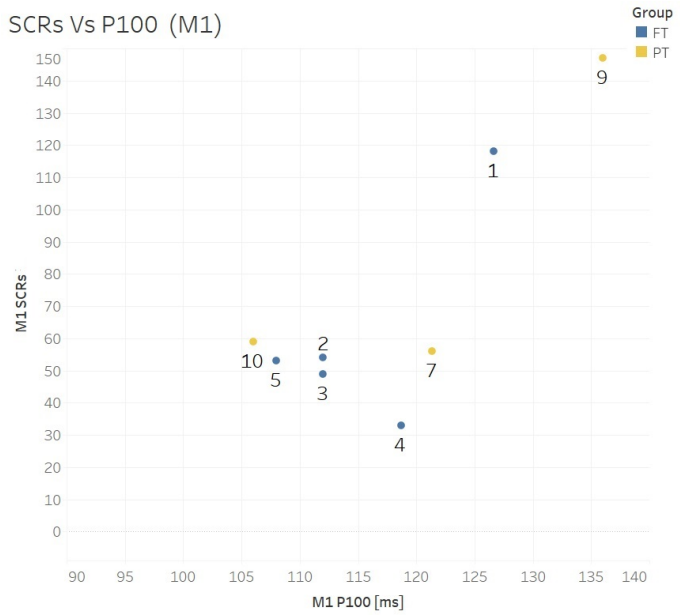

a) SCRs Vs. P100 at 4 months of age (M1).

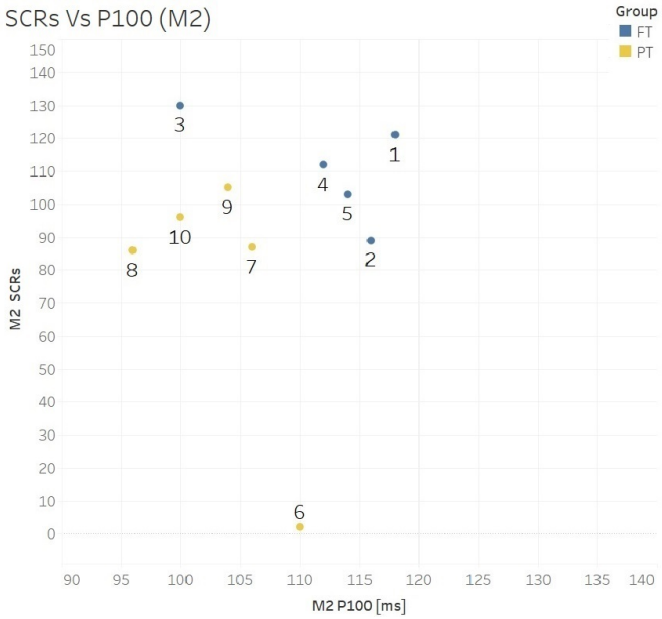

b) SCRs Vs. P100 at 12 months of age (M2).

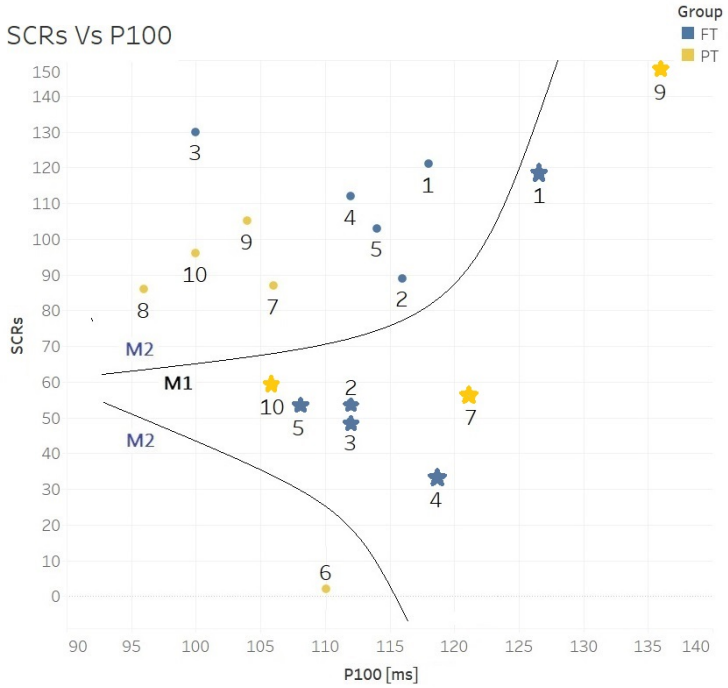

c) SCRs Vs. P100 at 4 months of age (M1), represented by star shapes and 12 months of age (M2) represented by dot shapes.

Figure 5.7: Evolution of the relation between SCRs and P100 latency for each subject. Preterm group represented in yellow and Full term group represented in blue.

In Figure 5.7 a), when examining the data at 4 months of age, individuals are primarily clustered in the lower-middle section of the graph. This clustering signifies lower SCR values and higher P100 values. Moving to Figure 5.7 b), a shift is observed, with individuals now positioned in the upper part of the graph, featuring higher SCR values. Along the P100 axis, they seem to centre around the 100-millisecond mark. Figure 5.7 c) combines both time points into a single graph. It becomes evident that individuals typically transition

from the lower-middle region to the upper-left area. This shift is associated with a broader dispersion of data points along the P100 axis, although concentrated around 100 milliseconds.

At the 12-month time point, it is noticeable that the yellow data points representing the PT Group form a tight cluster and occupy a distinct region from the blue data points of the FT Group. However, it is important to acknowledge that the sample sizes are relatively small, and the values are not significantly separated to conclusively assert that they belong to entirely distinct clusters.

During the M1 moment, it is noteworthy that individuals 1 and 9 emerge as potential outliers, characterised by higher P100 latencies and SCRs values. At the M2 moment, individual 6 stands out as an outlier, consistently maintaining a low value of SCRs.

In Figure 5.8, equivalent scatterplots have been produced, examining the associations between EDA Power and P100 latency.

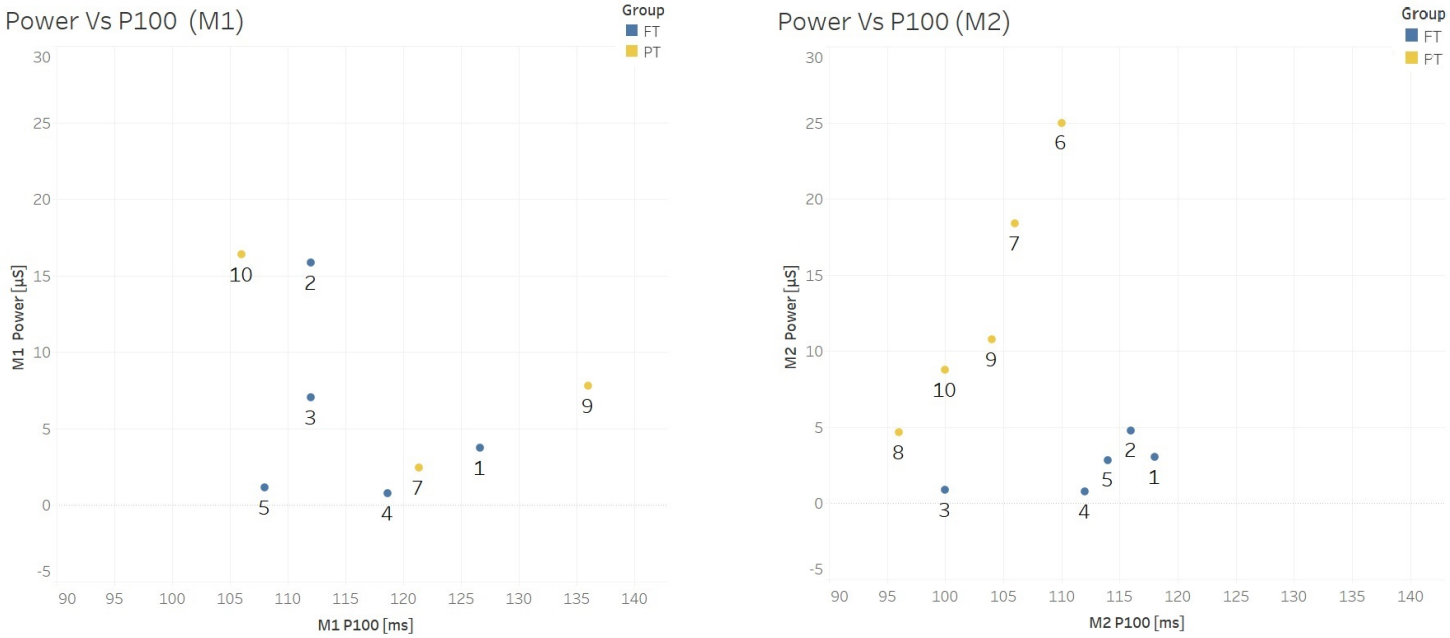

a) EDA Power Vs. P100 for each subject at 4 months (M1). b) EDA Power Vs. P100 for each subject at 12 months (M2).

Figure 5.8: Evolution of the relation between EDA Power and P100 latency for each subject at 4 months (M1) and 12 months (M2) of age.

In Figure 5.8 a), it becomes evident that the blue and yellow data points, denoting the FT and PT Groups, respectively, display a higher degree of dispersion. Notably, the groups show less consistent EDA Power values at moment M1.

Conversely, an opposite pattern is discernible in Figure 5.8 b). The blue data points representing the FT Group exhibit a more concentrated distribution, especially within the 0 to 5 microsiemens range of EDA Power. In contrast, the yellow data points of the PT Group display a higher degree of dispersion in the graphic, predominantly occupying the upper and left regions of the graph. This dispersion is characterised by varying EDA Power levels and P100 values closer to 100 milliseconds.

6

Discussion and Conclusions

In this concluding chapter of the dissertation, we conduct a meticulous review of the objectives, accomplishments, and pivotal milestones achieved. We synthesize the work done throughout the study, emphasizing the results and insights that have emerged during our research journey. We also engage in a thorough discussion of the results. Furthermore, we rigorously examine the limitations encountered, elucidating the specific boundaries within which our research was conducted. We reflect on the contributions made to the field and explore potential avenues for future research.

The primary objective of this exploratory work was to establish a relationship between EDA signals and VEPs, with the aim of enhancing the analysis and understanding of the development and evolution of the neurovisual system in full-term and preterm infants.

The objectives outlined in Section 1.2 have been successfully accomplished through a systematic series of tasks. While the normative base has been initiated, it is still in the process of development.

- First, we conducted simultaneous data collection of EDA and VEPs signals from infants at various developmental stages, including 4, 6, 9 and 12 months of age.
- Second, we focused on refining our signal processing tools and analytical platforms. This involved the implementation of new methods for effectively removing artifacts from VEPs signals and the development of a more selective platform tailored for analysing specific signal portions of interest.
- Third, we meticulously parameterised the acquired signals, carefully examining the data to identify components directly related to responses to visual stimuli while excluding irrelevant information.
- Lastly, through comprehensive descriptive data analysis, we validated the suitability of our chosen methods for signal analysis in very young individuals and established relationships between these signals. These cumulative efforts collectively contributed to the successful realization of our objectives in this exploratory study.

The existing literature on this topic is significantly limited. Existing studies have highlighted the usefulness of EDA in assessing emotions and stimulus responses in both children and adults, while VEPs have been effective in evaluating visual development in children. However, none of these studies have explored the relationship between these two domains in infants at such an early age, as far as we are aware. This deficiency in research hinders our understanding of the intricate nuances within their evolving neurovisual systems and our ability to effectively assess and diagnose potential complications or irregularities in this regard.

6.1 Discussion

In the research that precedes this dissertation, there are a series of challenges and limitations that were now confronted and successfully overcome. Notably, collaborative endeavors with parents and institutions facilitated the expansion of our subject pool, thereby enhancing the diversity and richness of our dataset. Furthermore, data acquisitions were conducted at multiple time points, including 4, 6, 9, and 12 months, for the same infants, affording a more comprehensive perspective on their developmental trajectories.

The protocols underwent a refinement process, leading to increased efficiency and improved reliability of our findings. The introduction of new tools, presented in Section 4.4, enabled the precise elimination of segments lacking stimuli related information, thereby maximizing the utilization of portions containing VEPs patterns. This improvement addressed several inherent limitations in our study, which will be discussed in detail in Section 6.2.

In the results analysis, we exclusively employed data from the assessments at 4 and 12 months. The study sample consisted of a total of 10 individuals, comprising 5 full-term infants constituting the FT Group and 5 preterm infants constituting the PT Group. Each parameter underwent individual evaluation for every subject, enabling the observation of their respective developmental progressions from 4 to 12 months. Additionally, we conducted a comparative analysis between the preterm and full-term infants, calculating the means of these parameters within each group and at both time points. This allowed us to assess whether the parameters evolved similarly across the different cohorts. Lastly, our investigation concentrated on identifying correlations between parameters of different signals through the creation of graphs illustrating the dispersion of individuals' EDA parameters concerning P100 latencies. The following results were obtained:

- **Parameter Temporal Analysis**

  A comparative analysis conducted at two specific temporal points, namely 4 and 12 months, for each parameter. P100 latencies mostly reduced or in some cases mantained. This observed pattern seamlessly aligns with the developmental and maturation processes inherent in the neurovisual systems of children, facilitating faster responses to stimuli [61]. Additionally, the results raise questions about the reliability of N75 as a parameter, as it may not be consistently present in some infants. Although the N75-P100 complex in VEPs represents the initial peaks to emerge in children, it is essential to recognize the substantial subjectivity in infant maturity. The methods presented may encounter challenges in detecting the N75 peak at such a young age, while the P100, with its higher amplitude, proves to be more easily detectable [16, 30, 34].

  Regarding the SCRs parameter, there were subjects where the values increased from 4 to 12 months, others where it decreased. More thorough analysis of the EDA signal enabled to see that some of the responses were probably affected by

confounding stimuli. Instances of saturation were also observed in the PT Group at 4 months. With additional data corroborating this occurence, it could potentially represent an intriguing characteristic in some extremely premature infants. Despite the presence of these saturation cases, the method appears to remain valid given that, at 12 months, the data aligns with the pattern observed in the rest of the group for in some cases, suggesting the possibility of a maturation recovery in these individuals [39]. With forthcoming analyses, including the 6 and 9 month age marks, it may become feasible to pinpoint the stage at which this saturation, resulting from skin immaturity, diminishes.

In the case of certain infants, mostly within the FT Group, a notable decline in the EDA Power value was observed from 4 to 12 months, while their SCRs increased. This observation aligns with a previous study conducted by Andrade [19], which reported an inverse correlation between stimulus reactivity and age in children older than 12 months. A plausible explanation for this phenomenon can be attributed to the limited capacity of these infants to respond to stimuli at 4 months, as their physiological systems may be primarily engaged in the intricate process of brain maturation. However, by the time they reach 12 months, their responses to stimuli become more pronounced and are channeled in a more focused and attentive manner, resulting in reduced EDA Power values.

Conversely, some infants exhibited an increase in SCRs and EDA Power values with age. Furthermore, Ferreira [61] reported similar findings in a study involving preterm infants with a two-month age gap. In such cases, the explanation could lie in their heightened reactivity to stimuli, coupled with a potentially underdeveloped ability to concentrate on the stimulus, as their cognitive systems are still actively engaged in the maturation process.

The existing literature lacks a comprehensive explanation for these results. However, a study by Visnovcova et al. [60] sheds light on the changes in the ANS during the early postnatal period. This research highlights substantial shifts in the sympathetic branch, reflected in EDA parameters, suggesting that a decrease in EDA Power potentially indicates diminished sympathetic activity, possibly associated with maturation in neural pathways and increased regulatory complexity, including a transition from sympathetic to parasympathetic dominance. Thus, the declining EDA Power with age can signify neurovisual system maturation, reinforcing our findings.

It is noteworthy that discernible differences emerge between measurements taken with an 8-month age gap (from 4 to 12 months). These distinctions can be indicative that age has an influence in the response to visual stimuli in both signals, which is consistent with the findings in [20] and supported by the literature in [46]. However, it is crucial to acknowledge that a larger sample size is necessary to employ statistical methods that can yield more significant findings.

- **Group Evolution Differences**

  Due to the VEPs being a more robust and extensively studied signal, it was possible to compare the developmental differences between the two study groups. In contrast, the EDA signal, being less well-studied, more sensitive to external factors and having encountered more issues, presented certain challenges. A smaller number of subjects was available for analysis due to signal saturation at 4 months, and the cases within the dataset were highly diverse. Given the substantial variability among these cases, it is challenging to establish a clear trend with certainty.

  In our examination of VEPs, between the two study groups, FT and PT, we obtained insights into their developmental trajectories and responses to stimuli. Specifically, both FT and PT infants exhibited a significant trend wherein P100 latencies tended to decrease with age. However, it is crucial to acknowledge the presence of diverse cases within the PT Group. The similar maturation pattern observed in the VEPs for both PT and FT Groups is consistent with the findings reported in previous studies, such as [45] and [49]. Additionally, a more pronounced developmental progression from 4 to 12 months was observed in the PT Group, which aligns with the suggested findings in [45] and [47].

- **Relationship Between EDA and VEPs**

  This investigation has established a compelling relationship between EDA and VEPs, potentially allowing for the differentiation of study groups based on their physiological responses. When examining the correlation between SCRs and P100 latency, a notable transition was observed in individuals' positions from the lower-middle region in the 4-month data to the upper-left area in the 12-month data. This transition was accompanied by higher SCRs and a wider dispersion of data points along the P100 axis while revolving around the 100 milliseconds, indicating increased variability in their responses to visual stimuli over time. At 12 months, the data points representing the PT Group seem to exhibit a distinct spatial distribution from those of the FT Group. This distinction suggests differences in the developmental trajectories of these two groups in response to visual stimuli.

  In terms of the relationship between EDA Power and P100 latency, our findings revealed dynamic changes in this association during the first year of life. Full-Term infants appeared to converge more densely by the age of 12 months, particularly within the range of 0 to 5 microsiemens of EDA Power. This concentration suggests that Full-Term infants exhibited a more consistent and limited range of EDA Power values and P100 latencies as they developed. In contrast, the PT Group showed a shift towards more dispersed data at 12 months, indicating increased variability in neural responses to visual stimuli.

  These results align with the literature, which suggests that infants follow varying rates of growth, with some adhering to a more typical developmental trajectory and

others progressing more slowly [16, 34]. The consistency of our findings with the literature suggests that our data analysis and treatment methods are appropriate. With a larger sample size, we hope to further explore and identify developmental trajectories.

These observations emphasize the significance of including EDA Power, SCRs, and P100 latencies in the examination of EDA and their correlation with VEPs in infants. Together, these parameters could offer valuable insights into the neurophysiological responses of infants to visual stimuli.

Exploring the relationship between VEPs and EDA parameters enables simultaneous analysis of both signals and presents a promising avenue for distinguishing individuals within the FT and PT Groups, especially as a more extensive dataset becomes accessible. This approach also facilitates the assessment of group behaviour at different temporal points, specifically 4 months (M1) and 12 months (M2).

6.2 Limitations

The study encountered several limitations related to equipment and data acquisition, data analysis, and interpretation of results.

6.2.1 Equipment and Data Acquisition

In our pursuit of assembling a comprehensive dataset spanning the ages of 4 to 12 months, we encountered notable challenges arising from the relatively limited number of infants who had completed the entire data collection protocol. This extended period of data acquisition, encompassing multiple phases at 4, 6, 9, and 12 months, contributed to the scarcity of infants who had undergone the entire process.

The data collection process proved intricate, primarily due to the complexity of the equipment involved. Connecting and handling these sensitive devices presented difficulties. Moreover, many data collection instances lacked crucial information, including discernible patterns of VEPs or the EDA responses to intended stimuli. There were some recordings that were not properly captured due to missing components, such as triggers, or issues with the software connection required for simultaneous collection of VEPs and EDA data. There were also situations where EDA data was not recorded.

Furthermore, logistical challenges emerged from the unavailability of parents with very young infants to partake in the data collection sessions. These sessions were frequently coordinated with vaccination days to streamline the process and alleviate the need for parents to make additional trips to the clinic. Consequently, this approach also imposed restrictions on the available time window for data acquisition. The confluence of logistical complexities and the stringent age-specific windows for each data collection moment (occurring specifically at 4, 6, 9, and 12-month marks) rendered it challenging to replicate or reschedule unsuccessful recordings.

During the actual acquisition process, another significant challenge stemmed from the inherent limitations of infants' attention spans and their susceptibility to agitation. Ensuring that infants were in an optimal state of calm and attentiveness to the stimulus proved exceedingly difficult. Factors such as sleepiness, hunger, or restlessness, which could diminish their inclination to pay attention, were hard to control. Consequently, the infants' limited capacity to sustain attention to stimuli and our inability to compel their focus on the intended stimulus posed additional constraints and limitations to the study.

6.2.2 Data Analysis

The data analysis process presented a multitude of challenges, primarily stemming from the inherent variability observed among infants. These young subjects exhibited substantial differences in their acquired signals, both in comparison to each other and to the signals typically encountered in adults. Given the tender age of these infants, it was not uncommon for some of them to display incomplete patterns, possibly lacking components like the N75 component, which is commonly observed in adults. Moreover, the success of VEPs recordings in these patients depended on their ability to remain alert, quiet, and capable of maintaining focus on the stimulus. In cases where patients were drowsy or exhibited variable attention, VEPs results were suboptimal, with the potential for misleading outcomes. Additionally, artifacts in the VEPs records were a notable concern, with head and body movements, including yawning, crying, and pacifier use, capable of generating artifacts of such magnitude that the VEPs signal became indiscernible. These challenges underscore the importance of stringent patient cooperation and artifact management in obtaining reliable VEPs data from infants [34].

Identifying reference points during data analysis proved to be a complex undertaking, primarily due to the distinctive and unpredictable nature of infant responses to stimuli. This complexity was further compounded by the limited knowledge about their reactions at this early stage of development.

Furthermore, the structural attributes of infants' heads introduced challenges. The small size of their heads and developing brains, exhibit variability from one infant to another and can undergo rapid changes between different data acquisition phases, that are only 2 or 3 months apart. This rendered the task of electrode placement highly complex. Precise electrode placement was crucial for accurate reception of signals elicited by the stimulus [63]. Notably, the C_Z electrode proved especially vulnerable to interference from infant eye movements or pacifier usage. Consequently, there were instances where certain electrodes failed to provide pertinent information due to these factors [16].

6.2.3 Interpretation of Results

The study grappled with complexities in interpreting the results, predominantly attributed to the intricate relationship between EDA signals and VEPs. This domain remains relatively uncharted, particularly concerning infants at such a tender age. Given that our study

represents an initial exploration into this area, it necessitates meticulous and cautious data analysis and interpretation.

The interpretation of EDA results was specially challenging due to its variability between individuals and potential variations within the same person under diverse stimuli or emotional states. Furthermore, external factors such as temperature fluctuations, patient movements, and background noise could occasionally be misinterpreted as actual response signals [43].

Despite these limitations, the study's findings have exhibited promise and suggest the feasibility of analysing these signals in very young infants, whose developmental journey is still in its early stages.

6.3 Contributions and Future work

The methodologies we employed created a robust platform for signal analysis, enhancing our capability to assess infant responses to stimuli and conduct thorough analyses of diverse cases. This approach has the potential to uncover valuable insights and contribute to the advancement of our understanding of the intricate dynamics between EDA and VEPs signals. These findings hold the potential to revolutionize the monitoring of signal evolution and enhance the early detection of indicators of immaturity in the future.

In future research, it would be influential to develop new methods for the analysis of the EDA signal and enhance the discrimination of stimuli-related SCRs from unrelated ones. In an upcoming research endeavor, we will leverage the complete dataset obtained from our longitudinal study, which encompasses signal collections at crucial developmental milestones, specifically at 4, 6, 9, and 12 months. This extended temporal perspective will enable us to conduct a comprehensive assessment, providing a holistic view of the developmental trajectories for both premature and full-term infants. Utilising this multifaceted dataset, our primary goal is to refine our ability to discern and elucidate the differences that distinguish these two study groups, ultimately establishing a more robust normative reference. This transformative approach aims to achieve the ultimate goal of early diagnosis and tailored interventions that cater to the unique needs of each infant. Such a paradigm shift increases the likelihood of promoting normative developmental trajectories for preterm infants from infancy into adulthood.

Bibliography

[1] J. M. Lourenço, *The NOVAthesis LaTeX Template User's Manual*, NOVA University Lisbon, 2021. [Online]. Available: https://github.com/joaomlourenco/novathesis/raw/main/template.pdf (cit. on p. i).

[2] A. Zimmermann, K. M. M. de Carvalho, C. Atihe, S. M. V. Zimmermann, and V. L. de Moura Ribeiro, "Visual development in children aged 0 to 6 years," *Arquivos Brasileiros de Oftalmologia*, vol. 82, pp. 173–175, 3 2019-03, ISSN: 16782925. DOI: 10.5935/0004-2749.20190034 (cit. on pp. xii, 6).

[3] W. Boucsein, "Methods of electrodermal recording," in *Electrodermal Activity*. Boston, MA: Springer US, 2012, pp. 87–258, ISBN: 978-1-4614-1126-0. DOI: 10.1007/978-1-4614-1126-0_2 (cit. on pp. xii, 8–11).

[4] J. F. Gould, B. G. Fuss, R. M. Roberts, C. T. Collins, and M. Makrides, "Consequences of using chronological age versus corrected age when testing cognitive and motor development in infancy and intelligence quotient at school age for children born preterm," *PLOS ONE*, vol. 16, no. 9, pp. 1–12, 2021-09. DOI: 10.1371/journal.pone.0256824 (cit. on pp. xii, 15).

[5] K. Blinowska and P. Durka, "Electroencephalography (EEG)," in *Wiley Encyclopedia of Biomedical Engineering*. Hoboken, NJ, USA: John Wiley & Sons, Inc., 2006-04. DOI: 10.1002/9780471740360 (cit. on pp. xii, 6).

[6] S. Wakim and M. Grewal, *23.4: Fetal Stage - Biology LibreTexts*, 2021. [Online]. Available: https://bio.libretexts.org/Bookshelves/Human_Biology/Book%5C%3A_Human_Biology_(Wakim_and_Grewal)/23%5C%3A_Human_Growth_and_Development/23.4%5C%3A_Fetal_Stage (visited on 2023-02-17) (cit. on pp. xiii, 4).

[7] S. Wakim and M. Grewal, *23.3: Embryonic Stage - Biology LibreTexts*, 2021. [Online]. Available: https://bio.libretexts.org/Bookshelves/Human_Biology/Book%5C%3A_Human_Biology_(Wakim_and_Grewal)/23%5C%3A_Human_Growth_and_Development/23.3%5C%3A_Embryonic_Stage (visited on 2023-02-17) (cit. on pp. xiii, 4).

[8] J. Stiles and T. L. Jernigan, "The basics of brain development," *Neuropsychology Review*, vol. 20, no. 4, pp. 327–348, 2010-12, ISSN: 10407308. DOI: 10.1007/S11065-010-9148-4 (cit. on pp. xiii, 4).

[9] J. E. Guyton Arthur C Hall, "Organization of the Nervous System, Basic Functions of Synapses, "Transmitter Substances"," in *Textbook of Medical Physiology*. W B Saunders, 2005, ch. 45, pp. 613–624 (cit. on pp. xiii, 3, 4).

[10] J. Jankovic, *Visual Evoked Potential - an overview | ScienceDirect Topics*. [Online]. Available: https://www.sciencedirect.com/topics/neuroscience/visual-evoked-potential (visited on 2023-02-19) (cit. on pp. xiii, 6–8).

[11] S. Wakim and M. Grewal, *23.2: Germinal Stage - Biology LibreTexts*, 2021. [Online]. Available: https://bio.libretexts.org/Bookshelves/Human_Biology/Human_Biology_(Wakim_and_Grewal)/23%3A_Human_Growth_and_Development/23.2%3A_Germinal_Stage (visited on 2023-02-17) (cit. on p. xiii).

[12] W. H. Organization, *Born too soon: the global action report on preterm birth*, 2012. [Online]. Available: https://iris.who.int/handle/10665/44864 (cit. on p. 1).

[13] *Preterm Infants - Pediatrics - MSD Manual Professional Edition*. [Online]. Available: https://www.msdmanuals.com/professional/pediatrics/perinatal-problems/preterm-infants (cit. on p. 1).

[14] M. Vieira, F. Ribeiro, and C. K. M. Formiga, "Principais instrumentos de avaliação do desenvolvimento da criança de zero a dois anos de idade," *Revista Movimenta*, vol. 2, pp. 23–31, 2009-01 (cit. on pp. 1, 12).

[15] L. Dubowitz, V. Dubowitz, and E. Mercuri, *Neurological assessment of the preterm and fullterm newborn infant* (Clinics in Developmental Medicine), en, 2nd ed. Cambridge, England: Mac Keith Press, 2007-02. DOI: 10.1016/s0387-7604(80)80003-9 (cit. on p. 1).

[16] M. J. Taylor and D. L. McCulloch, "Visual evoked potentials in infants and children," *Journal of clinical neurophysiology : official publication of the American Electroencephalographic Society*, vol. 9, pp. 357–372, 3 1992, ISSN: 0736-0258. DOI: 10.1097/00004691-199207010-00004 (cit. on pp. 1, 23, 35, 38, 39).

[17] G. Liebhardt, D. Sontheimer, and O. Linderkamp, "Visual-motor function of very low birth weight and full-term children at 3 1/2 to 4 years of age," *Early human development*, vol. 57, no. 1, pp. 33–47, 2000, ISSN: 0378-3782. DOI: 10.1016/S0378-3782(99)00056-0 (cit. on p. 1).

[18] E. H. Chung, J. Chou, and K. A. Brown, "Neurodevelopmental outcomes of preterm infants: a recent literature review," *Translational pediatrics*, vol. 9, no. Suppl 1, S3–S8, 2020-02, ISSN: 2224-4344. DOI: 10.21037/TP.2019.09.10 (cit. on pp. 1, 2).

[19] C. Andrade, "Estudo da Atividade Eletrodérmica em Bebés sujeitos a estímulos visuais," p. 127, 2022-09 (cit. on pp. 2, 10, 14, 36).

[20] A. Ferrão, "Estudo de Potenciais Evocados Visuais em Bebés," p. 100, 2022-09 (cit. on pp. 2, 14, 15, 18, 20, 36, 50, 51).

[21] A. C. C. De Paula Machado, S. R. De Oliveira, L. De Castro Magalhães, D. M. De Miranda, and M. C. F. Bouzada, "Sensory processing during childhood in preterm infants: A systematic review," *Revista Paulista de Pediatria*, vol. 35, no. 1, p. 92, 2017-01, ISSN: 19840462. DOI: 10.1590/1984-0462/;2017;35;1;00008 (cit. on pp. 3, 5).

[22] C. Tuvblad, J. Isen, L. A. Baker, A. Raine, D.-I. Lozano, and K. C. Jacobson, "The Genetic and Environmental Etiology of Sympathetic and Parasympathetic Activity in Children," *Behavior Genetics*, vol. 40, no. 4, pp. 452–466, 2010-02. DOI: 10.1007/s10519-010-9346-0 (cit. on p. 3).

[23] L. Thau, V. Reddy, and P. Singh, "Anatomy, Central Nervous System," *BMJ*, vol. 1, no. 4293, pp. 478–478, 2022-10, ISSN: 0959-8138. DOI: 10.1136/bmj.1.4293.478 (cit. on p. 4).

[24] J. E. Guyton Arthur C Hall, "Fetal and Neonatal Physiology," in *Textbook of Medical Physiology*. W B Saunders, 2005, ch. 83, pp. 1042–1052 (cit. on p. 5).

[25] E. Fitzgerald, J. P. Boardman, and A. J. Drake, "Preterm Birth and the Risk of Neurodevelopmental Disorders - Is There a Role for Epigenetic Dysregulation?" *Current Genomics*, vol. 19, p. 507, 7 2018-08, ISSN: 13892029. DOI: 10.2174/1389202919666171229144807 (cit. on p. 5).

[26] S. Prasad and S. L. Galetta, "Anatomy and physiology of the afferent visual system," *Handbook of Clinical Neurology*, vol. 102, pp. 3–19, 2011, ISSN: 00729752. DOI: 10.1016/B978-0-444-52903-9.00007-8 (cit. on p. 5).

[27] J. E. Guyton Arthur C Hall, "The Eye: I. Optics of Vision," in *Textbook of Medical Physiology*. W B Saunders, 2005, ch. 49, pp. 613–624 (cit. on p. 5).

[28] J. E. Guyton Arthur C Hall, "The Eye: II. Receptor and Neural Function of the Retina," in *Textbook of Medical Physiology*. W B Saunders, 2005, ch. 50, pp. 626–637 (cit. on pp. 5, 6, 9).

[29] S. P. Johnson, "Development of visual perception," *Wiley Interdisciplinary Reviews: Cognitive Science*, vol. 2, pp. 515–528, 5 2011-09, ISSN: 1939-5086. DOI: 10.1002/WCS.128 (cit. on p. 6).

[30] "ISCEV standard for clinical visual evoked potentials: (2016 update)," *Documenta ophthalmologica. Advances in ophthalmology*, vol. 133, no. 1, pp. 1–9, 2016-08, ISSN: 1573-2622. DOI: 10.1007/S10633-016-9553-Y (cit. on pp. 6–8, 19, 35).

[31] A. S. Blum and S. B. Rutkove, Eds., *The clinical neurophysiology primer*, en. Totowa, NJ: Humana Press, 2007-09. DOI: 10.1007/978-1-59745-271-7 (cit. on p. 7).

[32] O. E. Arslan, "Computational Basis of Neural Elements," *Artificial Neural Network for Drug Design, Delivery and Disposition*, pp. 29–82, 2016-01. DOI: 10.1016/B978-0-12-801559-9.00003-X (cit. on p. 7).

[33] R. Kothari, P. Bokariya, S. Singh, and R. Singh, "A Comprehensive Review on Methodologies Employed for Visual Evoked Potentials," *Scientifica*, vol. 2016, 2016, ISSN: 2090908X. DOI: 10.1155/2016/9852194 (cit. on p. 7).

[34] E. E. Birch and V. Subramanian, "Chapter 23 – visual evoked potentials in infants and children," 2012. [Online]. Available: https://api.semanticscholar.org/CorpusID:151513398 (cit. on pp. 7, 19, 35, 38, 39).

[35] D. J. Creel, "Visually evoked potentials," *Handbook of Clinical Neurology*, vol. 160, pp. 501–522, 2019-01, ISSN: 0072-9752. DOI: 10.1016/B978-0-444-64032-1.00034-5 (cit. on p. 8).

[36] M. J. Aminoff, *Aminoff's electrodiagnosis in clinical neurology*, 6th ed. London, England: W B Saunders, 2012-03 (cit. on p. 8).

[37] M. E. Dawson, A. M. Schell, D. L. Filion, and G. G. Berntson, "The Electrodermal System," *Handbook of Psychophysiology*, pp. 157–181, 2009-12. DOI: 10.1017/CBO9780511546396.007 (cit. on p. 9).

[38] R. C. Reed, D. E. Johnson, and A. M. Nie, "Preterm Infant Skin Structure Is Qualitatively and Quantitatively Different From That of Term Newborns," *Pediatric and Developmental Pathology*, vol. 24, no. 2, pp. 96–102, 2021-04, ISSN: 16155742. DOI: 10.1177/1093526620976831/ASSET/IMAGES/LARGE/10.1177_1093526620976831-FIG5.JPEG (cit. on p. 9).

[39] M. O. Visscher, A. N. Carr, and V. Narendran, "Premature infant skin barrier maturation: Status at full-term corrected age," *Journal of Perinatology 2020 41:2*, vol. 41, pp. 232–239, 2 2020-06, ISSN: 1476-5543. DOI: 10.1038/s41372-020-0704-3 (cit. on pp. 9, 30, 36).

[40] B. D. Hodge, T. Sanvictores, and R. T. Brodell, "Anatomy, Skin Sweat Glands," *StatPearls*, 2022-10 (cit. on p. 9).

[41] M. El-Azazy, M. Min, and P. Annus, *Electrochemical Impedance Spectroscopy*. Rijeka: IntechOpen, 2020-12, ISBN: 978-1-78985-216-5. DOI: 10.5772/intechopen.87884 (cit. on p. 10).

[42] H. F. Posada-Quintero and K. H. Chon, "Innovations in Electrodermal Activity Data Collection and Signal Processing: A Systematic Review," *Sensors 2020, Vol. 20, Page 479*, vol. 20, no. 2, p. 479, 2020-01, ISSN: 1424-8220. DOI: 10.3390/S20020479 (cit. on pp. 10, 11).

[43] R. Zangróniz, A. Martínez-Rodrigo, J. M. Pastor, M. T. López, and A. Fernández-Caballero, "Electrodermal Activity Sensor for Classification of Calm/Distress Condition," *Sensors (Basel, Switzerland)*, vol. 17, no. 10, 2017-10, ISSN: 14248220. DOI: 10.3390/S17102324 (cit. on pp. 11, 40).

[44] M. A. R. D. Israel, Y. Pileggi, T. de Vicente Krambeck, and F. C. P. Piveta, "Intervenção precoce no desenvolvimento neuromotor de lactentes prematuros de risco," *Revista FisiSenectus*, vol. 8, pp. 1–18, 1 2020-08, ISSN: 2318-3381. DOI: 10.22298/RFS.2020.V8.N1.5171 (cit. on p. 12).

[45] M. S. Roy, M. Barsoum-Homsy, J. Orquin, and J. Benoit, "Maturation of Binocular Pattern Visual Evoked Potentials in Normal Full-Term and Preterm Infants from 1 to 6 Months of Age," *Pediatric Research 1995 37:2*, vol. 37, pp. 140–144, 2 1995, ISSN: 1530-0447. DOI: 10.1203/00006450-199502000-00002 (cit. on pp. 12, 37).

[46] C. Balachandran, A. I. Klistorner, and F. Billson, "Multifocal VEP in children: its maturation and clinical application," *British Journal of Ophthalmology*, vol. 88, pp. 226–232, 2 2004-02, ISSN: 0007-1161. DOI: 10.1136/BJO.2003.018390 (cit. on pp. 12, 36).

[47] G. Ruberto *et al.*, "Compared progression of visual-evoked potentials in preterm and term newborns.," *Journal Francais D'ophtalmologie*, vol. 27, pp. 1031–1038, 9 Pt 1 2004-11, ISSN: 0181-5512. DOI: 10.1016/S0181-5512(04)96260-2 (cit. on pp. 12, 37).

[48] D. B. Birtles, O. J. Braddick, J. Wattam-Bell, A. R. Wilkinson, and J. Atkinson, "Orientation and motion-specific visual cortex responses in infants born preterm," *NeuroReport*, vol. 18, pp. 1975–1979, 18 2007-12, ISSN: 09594965. DOI: 10.1097/WNR.0B013E3282F228C8 (cit. on p. 12).

[49] J. J. Feng, W. P. Wang, S. J. Guo, Z. W. Liu, and X. Xu, "Flash Visual Evoked Potentials in Preterm Infants," *Ophthalmology*, vol. 120, pp. 489–494, 3 2013-03, ISSN: 0161-6420. DOI: 10.1016/J.OPHTHA.2012.08.025 (cit. on pp. 12, 37).

[50] E. Tremblay *et al.*, "Delayed Early Primary Visual Pathway Development in Premature Infants: High Density Electrophysiological Evidence," *PLOS ONE*, vol. 9, e107992, 9 2014-09, ISSN: 1932-6203. DOI: 10.1371/JOURNAL.PONE.0107992 (cit. on p. 12).

[51] M. Michalczuk, B. Urban, B. Chrzanowska-Grenda, M. Oziębło-Kupczyk, and A. Bakunowicz-Łazarczyk, "An influence of birth weight, gestational age, and apgar score on pattern visual evoked potentials in children with history of prematurity," *Neural Plasticity*, vol. 2015, 2015, ISSN: 16875443. DOI: 10.1155/2015/754864 (cit. on p. 12).

[52] A. Kharal, S. Khanal, J. B. Shrestha, G. S. Shrestha, and N. Paudel, "Flash VEP in clinically stable pre-term and full-term infants," *Documenta Ophthalmologica*, vol. 141, pp. 259–267, 3 2020-12, ISSN: 15732622. DOI: 10.1007/S10633-020-09773-0/FIGURES/3 (cit. on p. 13).

[53] A. Martínez-Rodrigo, R. Zangróniz, J. M. Pastor, and A. Fernández-Caballero, "Arousal level classification in the ageing adult by measuring electrodermal skin conductivity," *Lecture Notes in Computer Science (including subseries Lecture Notes in Artificial Intelligence and Lecture Notes in Bioinformatics)*, vol. 9456, pp. 213–223, 2015, ISSN: 16113349. DOI: 10.1007/978-3-319-26508-7_21/COVER (cit. on p. 13).

[54] A. Scarpa, P. H. Venables, A. Raine, and S. A. Mednick, "Heart rate and skin conductance in behaviorally inhibited Mauritian children," *Journal of Abnormal Psychology*, vol. 106, pp. 182–190, 2 1997, ISSN: 0021843X. DOI: 10.1037/0021-843X.106.2.182 (cit. on p. 13).

[55] D. C. FOWLES, G. KOCHANSKA, and K. MURRAY, "Electrodermal activity and temperament in preschool children," *Psychophysiology*, vol. 37, pp. 777–787, 6 2000-11, ISSN: 1469-8986. DOI: 10.1111/1469-8986.3760777 (cit. on p. 13).

[56] H. Storm, "Skin conductance and the stress response from heel stick in preterm infants," *Archives of Disease in Childhood - Fetal and Neonatal Edition*, vol. 83, F143–F147, 2 2000-09, ISSN: 1359-2998. DOI: 10.1136/FN.83.2.F143 (cit. on p. 13).

[57] K. G. Hernes, L. Mørkrid, A. Fremming, S. Ødegården, Ø. G. Martinsen, and H. Storm, "Skin Conductance Changes During the First Year of Life in Full-Term Infants," *Pediatric Research 2002 52:6*, vol. 52, pp. 837–843, 6 2002, ISSN: 1530-0447. DOI: 10.1203/00006450-200212000-00005 (cit. on p. 13).

[58] J. Ham and E. Tronick, "A procedure for the measurement of infant skin conductance and its initial validation using clap induced startle," *Developmental Psychobiology*, vol. 50, pp. 626–631, 6 2008-09, ISSN: 1098-2302. DOI: 10.1002/DEV.20317 (cit. on p. 13).

[59] P. H. Ellaway, A. Kuppuswamy, A. Nicotra, and C. J. Mathias, "Sweat production and the sympathetic skin response: improving the clinical assessment of autonomic function," *Autonomic neuroscience : basic & clinical*, vol. 155, pp. 109–114, 1-2 2010-06, ISSN: 1872-7484. DOI: 10.1016/J.AUTNEU.2010.01.008 (cit. on p. 13).

[60] "Entropy Analysis of Neonatal Electrodermal Activity during the First Three Days after Birth," *Entropy 2022, Vol. 24, Page 422*, vol. 24, p. 422, 3 2022-03, ISSN: 1099-4300. DOI: 10.3390/E24030422 (cit. on pp. 13, 36).

[61] A. I. Ferreira, A. Ferrão, C. Andrade, M. Baptista, C. Quaresma, and C. Quintão, "Electrophysiological answer to a checkerboard stimulus: A pilot study," *HEALTHINFO 2022: The Seventh International Conference on Informatics and Assistive Technologies for Health-Care, Medical Support and Wellbeing*, pp. 32–38, 2022. DOI: 10.5172/HESR.2013.3223 (cit. on pp. 16, 35, 36).

[62] *g.NAUTILUS RESEARCH | Wearable EEG Headset | g.tec medical engineering GmbH*. [Online]. Available: https://www.gtec.at/product/gnautilus-research/ (cit. on p. 19).

[63] F. D. Russo, A. Martínez, M. I. Sereno, S. Pitzalis, and S. A. Hillyard, "Cortical sources of the early components of the visual evoked potential," *Human brain mapping*, vol. 15, pp. 95–111, 2 2002, ISSN: 1065-9471. DOI: 10.1002/HBM.10010 (cit. on pp. 23, 39).

A

Behavioural Analysis

In this appendix, you will find detailed records pertaining to the behaviour of each infant during the data acquisition sessions in Table A.1. Additionally, the form used for documenting these observations is included for reference.

Table A.1: Behavioural analysis of the acquisitions. Abbreviations: ID, identification of the subject; GA, Gestational Age of the subjects in weeks and days; M1, acquisitions at 4 months of age; M2, acquisitions at 12 months age; FT, Full-Term Group; PT, Preterm group.

ID	Group	GA [weeks+days]	M1	M2 - Take 1	M2 - Take 2
1	FT	38+1	Alert though sleepy. Attempted to touch the cap 1/2 times.	Fixated for 10/15 seconds, then became restless and started trying to remove the cap.	Similar performance, slightly better.
2	FT	38	Restless, fell asleep after the acquisition.	As soon as the cap was placed, the infant began to cry.	Take 1 possibly better than Take 2.
3	FT	41	Attentive and active.	The baby appeared sleepy and hungry.	Take 2 may be slightly better.
4	FT	40	Restless. Cooperated but occasionally distracted.	Started crying from the beginning.	Also crying and standing.
5	FT	40	Cooperative and interested in the stimulus; Looked away but resumed.	First one maybe better than the second. In both, she did not seem receptive to the stimulus.	
6	PT	31+5	Chatty and observant. Attentive to the stimulus.	Kept looking at the stimulus but would become unfocused and disinterested. Both attempts were the same.	
7	PT	27	Restless after putting on the small cap. Then adapted and began to look.	Medium cap, the baby seems to not particularly like the stimulus in both attempts.	
8	PT	31+6	Attentive and cooperative.	Kept putting the toy in the mouth. Kept standing up for most of the signal. Tried to remove the reference electrode.	Irritable but more focused on the stimulus. Overall performance is intermediate.
9	PT	29+3	Tonic and restless baby; difficulty in bringing upper limbs to the midline; stressed, and seemingly sleepy.	Very agitated baby initially. The 2^{nd} take seemed better than the 1^{st} one. In the 1^{st} take, the clip from the earlobe was removed.*	
10	PT	29+1	Small cap. Baby inattentive and restless	Cooperative baby during equipment placement. Seemed to dislike the stimulus, and was very restless during it. The first take was better than the second. Removed the clip during the first one.*	

*The clip on the earlobe was quickly replaced and the artefacts removed.

The table columns are arranged in the following sequence: Subject ID, Sample Group, Gestational Age, and Behavioral Notes from two distinct extraction moments. M1 designates the 4-month assessment, while M2 represents the 12-month evaluation. Both Take 1 and Take 2 data were collected, with a 10-minute interval between the two assessments.

ESTUDO DO DESENVOLVIMENTO DAS COMPETÊNCIAS VISUAIS E MOTORAS EM BEBÉS PRÉ TERMO

GRELHA DE REGISTO DA RECOLHA DE DADOS

Participante ___ ___ ___

(a preencher pelo investigador)

	1ª Av	2ª Av	3ª Av	4ª Av
Tempo de preparação				
Comportamento geral do bebé				
Distância do bebé ao ecrã				
Luminosidade na sala				
Posicionamento dos elétrodos				
FZ				
CZ				
OZ				
PO7				
PO8				

	1ª Av.	2ª Av.	3ª Av.	4ª Av.		Observ.
Fixação do estímulo					Permanente	
					Desfocou 1-2 x, mas retomou	
					Desfocou mais de 3x, mas retomou	
					Predominantemente desatento ao estímulo	

Observações: (sono profundo; sono superficial; sonolência; calma alerta; alerta ativo; choro)

Data 1ª av.	Data 2ª av.	Data 3ª av.	Data 4ª av.

B

Acquisition Equipment for VEPs and EDA

Within this appendix, you will find the materials utilised for the acquisition of the Visual Evoked Potential (VEPs) and Electrodermal Activity (EDA). This section aims to provide an understanding of their placement and their role in the data collection process.

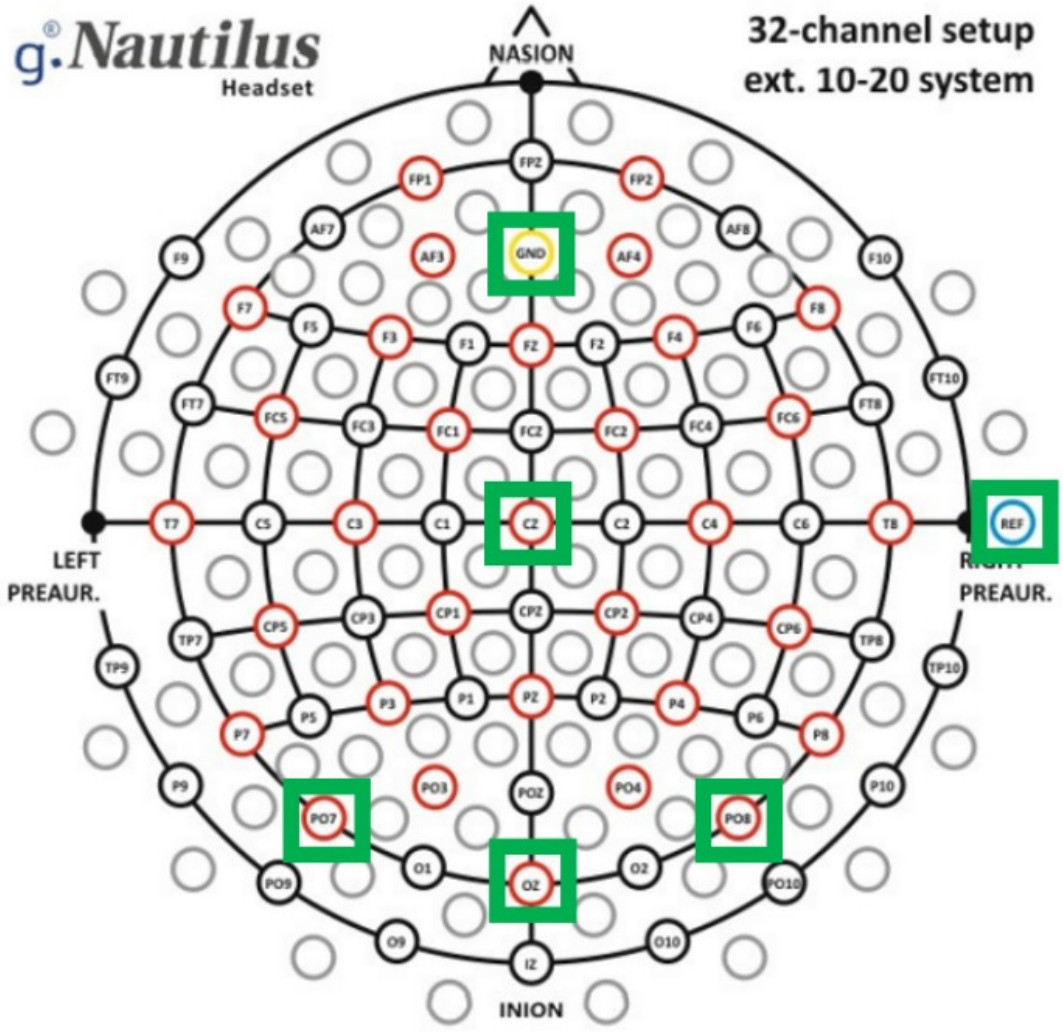

Figure B.1: *g.Nautilus*® electrode placement adapted from [20]. Active electrodes in red ($P0_8$, $P0_7$, O_Z and C_Z), ground electrode in yellow (GND) and reference earlobe electrode in blue (REF). All the electrodes used are highlighted in green.

Figure B.2: *g.Nautilus*® equipment for Electroencephalogram (EEG) acquisition, adapted from [20].

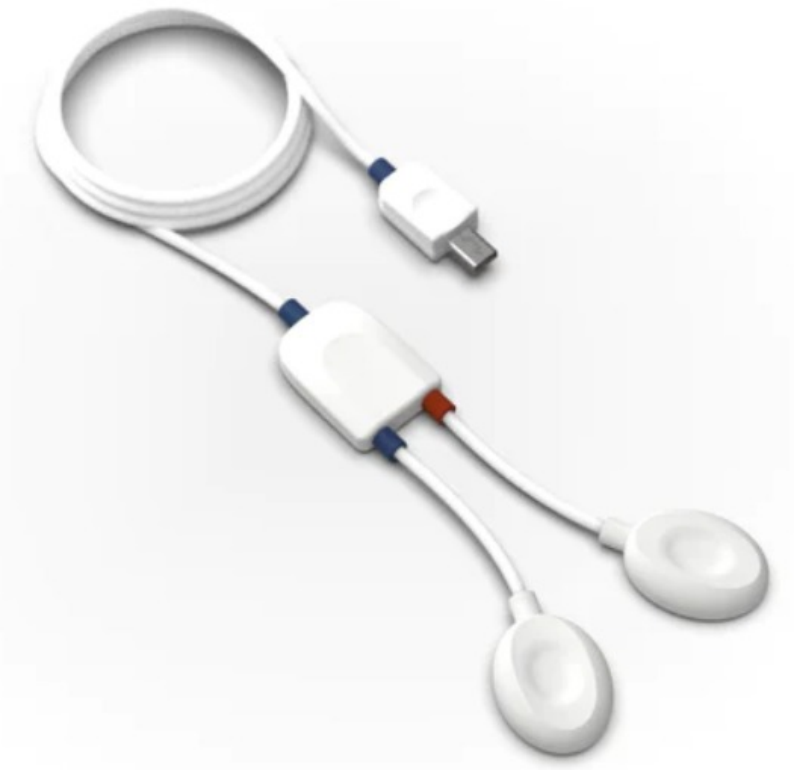

Figure B.3: EDA sensor containing two electrodes.

Figure B.4: *Biosignalsplux*®equipment for EDA acquisition. Connects with EDA sensor through one of the analog ports.

C

Informed Parental Consent

In this appendix, you will find an Informational Document and a Consent Form.

The Informational Document comprises a comprehensive description of the study, elucidating all procedures encompassing the data collection and assessments to which the infants are subjected. This document is provided to the parents, alongside the Parental Consent Form, which requires their signature should they wish for their infants to participate in the study.

Título do estudo: Desenvolvimento das competências visuais e motoras em bebés ex pré-termo

Áreas/Unidades: Sector de Neonatologia e Serviço de Oftalmologia (CHULC, EPE) e Unidade de Saúde Familiar da Baixa (ACES Central, ARS LVT) e

Descrição do estudo:

A presente investigação desenvolve-se no âmbito do Doutoramento em Engenharia Biomédica da Faculdade de Ciências e Tecnologia da Universidade Nova de Lisboa (FCT UNL) e conta com a participação do Centro Hospitalar Universitário Lisboa Central (CHULC) e da Unidade de Saúde Familiar da Baixa (ACES Central, ARS LVT).

Tem como investigadora principal a aluna de Doutoramento Ana Isabel Ferreira que poderá ser contactada através do e-mail aix.ferreira@campus.fct.unl.pt. A orientação do estudo é realizada pelas Professoras Carla Quintão e Cláudia Quaresma.

O estudo tem por objetivo identificar o impacto do nascimento pré-termo no desenvolvimento das competências visuais e motoras, durante os primeiros 12 meses de vida. Nesta sequência foram definidos um conjunto de objetivos específicos, de entre os quais se destaca:

- Caracterizar o desempenho dos bebés (ex pré-termo e de termo), ao nível das tarefas visuomotoras, aos 4, 6, 9 e 12 meses;

- Analisar o percurso de desenvolvimento, ao nível das competências visuomotoras, nos bebés ex pré-termo e nos bebés termo;

- Comparar o curso do desenvolvimento das competências visuomotoras nos bebés do grupo de estudo (bebés ex pré-termo) com os bebés do grupo controlo (bebés de termo);

Para responder aos objetivos delineados pretende-se avaliar 35 bebés ex pré-termo e 35 bebés de termo, aos 4, 6, 9 e 12 meses de vida, tal como se apresenta na figuranº1.

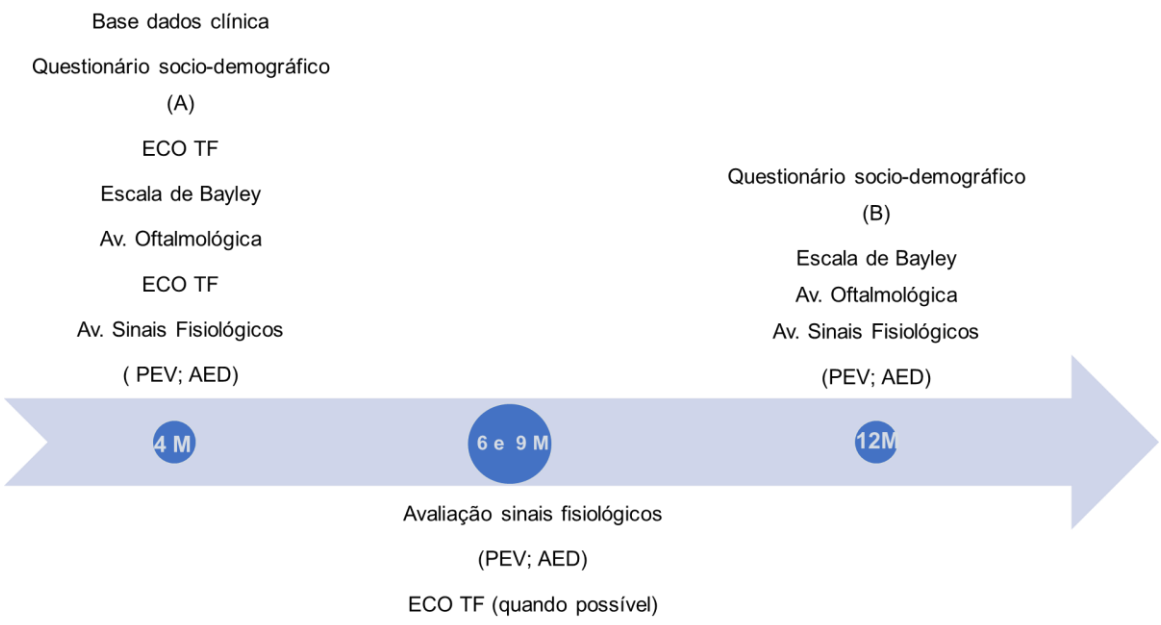

Figura nº1: Momentos de aplicação da avaliação

Será criada uma **base de dados** que permitirá a compilação de informação clínica sobre o bebé e a causa da prematuridade. Prevê-se que esta base de dados inclua a informação sobre a gravidez, o nascimento e o desenvolvimento nos primeiros meses de vida.

Os dados a constar nesta base de dados serão recolhidos pelo médico e registados pela aluna de doutoramento no início da avaliação (4 meses), uma vez que reportam à história de vida do bebé. Salienta-se que estes dados não acrescem aos procedimentos de rotina, uma vez que já são habitualmente recolhidos na prática clínica. Não implicam a interação da doutoranda com o bebé.

O **questionário sociodemográfico** será entregue aos pais pelo médico, correspondendo ao segundo passo do protocolo de recolha de dados.

Destina-se a ser preenchido pelos pais e irá ser aplicado tanto ao grupo controlo (bebés de termo) quanto ao grupo em estudo (bebés nascidos de pré-termo). Será constituído pela parte A, a aplicar no início do estudo, logo aos 4 meses, e pela parte B, a aplicar no final, aos 12 meses. A parte A incluirá questões relacionadas com os dados

sociodemográficos da família, enquanto a parte B será constituída por questões relativas ao percurso e competências do bebé, nos primeiros 12 meses de vida.

A **ecografia transfontanelar** é uma técnica de avaliação não invasiva, totalmente inócua para o bebé, rápida e com valor prognóstico. Por estes motivos é um método de primeira linha para avaliar a anatomia do sistema nervoso central no bebé pré-termo ou de risco. É proposta a sua realização, pelo médico neonatalogista com treino em ecografia cerebral, no primeiro e último momento do estudo (4 e 12 meses de vida respetivamente).

A **escala de desenvolvimento infantil de Bayley** (III edição) é um instrumento de administração individual que avalia o desenvolvimento de bebés, nos primeiros 42 meses de vida. É aplicado por rotina aos bebés pré-termo nascidos na Maternidade Dr. Alfredo da Costa e poderá também ser aplicado pela aluna de doutoramento aos bebés dos dois grupos de estudo. Neste procedimento há interação entre o avaliador e o bebé, estando presentes os pais do bebé. Serão necessários cerca de 20 minutos para a aplicação da escala de avaliação.

A **avaliação visual geral** será realizada pelos técnicos de ortóptica no Serviço de Oftalmologia do H.D.E. (CHULC). Prevê-se que esta avaliação possa ser realizada no momento inicial e no final, ou seja aos 4 e aos 12 meses de vida do bebé pré-termo e de termo. Com este procedimento será recolhida informação sobre a acuidade, conjugação dos dois olhos e motilidade ocular. Nos bebés ex pré-termo, para além destes parâmetros será também necessária a informação acerca da retina no momento do nascimento, sendo essa informação obtida através da avaliação do oftalmologista pediátrico e cuja informação já se encontra registada no processo.

A **avaliação dos sinais fisiológicos** será a última etapa da recolha de dados. Será registado o sinal de Electroencefalografia (através do equipamento *g.Nautilus*), o sinal da atividade eletrotérmica (recorrendo ao equipamento *Biosignalsplux*)e registado o comportamento do bebé durante esta avaliação.

Inicialmente, com o bebé sentado ao colo dos pais, é colocado o sensor para registo da avaliação eletrotérmica no bordo externo do pé. De seguida é colocada a touca no couro cabeludo do bebé com o respetivo gel. Prevê-se que estes procedimentos preparatórios demorem cerca de 15 minutos, desde que o bebé esteja calmo e colaborante. Salienta-se que estes procedimentos são totalmente inócuos para o bebé e para os pais, tendo sido já utilizados em várias investigações científicas, em diferentes centros de referência.

Só depois do bebé estar com o equipamento devidamente colocado, calmo, sentado no colo dos pais será ligado o ecrã. Este estará posicionado a 70 cm de distância, e aí será apresentado o estímulo que inclui dois padrões reversos de xadrez, tal como se apresenta na figura 2.

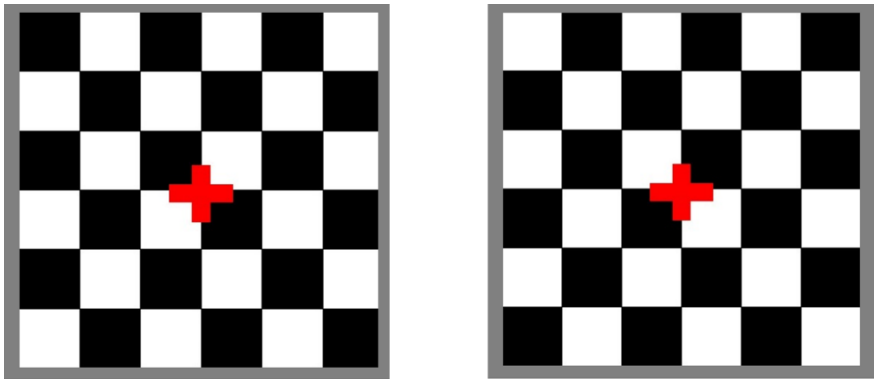

Figura 2: Estímulos a apresentar aos bebés

Este paradigma já foi testado e aplicado em bebés, a fim de medir a atividade elétrica, na via dorsal e na via ventral, sendo seguro e fidedigno.

Este paradigma experimental será aplicado em cada um dos momentos do estudo, ou seja, aos 4, 6, 9 e 12 meses. A apresentação do estímulo e a recolha do sinal acontecerá durante 120 segundos.

Todos os dados recolhidos serão armazenados digitalmente, não havendo lugar a registo vídeo e/ou áudio dos participantes e familiares. Será utilizada uma chave alfanumérica para codificação dos elementos de identificação dos participantes. O tratamento e análise de dados serão realizados pelo investigador principal sendo garantido o anonimato dos participantes. Os dados serão conservados enquanto o estudo estiver a decorrer e até ser publicado e apresentado em congresso.

Todas as metodologias de recolha de dados são inofensivas para os bebés, tendo sido já utilizadas em estudos anteriores. Não se prevê qualquer efeito adverso, contudo caso haja sinal de desconforto durante a aplicação da avaliação, o procedimento será interrompido. A interrupção pode também acontecer a pedido dos pais, sem qualquer prejuízo para os cuidados clínicos habitualmente disponibilizados para o bebé / família. Em qualquer momento os pais/tutores legais podem contactar o encarregado de Proteção de Dados (através do e-mail epd@chlc.min-saude.pt), ou mesmo a Comissão Nacional de Proteção de Dados (através do contacto cnpd@cnpd.pt)

Prevê-se que a recolha de dados decorra durante um ano, mais concretamente de fevereiro de 2022 a junho de 2023.

Os resultados serão publicados em revistas científicas e com revisão por pares, estando assegurada a confidencialidade e anonimato dos participantes.

CONSENTIMENTO ESCLARECIDO PARA PARTICIPAÇÃO EM

ESTUDOS DE INVESTIGAÇÃO EM SAÚDE

Área/Unidade: Sector de Neonatologia e Serviço de Oftalmologia (CHULC, EPE) e Unidade de Saúde Familiar da Baixa (ACES Central, ARS LVT)

Título do estudo: Desenvolvimento das competências visuais e motoras em bebés ex pré-termo

Procedimentos principais: Os bebés, nascidos de pré-termo e de termo, serão avaliados aos 4, 6, 9 e 12 meses de vida, presencialmente e por consulta dos processos clínicos. Estes momentos decorrem no âmbito das consultas de rotina. As metodologias de avaliação e de recolha de dados são inofensivas para os bebés, tendo sido já utilizadas em estudos anteriores. Não se prevê qualquer efeito adverso, contudo caso haja sinal de desconforto durante a aplicação da avaliação, o procedimento será interrompido.

As avaliações estão incluídas nos procedimentos de rotina já praticados para estas crianças, no acompanhamento do desenvolvimento do seu crescimento.

No folheto de informação complementar está descrita a informação detalhada de cada uma das metodologias de recolha de dados e sobre a sequência de aplicação.

Os dados recolhidos serão tratados e analisados pelo investigador principal sendo garantido o anonimato dos participantes, através de codificação alfanumérica. Os resultados científicos serão publicados em revistas com revisão por pares.

O participante pode abandonar o estudo em qualquer momento, a pedido dos pais/tutores legais, sem qualquer prejuízo para os cuidados clínicos habitualmente disponibilizados para o bebé / família. Podem ainda, contactar o encarregado de Proteção de Dados (através do e-mail epd@chlc.min-saude.pt), ou mesmo a Comissão Nacional de Proteção de Dados (através do contacto cnpd@cnpd.pt).

Confirmo que expliquei ao participante, ou ao seu representante legal, de forma adequada e inteligível, os procedimentos, assim como os potenciais riscos e inconvenientes, e que entreguei o folheto de informação complementar.

Assinatura do investigador ……..……

Nº aluno doutoramento…… Cédula Profissional …… Data: ___ / ___ / ____

A preencher pelo participante ou pelo seu representante legal

Declaro que me foram explicados de forma adequada e inteligível o objetivo e natureza da investigação e o(s) procedimento(s) a(os) que serei sujeito. Foram-me explicados os potenciais riscos e inconvenientes do(s) procedimento(s) proposto(s), que foram por mim compreendidos e aceites, concordando em participar no estudo.

Nome do Participante: .....

Representante Legal*: ..... Qualidade: ……...……

Documento de Identificação:.....Validade: ……

Assinatura: ..... Data: ___ / ___ / _____

* O representante legal deverá fazer prova dos seus poderes para representar do participante.

RETIRADA DO CONSENTIMENTO PARA PARTICIPAÇÃO EM

ESTUDOS DE INVESTIGAÇÃO EM SAÚDE

A relação investigador-participante é baseada na confiança mútua. O CHULC, EPE dispõe de procedimentos que permitem salvaguardar os direitos de ambos.

O investigador obriga-se a informar o participante ou o representante legal da sua liberdade de retirar, em qualquer momento, o consentimento para participar no estudo.

Áreas/Unidades: Sector de Neonatologia e Serviço de Oftalmologia (CHULC, EPE) e Unidade de Saúde Familiar da Baixa (ACES Central, ARS LVT)

Título do estudo: Desenvolvimento das competências visuais e motoras em bebés pré-termo

Confirmo que expliquei ao participante, ou ao seu representante legal, de forma adequada e inteligível, que a opção de retirar o consentimento de participação neste estudo em nada afeta ou afetará a sua relação com a Unidade de Saúde Familiar da Baixa ou os seus profissionais.

Assinatura do investigador ……..

Nº aluno doutoramento…… Cédula Profissional …… Data: ___ / ___ / ____

A preencher pelo participante ou pelo seu representante legal

Declaro que me foram explicados de forma adequada e inteligível o objetivo e natureza da investigação e o(s) procedimento(s) inerentes à participação neste estudo. Declaro ainda que, embora tendo concordado previamente em participar no estudo, decido agora deixar de participar nele, tendo-me sido esclarecido que se manterá inalterada a minha condição prévia de utente da Unidade de Saúde Familiar da Baixa.

Nome do Participante: .....

Representante Legal*: ..... Qualidade: …….....

Documento de Identificação: .....Validade: ……..……

Assinatura: ..... Data: ___ / ___ / _____

* O representante legal deverá fazer prova dos seus poderes para representar do participante.

|__| O participante ou o seu representante legal declararam verbalmente a retirada do consentimento previamente concedido para participação neste estudo.

D

Image Detailed Improvements

In this appendix, we provide a comprehensive overview of the enhancements implemented for artefact removal and the GUIDE platform in the context of VEPs. A comparison between the previous and updated methods is made, illustrating their application on two subjects. One subject exhibits a high-quality signal with minimal artefacts and strong concentration, Subject A, while the other subject demonstrates a less focused state and more signal artefacts, Subject B.

D.1 Artefact Removal for VEPs

The previous approach posed challenges in identifying artifacts and ensuring their proper removal. To address this issue, the first step involved preprocessing the electrode signals before artifact removal. This entailed applying filters and eliminating the offset, as described in Section 4.4.1. Figure D.1 illustrates how these preprocessing techniques enhance the visibility of artifacts.

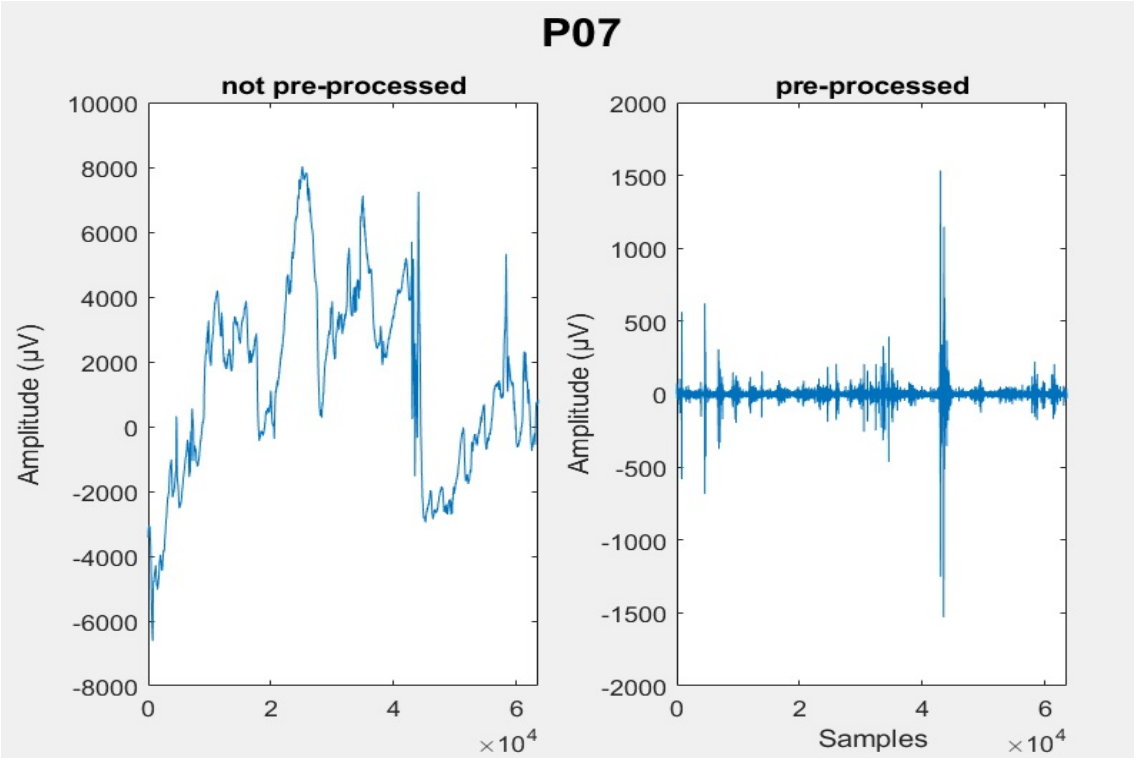

Figure D.1: Difference between preprocessed and non preprocessed EEG signal. The electrode $P0_7$ is used in this example.

Section 4.4.1 provides an explanation of both the previous and new methods, along with the limitations that have been addressed. Subsequent Figure D.2 illustrates an example featuring Subject using the new and previous method. This subject demonstrated strong focus during the entire acquisition, and had a high-quality signal with minimal artifacts. However, using the previous method, the excessive artifact removal resulted in signal degradation.

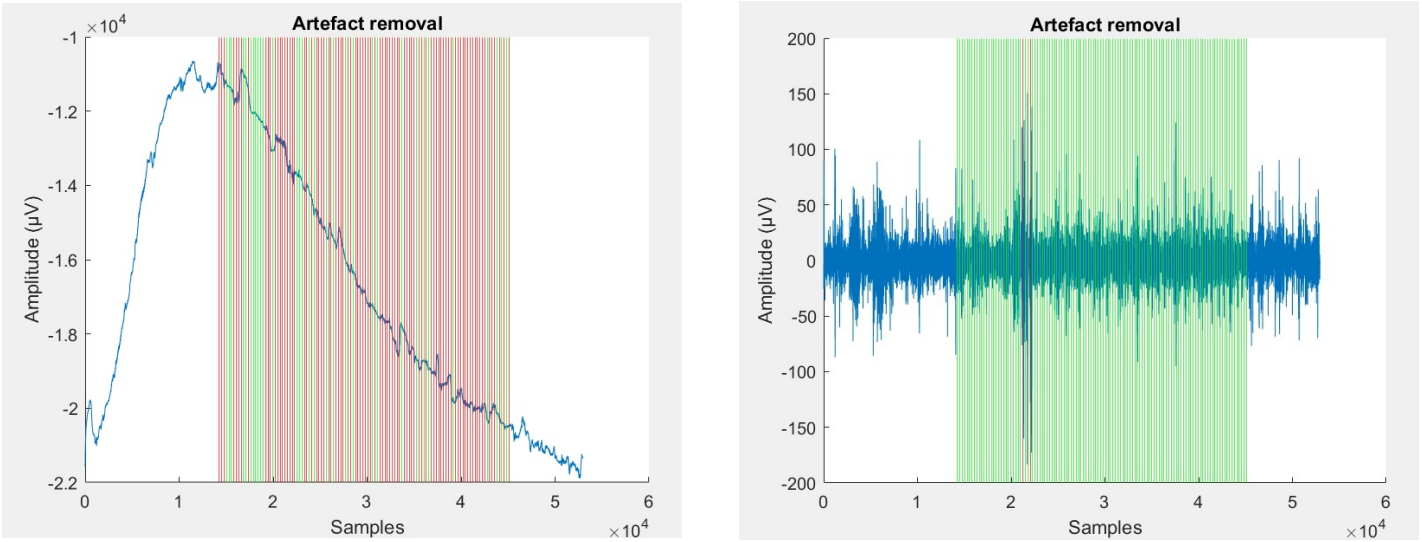

a) Subject A artefact removal using the previous method. b) Subject A artefact removal using the new method.

Figure D.2: Subject A artefact removal using the previous method Vs the new method. The electrode $P0_7$ is used in this example. The red lines represent the segments of signal being removed, while the green ones segments that were not removed.

Another comparison between the two methods can be observed in Figure D.3. This example features Subject B, who exhibited reduced focus and interest during data acquisition. In this case, there was no excessive artifact removal, as the artifacts' amplitudes were significantly larger in comparison to the rest of the signal. Nevertheless, it is notably more manageable to identify the artifacts using the new method.

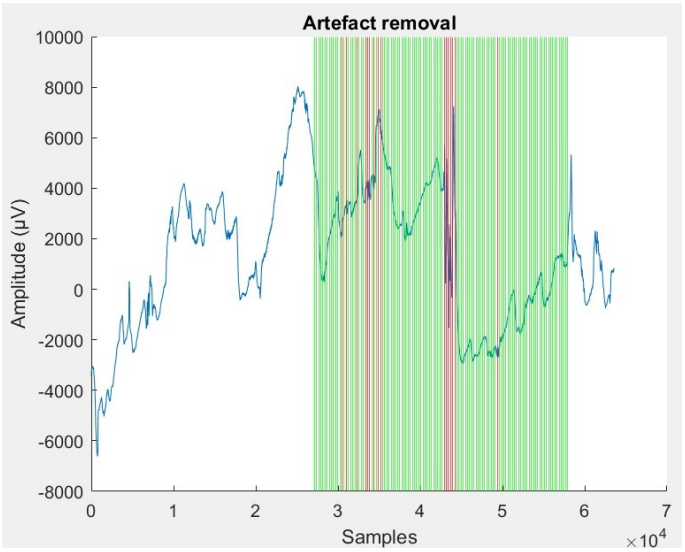

a) Subject B artefact removal using the previous method.

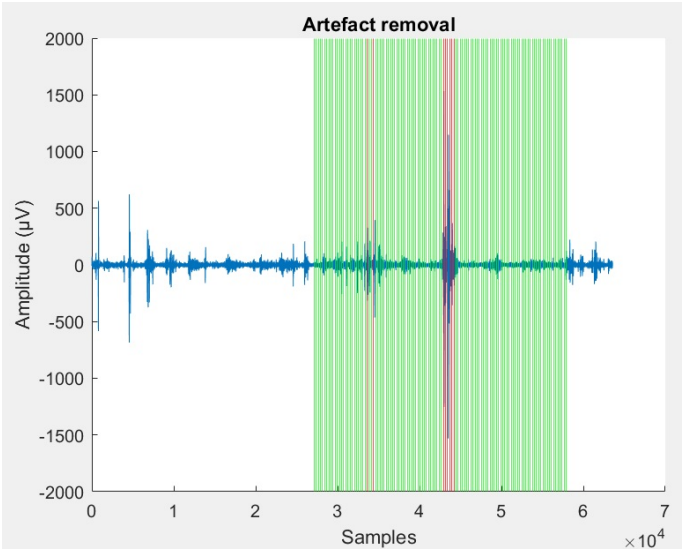

b) Subject B artefact removal using the new method.

Figure D.3: Subject B artefact removal using the previous method Vs the new method. The electrode $P0_7$ is used in this example. The red lines represent the segments of signal being removed, while the green ones segments that were not removed.

Despite the visual appearance of more noise in Subject A's signal, it's worth noting that the amplitude values are very low, indicating the presence of very few artifacts. There are no high-amplitude artifacts distinguishable from the rest of the signal.

D.2 GUIDE platform for VEPs

The differences between the new and previous GUIDE platforms are explained in Section 4.4.2, and it is also elucidated how the new platform functions, should be utilized, and the involved improvements. The following Figures are obtain from Subject A.

These figures illustrate the main distinctions between the pages of the GUIDE platform. First, we have the covers of the previous and new platforms in Figure D.4 and Figure D.5, respectively, followed by an example of a previous analysis page in Figure D.6 and a new analysis page in Figure D.7. Lastly in Figure D.8 and Figure D.9, we present the "Artifact" pages, where the artifacts are identified for each active electrode.

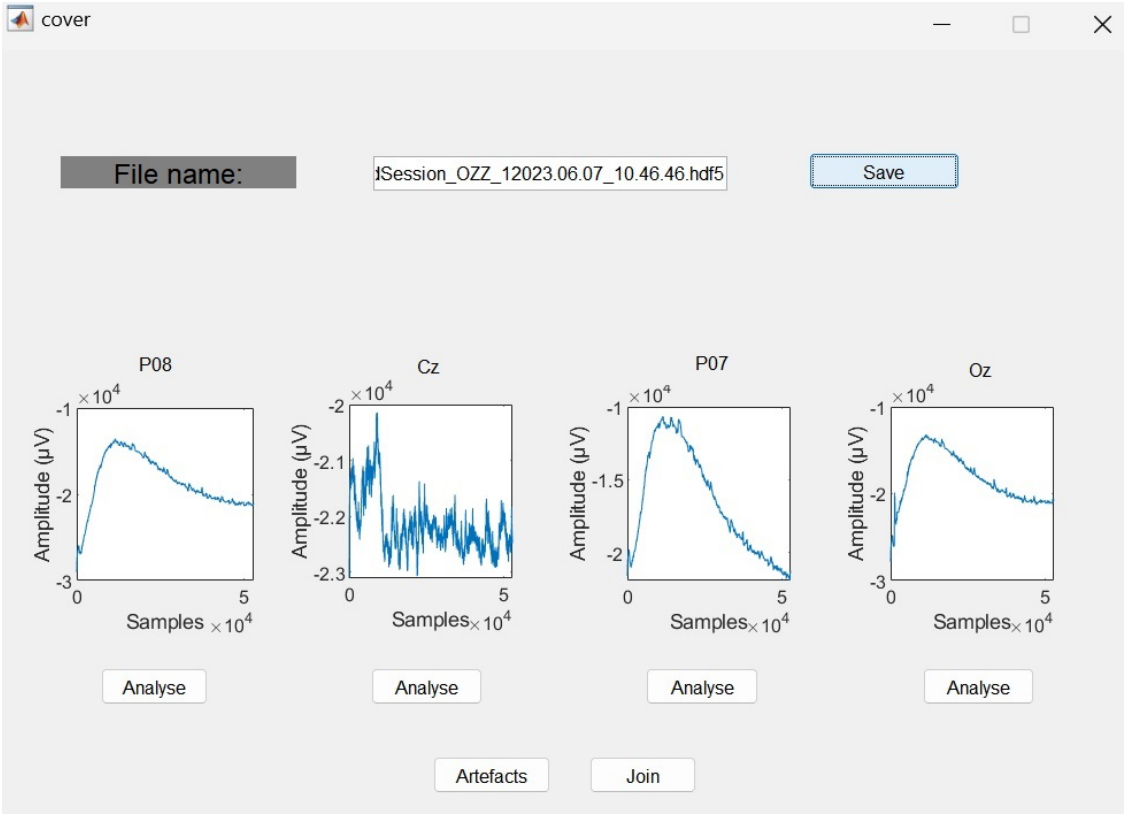

Figure D.4: Previous GUIDE platform cover.

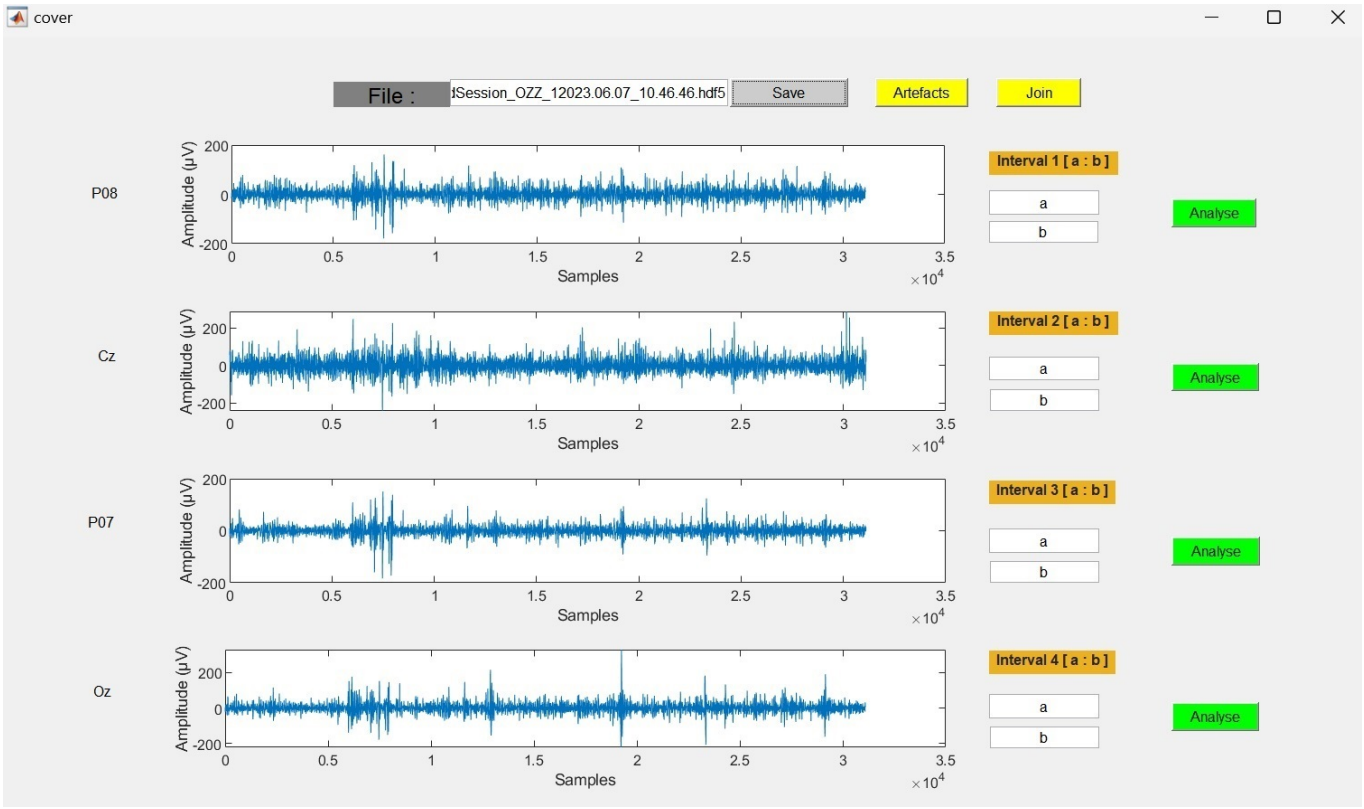

Figure D.5: New GUIDE platform cover.

As explained in Section 4.4.2, the new GUIDE platform cover page allows for the selection of intervals where the signal appears to be less affected by artifacts, thus improving the artifact removal process. A comparison of the "Analyse" pages from the previous method (Figure D.6) and the new method (Figure D.7) reveals the impact of this artifact removal enhancement. The VEPs are more noticeable in Figure D.7. The grey lines, which indicate the moments of stimulation, further aid in understanding the subject's response to the stimulus.

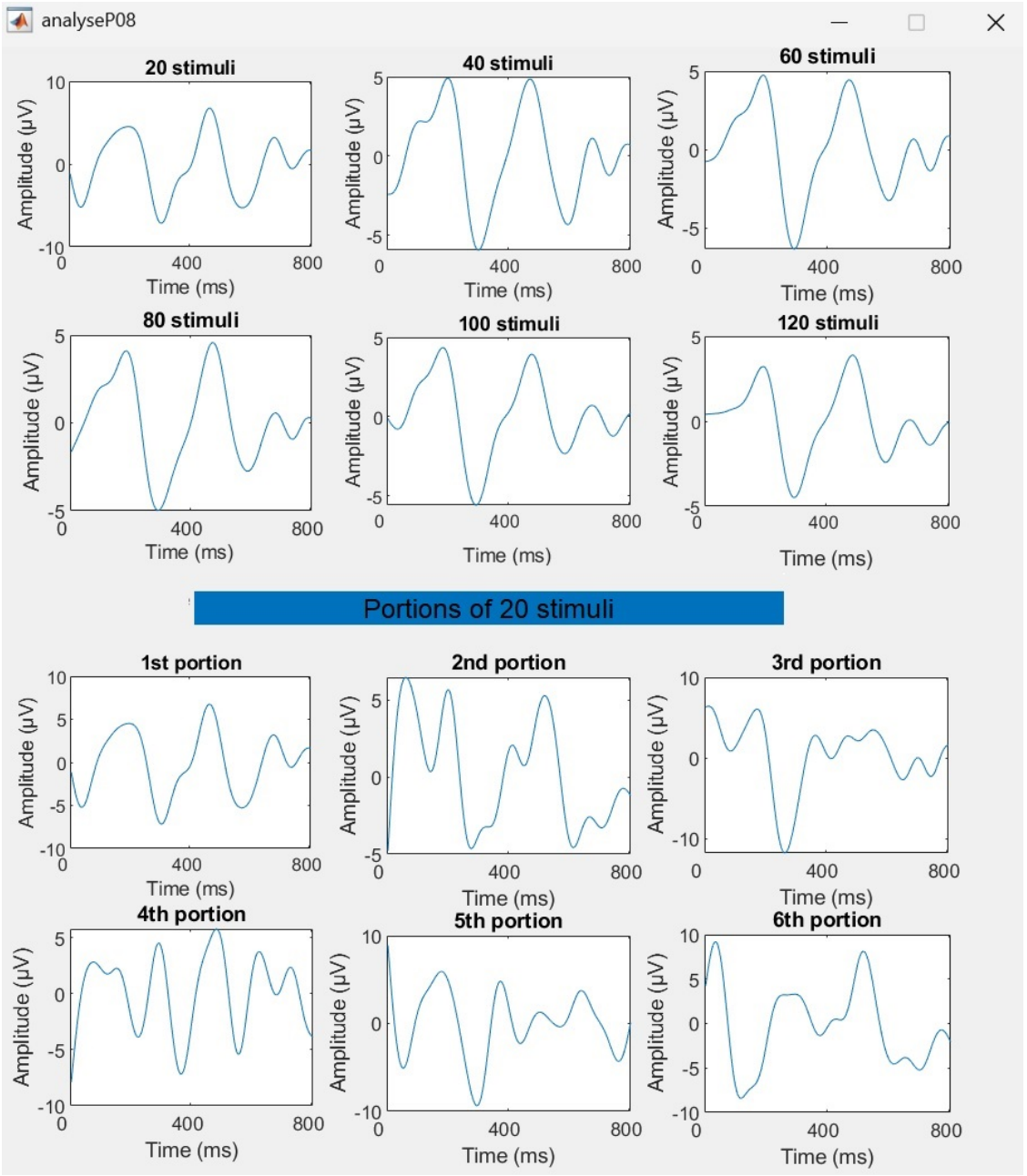

Figure D.6: Previous GUIDE platform "Analyse" page. The electrode $P0_8$ is used in this example.

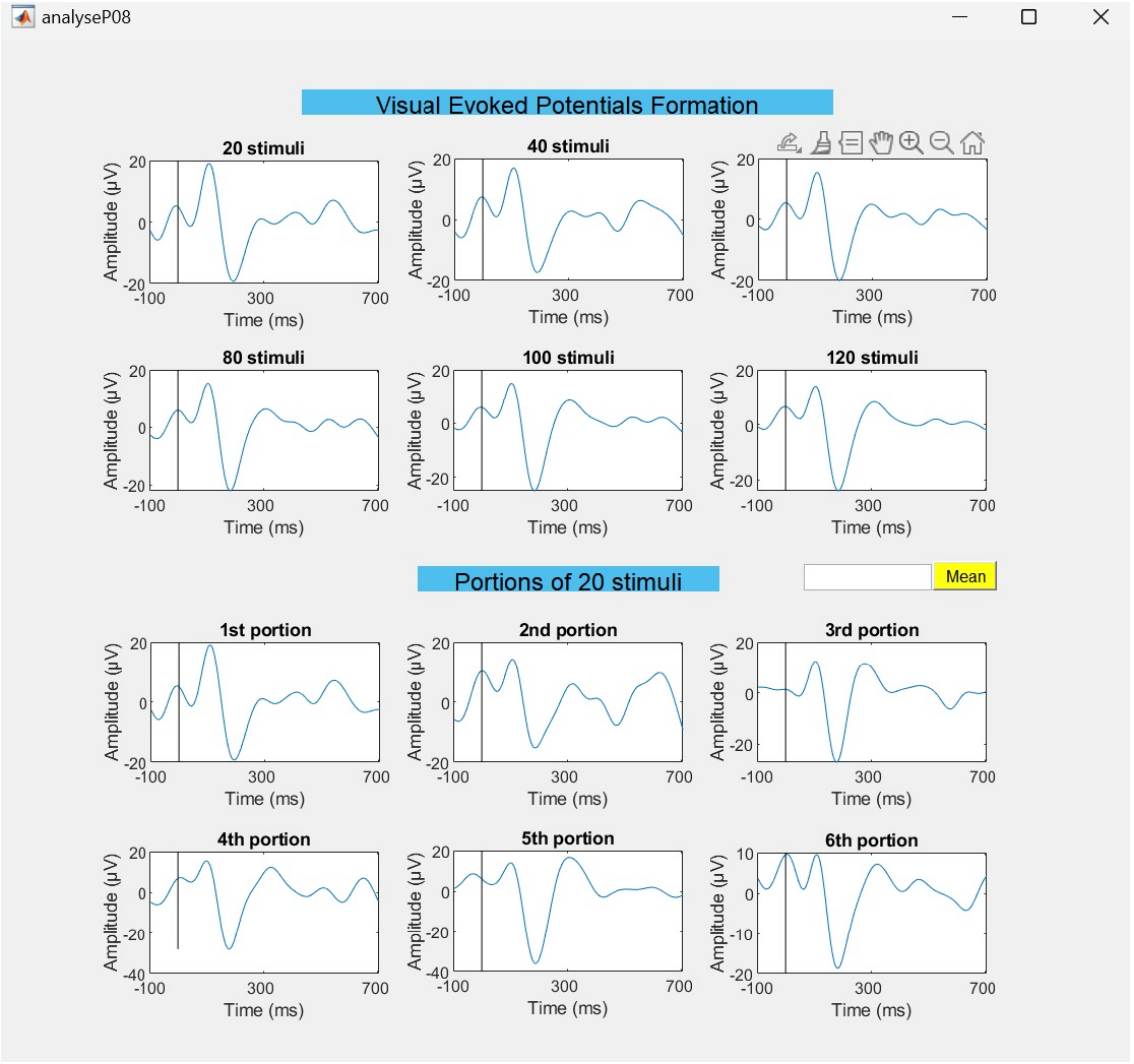

Figure D.7: New GUIDE platform "Analyse" page. The electrode $P0_8$ is used in this example.

In these last pages, the "Artefacts" pages, the impact of the new artifact removal method is particularly noticeable. In the old method, the signal is almost entirely rendered unusable and truncated, and the artifacts are incorrectly identified, as illustrated in Figure D.8.

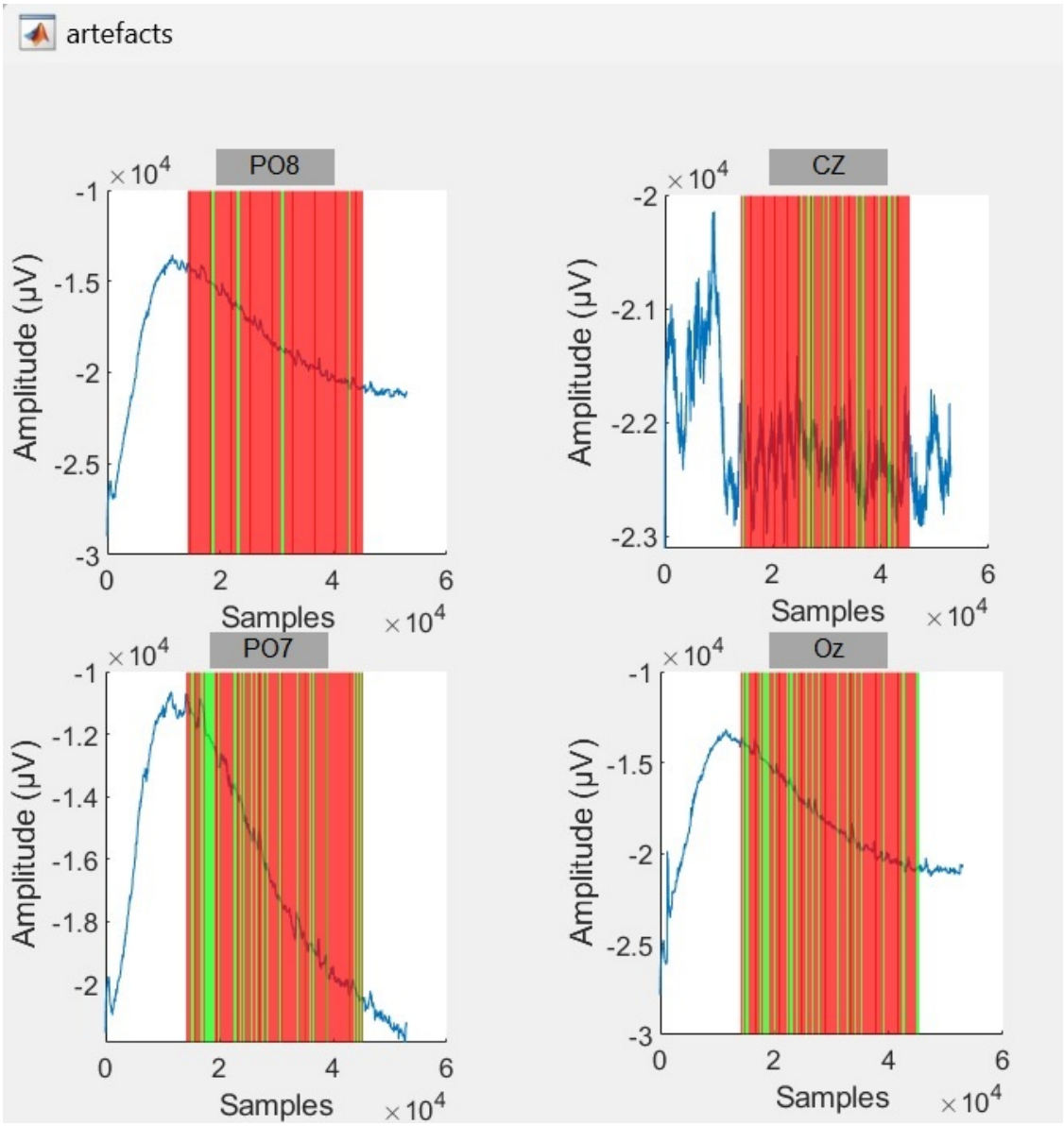

Figure D.8: Previous GUIDE platform "Artefacts" page.

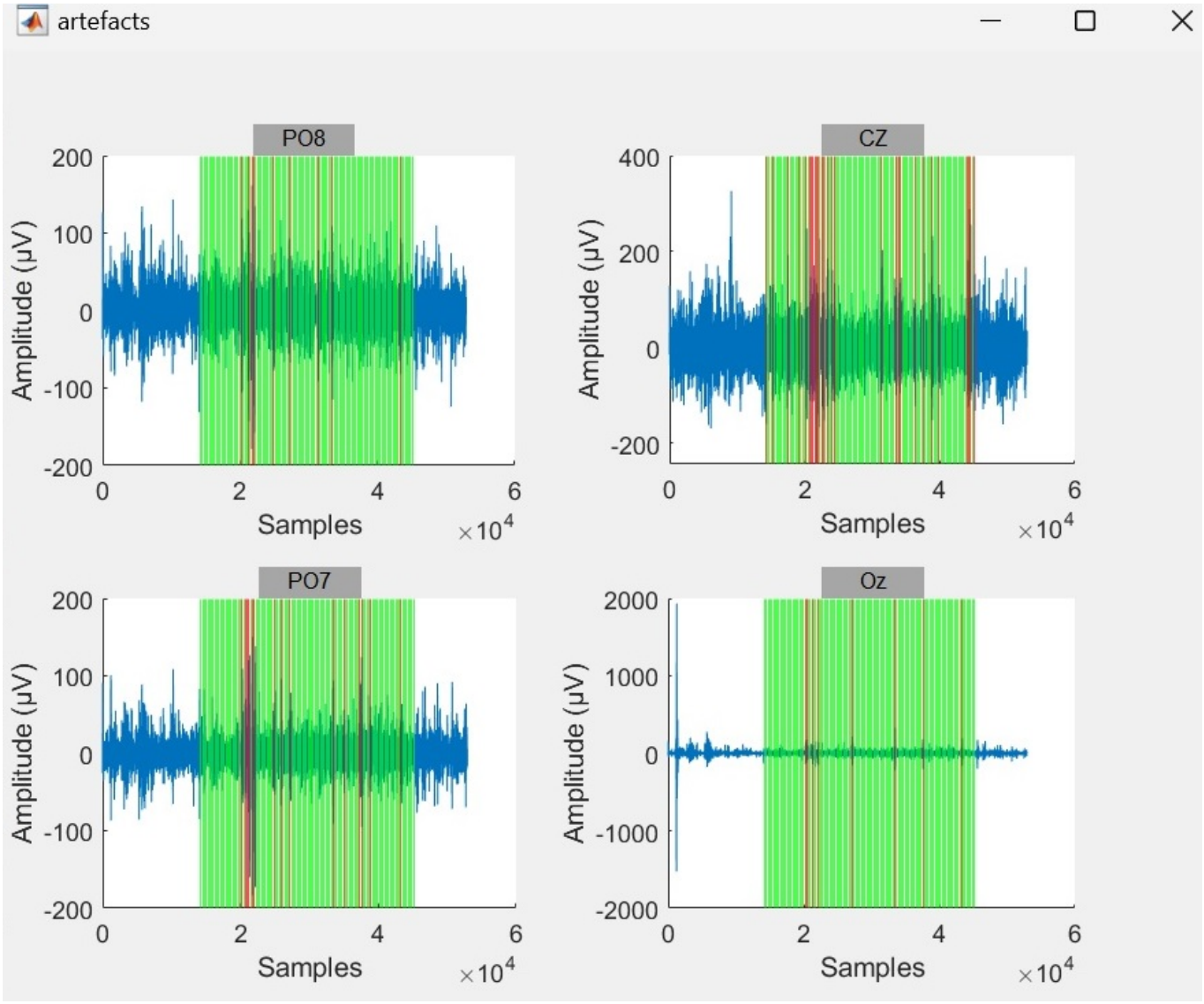

Figure D.9: New GUIDE platform "Artefacts" page.

This Appendix provides a more detailed understanding of the adaptations and improvements made that enhanced the efficiency of processing VEPs signals.

E

Detailed Signals Parametrisation

This appendix provides a comprehensive outline of the essential procedures for deriving the requisite parameters for data analysis from the acquired signals. To illustrate this process, we will employ the 4 month acquisition of subject with ID 3 as an example, starting with the parametrisation of VEPs and subsequently addressing EDA. It is imperative to note that these procedures are carried out for each acquisition, thus requiring application for the assessment at 4 months and for both takes at 12 months.

E.1 Visual Evoked Potentials Parametrisation

The initial step involves opening the MATLAB® software, entering the name of the *g.Nautilus*® file, and subsequently pressing the "Save" button, as seen in Figure E.1.

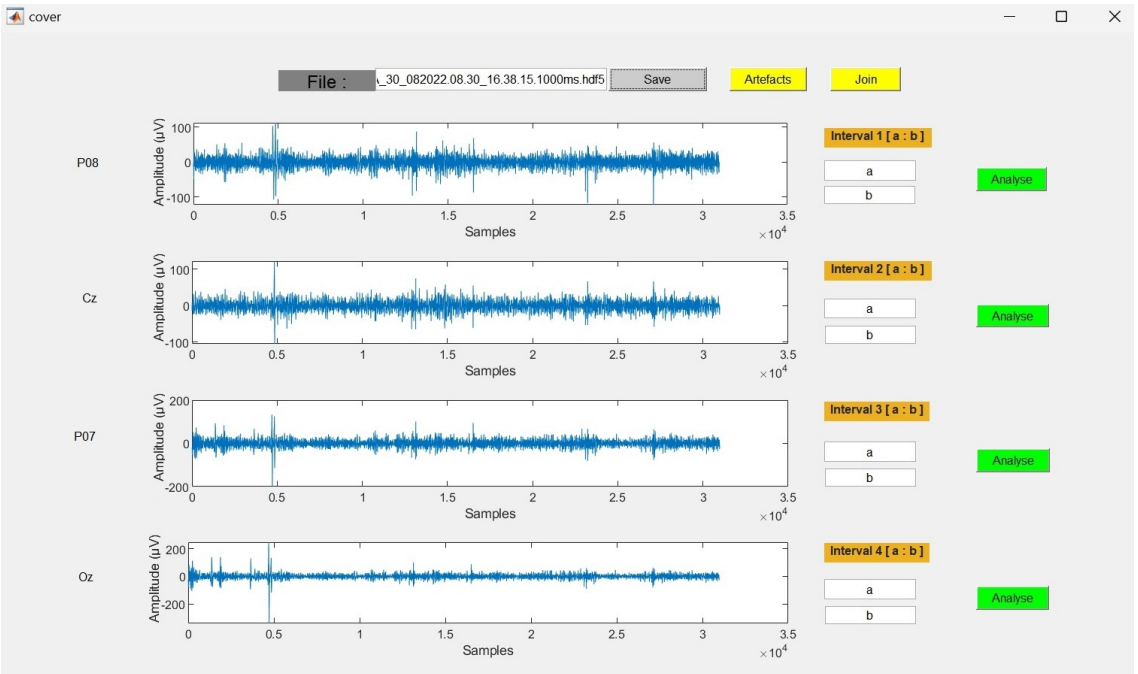

Figure E.1: GUIDE cover page file upload from 4 months acquisition of subject ID 3.

Subsequently, as despicted in Figure E.2, we select the interval where the signal appears to be relatively free from artifacts, which will serve as the foundation for calculating the standard deviation used to exclude artifacts, as explained in Section 4.4.1.

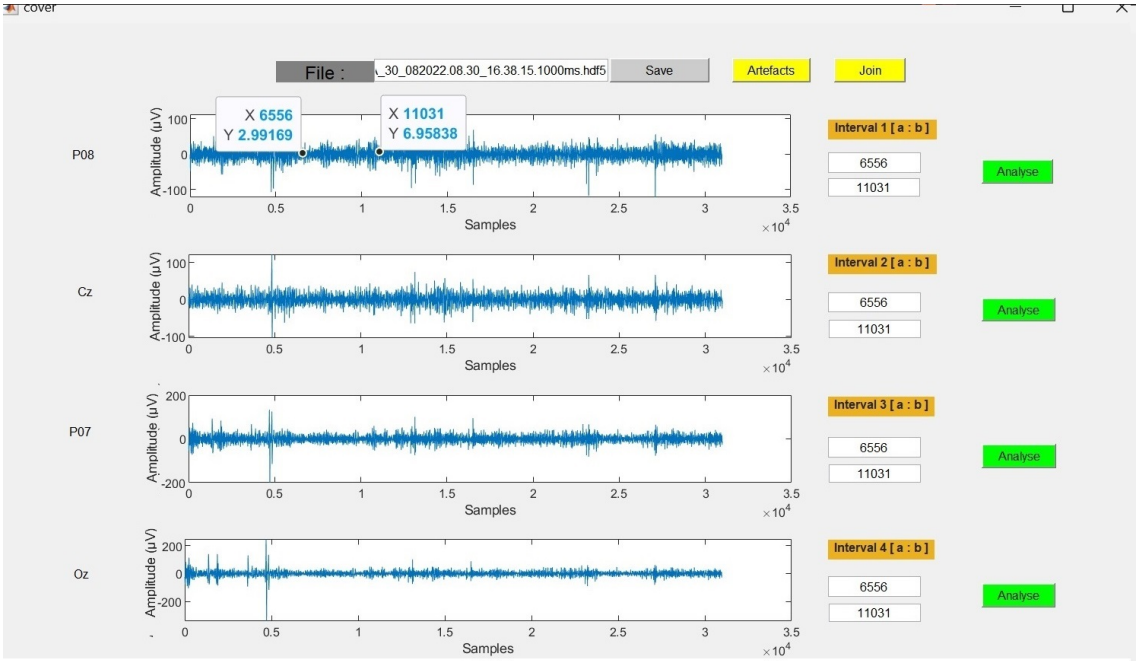

Figure E.2: GUIDE cover page with interval selection for standard deviation calculation.

An additional step involves clicking the "Join" button to get a preliminary view of the electrodes that seem to exhibit VEPs patterns, as seen in Figure E.3. It is possible to see that electrode $P0_7$ and O_Z have an easily recognizable VEPs pattern in comparison with the others.

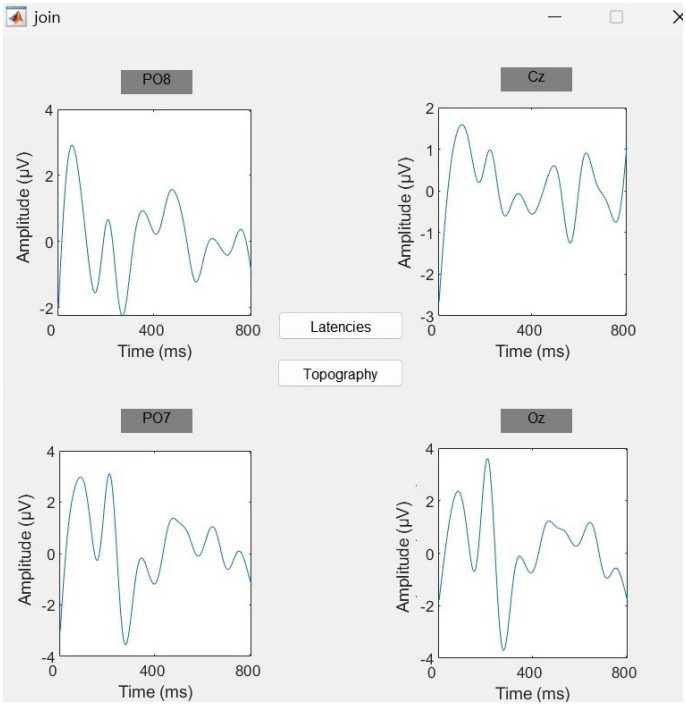

Figure E.3: GUIDE "Join" page.

The subsequent step is to click the "Analyse" button for each of the electrodes and

review the generated graphs. Detailed explanations regarding the content of these graphs can be found in Section 4.4.2. In this example, Figure E.4 contains the electrode $P0_7$ under analysis.

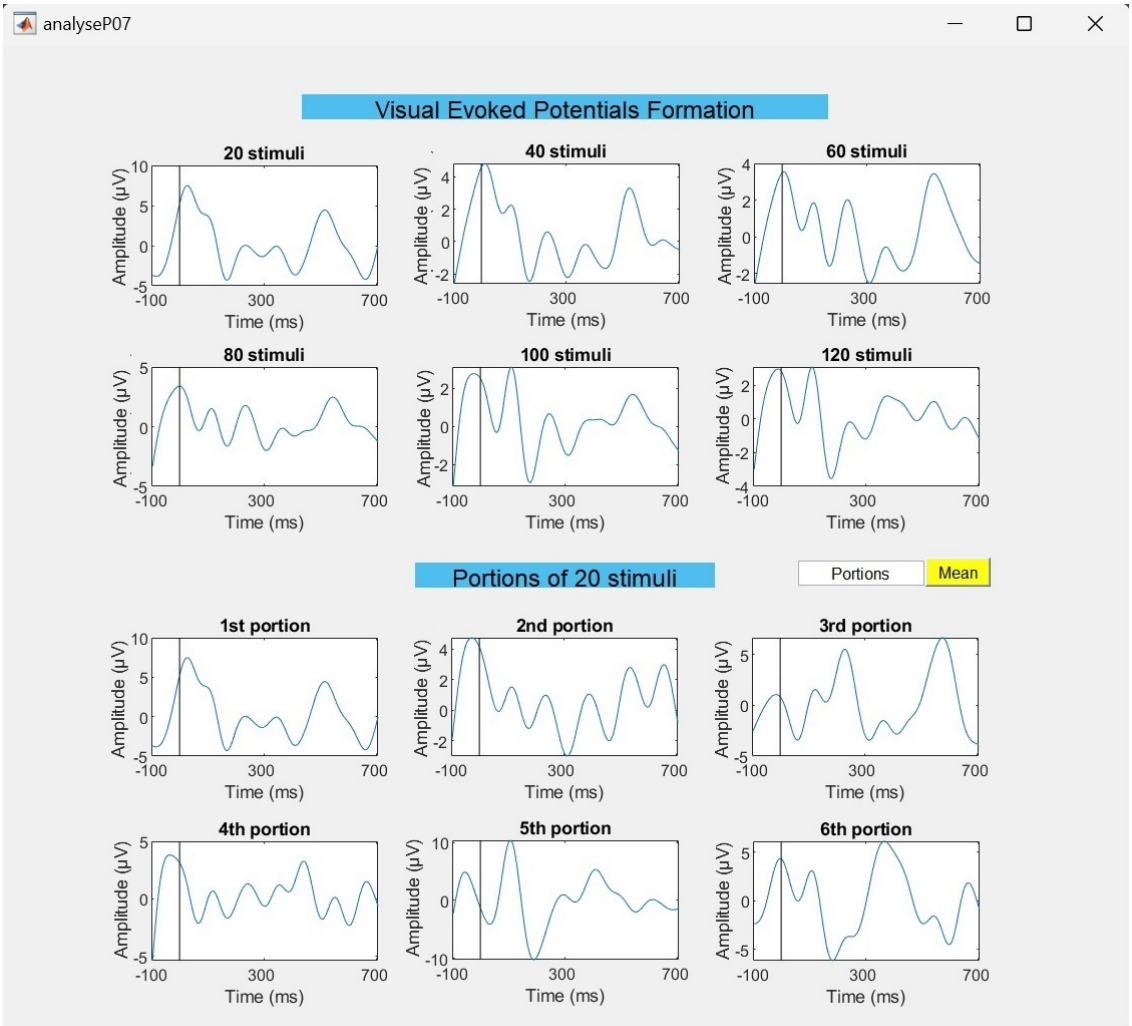

Figure E.4: GUIDE "Analyse" page for electrode $P0_7$ for 4 months acquisition of subject ID 3. The grey line marks the moment of application of a stimulus.

From these graphs, we attempt to identify a pattern and ascertain the signal portions where attention to the stimulus and the corresponding VEPs can be discerned. We monitor the potential locations of the N75 and P100 peaks.

In Figure E.5 we can observe a progression in the top graphs. The "40 stimuli" graph (second graphic from the top) begins to exhibit the initial stages of a pattern, while the "60 stimuli" graph displays a more pronounced pattern. The "80 stimuli" graph appears to be less defined compared to the previous graphs, but the "100 stimuli" graph represents an improvement, and the "120 stimuli" graph displays a highly recognizable VEPs pattern.

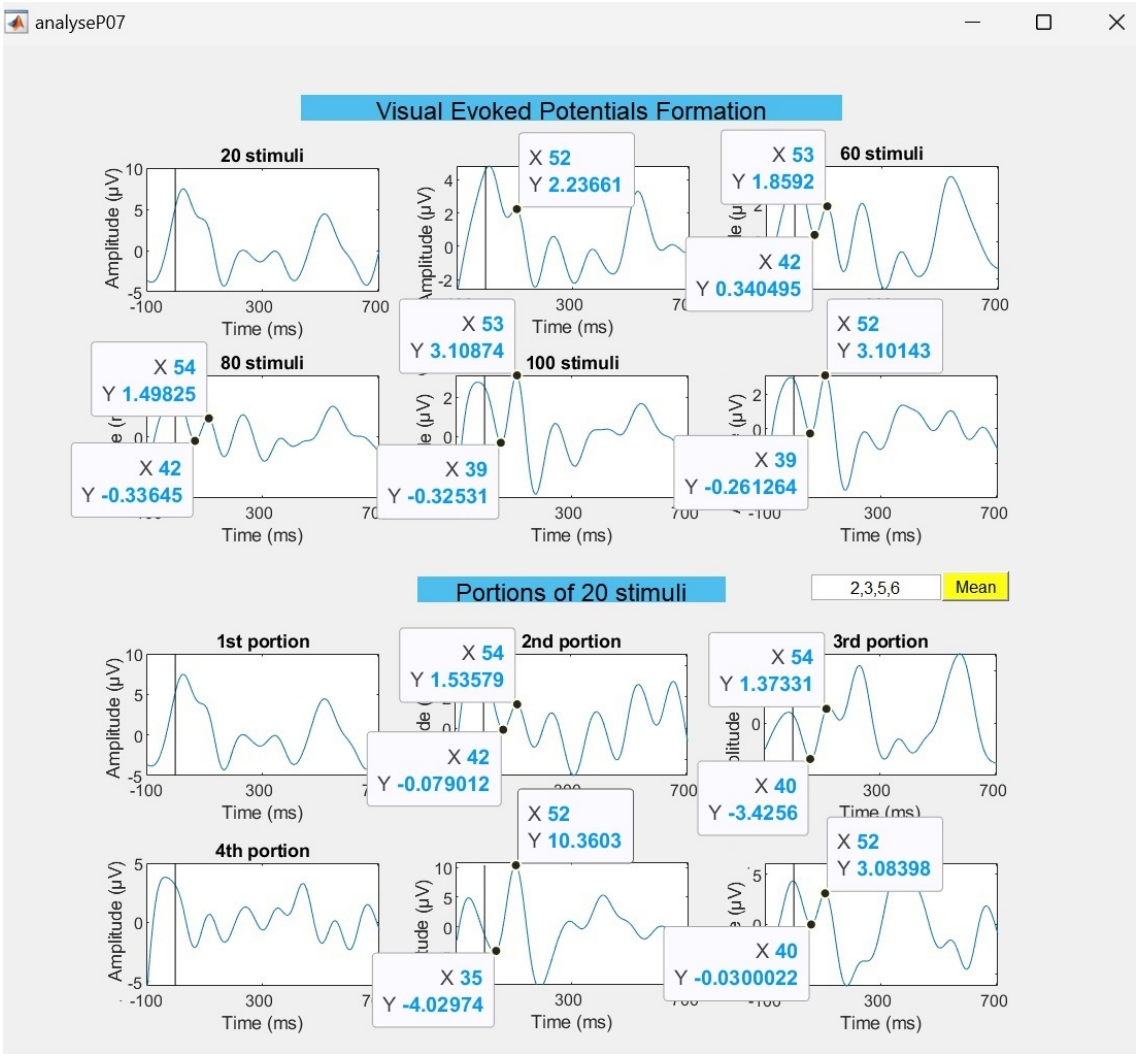

Figure E.5: GUIDE "Analyse" page for electrode $P0_7$. Finding the N75 and P100 peeks.

When observing the first six graphs with the last ones, information suggests that during the 1^{st} portion of the signal, the subject's attention may not have been fully engaged. However, as we progress through the 2^{nd} and 3^{rd} portions, attention seems to increase. In the 4^{th} portion, attention may have waned slightly, but it is regained in the 5^{th}, and 6^{th} portions of the signal.

With this analysis concluded, we can identify the portions where VEPs appear to be present and indicate the corresponding graph numbers alongside the "Mean" button, separated by commas. In this scenario, the optimal portions for selection would include the 2^{nd}, 3^{rd}, 5^{th}, and 6^{th} portions.

Upon clicking the "Mean" button, we obtain a signal that represents the average of the selected portions, potentially comprising the segments where the subject is most attentive to the stimulus.

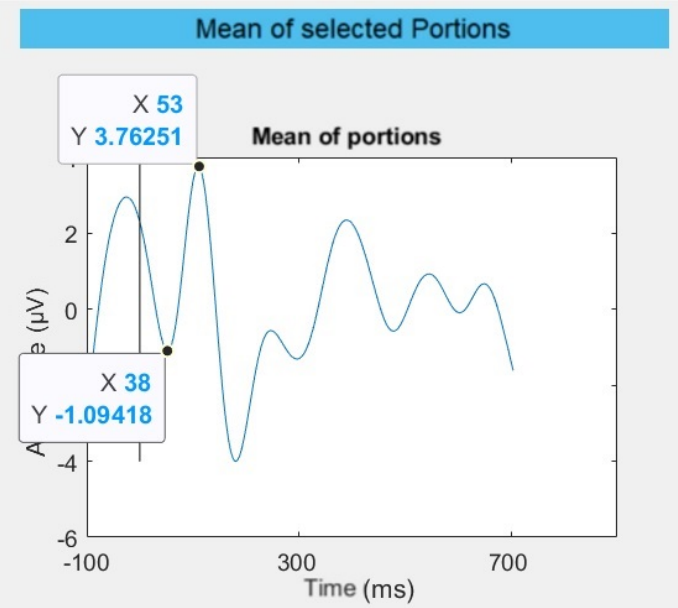

Figure E.6: GUIDE "Mean of selected portions" page for N75 and P100 selection.

When comparing to a reference VEPs signal (like figure 2.4), we identify the N75 and P100 peeks. The marked points in Figure E.6 are then extracted to an Excel spreadsheet, according to Table E.1. The entire process of analysis is subsequently applied to the remaining three electrodes, where, at times, no pattern of evoked potentials is found, resulting in the exclusion of those electrodes.

Table E.1: Excel table for the 4 months acquisition of Subject ID 3 after VEPs parameter extraction of the four electrodes in sample number X.

$P0_8$				**C_Z**				**$P0_7$**				**O_Z**			
N75		P100		N75		P100		N75		P100		N75		P100	
X	Y	X	Y	X	Y	X	Y	X	Y	X	Y	X	Y	X	Y
38	-1.01	52	1.94	38	-2.12	55	2.49	38	-1.09	53	3.76	38	1.50	53	3.53

Once all the points are extracted into Excel, an average of the N75 and P100 latency values is computed with the electrodes that were not excluded. This yields a single N75 latency value and a single P100 latency value for each assessment, which constitute our parameters for evaluation.

The last step is using the conversion Equation 4.2 to translate the information from samples to latency values obtaining our VEPs parameters, as depicted in Table E.2.

Table E.2: Parameters converted from sample number to latencies in milliseconds.

N75	**P100**	**N75 [ms]**	**P100 [ms]**
38	53.25	52	113

E.2 Eletrodermal Activity Parametrisation

The initial step in extracting EDA parameters involves running a MATLAB® script. This script is designed to extract signal information from the *opensignals*® file and trigger information from the *g.Nautilus*® file. By executing the script, two files are generated: one containing the subject's EDA data and another containing the stimulus moments.

Subsequently, the *Ledalab*® application is launched, and the data and stimulus files previously generated are imported, creating a *.mat* file, as illustrated in Figure E.7.

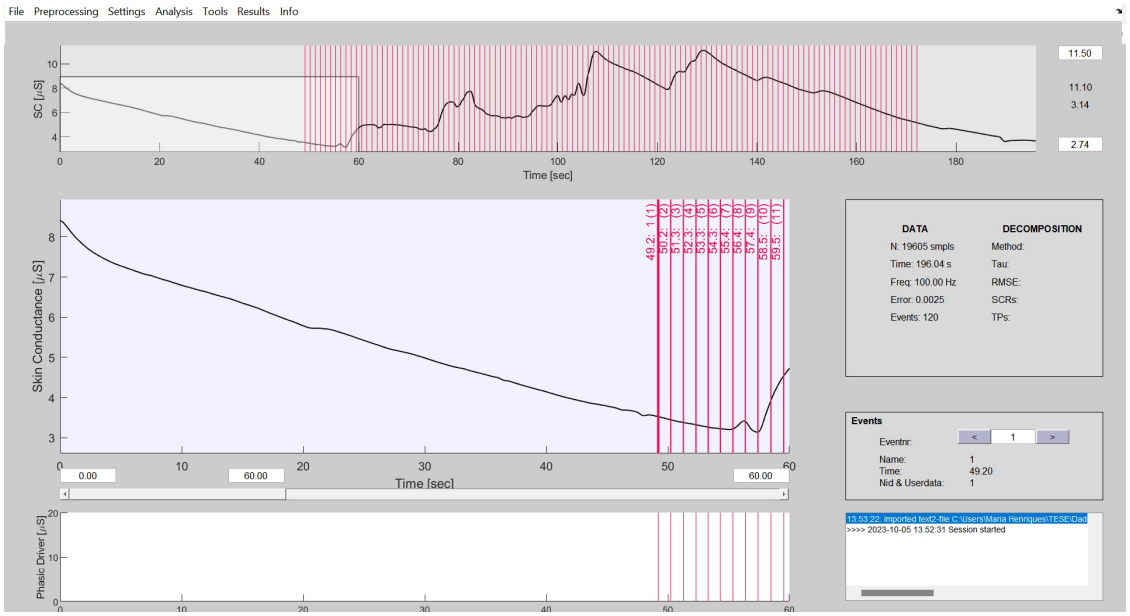

Figure E.7: Ledalab® software data and event upload. The red lines represent the triggers.

The following step entails executing the DDA process to decompose the signal into its tonic and phasic components, resulting in the file depicted in Figure E.8. From this file, the SCRs parameter, highlighted in green, is directly extracted.

Figure E.8: *Ledalab*® software after DDA process. The top graph contains the entire EDA signal, the middle graph contains the tonic component and the bottom graph the phasic component of the signal. The SCRs number is highlighted in green, in the right part of the image. The "Results" menu is highlighted in orange.

Afterwards, by selecting the "Results" command from the menu bar, it is possible to extract the multiple values from the *.mat* file to an Excel spreadsheet. To do so, it is necessary to specify the values for the response window, as despicted in Figure E.9. The justification behind the selection of these values is elucidated in Section 4.4.3.

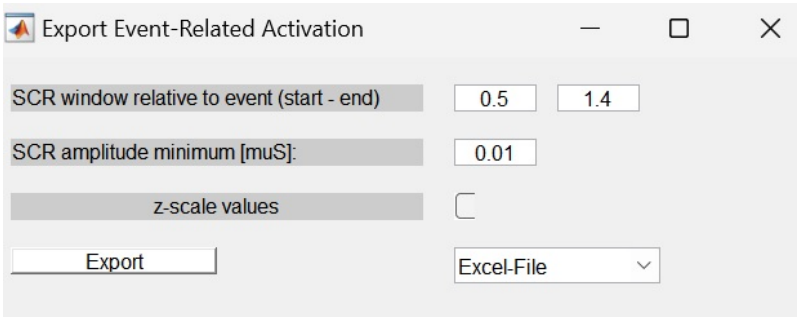

Figure E.9: *Ledalab*® Selection of values for the response window. The parameters where extracted between a 0.5 to 1.4 seconds of time, and 0.01 microsiemens of amplitude window.

Based on the Excel spreadsheet generated, as exemplified in Table E.3, the EDA Power parameter is computed. This calculation is performed by taking the average of the column titled "Global.Mean [muS]", i.e., the mean Skin Conductance value within the response window.

Table E.3: Excel table containing the values extracted from *Ledalab*® within the response window selected.

Event .Nr	Event .NID	Event. Name	DDA. nSCR	DDA. Latency [s]	DDA. AmpSum [muS]	DDA. AreaSum [muSxs]	DDA. Tonic [muS]	TTP. nSCR	TTP. Latency [s]	TTP. AmpSum [muS]	Global. Mean [muS]	Global.Max Deflection [muS]
1	1	1	0		0	0	0.871388	0		0	3.454887	0
2	2		0		0	0	0.862142	0		0	3.38539	0
3	3		0		0	0	0.852607	0		0	3.329293	0
4	4		0		0	0	0.84288	0		0	3.268802	0
5	5		1	0.654	0.023823	1.08305	0.833353	0		0	3.228023	0
6	6		1	0.976	0.29106	4.89494	0.823565	1	0.746	0.216751	3.226889	0.089272
7	7		0		0	0	0.813422	0		0	3.371637	0.088478
8	8		0		0	0	0.803323	1	1.002	1.845528	3.178003	0.169983
9	9		1	0.532	2.067688	98.00985	0.792775	0		0	3.822331	0.705185
10	10		0		0	0	0.781775	0		0	4.486645	0.410988
⋮	⋮	⋮	⋮	⋮	⋮	⋮	⋮	⋮	⋮	⋮	⋮	⋮
120	120		0		0	0	0.192586	0		0	5.05163	0

In this manner, we obtain the parameters SCRs and EDA Power from the EDA signal of the 4 months evaluation of the subject.

F

Sample Subjects Dataset

In this appendix, the dataset containing all the parameters extracted from the VEPs and EDA signals of the sample subjects are presented in Table F.1.

Table F.1: Dataset containing all the parameters extracted from VEPs and EDA signal from the sample subjects, from 4 months (M1) and 12 months (M2) acquisition. Missing data values for subject ID 6 and 8 correspond to the EDA saturation cases. Abbreviations: ID, identification of the subject over which values were calculated; M1, acquisitions at 4 months of age; M2, acquisitions at 12 months age; FT, Full-Term Group; PT, Preterm group.

ID	Group	Gestational Age [weeks + days]	M1				M2			
			M1_N75 [ms]	M1_P100 [ms]	M1_nSCR	M1_Power [μS]	M2_N75 [ms]	M2_P100 [ms]	M2_nSCR	M2_Power [μS]
1	FT	38+1	56.00	126.67	118.00	3.74	42.00	118.00	121.00	3.04
2	FT	38	48.00	112.00	54.00	15.85	60.00	116.00	89.00	4.80
3	FT	41	54.00	112.00	49.00	7.05	54.67	100.00	130.00	0.86
4	FT	40	57.33	118.67	33.00	0.80	60.00	112.00	112.00	0.77
5	FT	40	46.67	108.00	53.00	1.14	58.00	114.00	103.00	2.86
6	PT	31+5	66.00	122.00			54.00	110.00	2.00	25.00
7	PT	27	45.33	121.33	56.00	2.46	50.00	106.00	87.00	18.41
8	PT	31+6	52.00	120.00			48.00	96.00	86.00	4.69
9	PT	29+3	50.67	136.00	147.00	7.82	42.00	104.00	105.00	10.78
10	PT	29+1	48.00	106.00	59.00	16.40	53.33	100.00	96.00	8.78

The table columns are organized starting with the subject ID, the sample group, gestation age and finally the VEPs and EDA parameters. Groups FT (Full-Term) and PT (Preterm) are highlighted in blue and yellow, respectively. The parameters are separated according to the moment of extraction, with M1 being at 4 months and M2 at 12 months. The values reported are the N75 and P100 latencies, in millisecond units, SCRs and EDA Power in microsiemens.